OPTICAL AND DIELECTRIC PROPERTIES OF METALLIC CALCIUM, MODELED GENERALIZED OSCILLATOR STRENGTH FUNCTION OF CALCIUM, INTERACTION CROSS SECTIONS OF ELECTRONS, PROTONS, AND ALPHA PARTICLES WITH CALCIUM

by

Irakli G. Jorjishvili

January 2013

Director of Dissertation: Michael Dingfelder, PhD.

Major Department: Physics.

Keywords: calcium, optical, dielectric, oscillator strength, excitation energy, ionization potential, interaction cross sections.

Abstract

An analysis of the optical and the dielectric properties of calcium, determined from the literature, was performed. The optical functions of calcium were used for a calculation of the energy loss function of calcium. The energy loss function of calcium was used for a calculation of the oscillator strengths of electrons from the shells of calcium atoms and the bands of metallic calcium. The function was also used for a calculation of the mean excitation energies of

electrons from the shells and the bands of calcium. The mean excitation energy of electrons from the whole atoms of calcium was found equal to 172 eV. The oscillator strengths and the partial mean excitation energies were used for modeling the generalized oscillator strength (GOS) function of calcium. The GOS function of calcium was first constructed with the Dirac's delta functions, and later with Gaussian functions adjusted for small and for large energy losses. The GOS function of calcium was used for a calculation of the energy loss and recoil energy differential interaction cross sections of charged particles with calcium. Calculations of the cross sections were performed for electrons, protons, and alpha particles. It was also shown that interaction cross sections of charged particles heavier then protons and fully stripped from electrons can be calculated from proton interaction cross sections by charge, mass, and speed scaling. The energy loss differential interaction cross sections were calculated by integration of the double differential interaction cross sections by the recoil energy. The inverse mean free path, the stopping power, and the energy straggling of electrons, protons, and alpha particles in calcium were also calculated. Calculated interaction cross sections can be used in computer simulations of a passage of energetic charged particles through media containing calcium. Such computer simulations can help for an assessment of the radiation damage induced by energetic charged particles to media in question.

OPTICAL AND DIELECTRIC PROPERTIES OF METALLIC CALCIUM, MODELED GENERALIZED OSCILLATOR STRENGTH FUNCTION OF CALCIUM, INTERACTION CROSS SECTIONS OF ELECTRONS, PROTONS, AND ALPHA PARTICLES WITH CALCIUM

A Dissertation

Presented to the Faculty of the Department of Physics

East Carolina University

In Partial Fulfillment of the Requirements for the Degree

PhD

by

Irakli G. Jorjishvili

January 2013

OPTICAL AND DIELECTRIC PROPERTIES OF METALLIC CALCIUM, MODELED GENERALIZED OSCILLATOR STRENGTH FUNCTION OF CALCIUM, INTERACTION CROSS SECTIONS OF ELECTRONS, PROTONS, AND ALPHA PARTICLES WITH CALCIUM

by

Irakli G. Jorjishvili

APPROVED BY:

DIRECTOR OF DISSERTATION: _____ MICHAEL DINGFELDER, PHD

COMMITTEE MEMBER: _____ ROBERTA JOHNKE, PHD

COMMITTEE MEMBER: _____ GREGORY LAPICKI, PHD

COMMITTEE MEMBER: _____ JEFFERSON SHINPAUGH, PHD

COMMITTEE MEMBER: _____ LARRY H. TOBUREN, PHD

CHAIR OF THE DEPARTMENT OF PHYSICS: _____ JOHN C. SUTHERLAND, PHD

DEAN OF THE GRADUATE SCHOOL: _____ PAUL J. GEMPERLINE, PHD

Contents

Introduction

The cosmos is not merely an empty space. The cosmos is filled, at a very low density, with ions and electrons, and also with neutrons in the proximity to larger terrestrial objects such as planets or moons which lack atmosphere or magnetic field. Collectively energetic particles in space along with X-rays and γ rays are called the space radiation.

Radiation in space is roughly divided into four categories based on the source. Low energy electrons and protons, trapped within the Earth's magnetosphere, make the so-called Van Allen belts around the Earth. The continuous flow of charged particles from the Sun is known as the solar wind. Massive ejections of plasma from the Sun into the space during solar flares are known as the solar particle events. The fourth category of radiation in space is the galactic cosmic rays. The galactic cosmic rays are high kinetic energy highly charged particles originating outside the solar system.

The galactic cosmic rays are responsible for the secondary radiation near massive objects in space. Collisions of galactic cosmic ray particles with nuclei of atoms of objects present in space may result in nuclear reactions. The spallation products of nuclear reactions, ejected neutrons, and also ejected atomic electrons may contribute to the overall radiation environment near massive objects in space. The objects in space, with which the galactic cosmic rays may collide, may be surfaces of planets or moons, atmosphere, structures of man made satellites, structures of piloted spacecrafts, or even bodies of the astronauts.

The trapped radiation and the solar wind are important for low earth orbit space flights because these are the most predominant sources of exposure of the astronauts to radiation in space. Solar particle events are important for both low earth orbit and deep space flights. However, there are

measures which can be used for dealing with solar particle events during space flights. Spacecrafts can, for example, be equipped with radiation shelters, heavily shielded confinements on board of spacecrafts, where the astronauts could stay for the duration of a solar particle event. However, there is no effective method for shielding against galactic cosmic ray particles in space. The astronauts will unavoidably be exposed to the galactic cosmic rays in deep space flights.

An exposure of the astronauts to the galactic cosmic rays, as well as to any other ionizing radiation or a carcinogenic agent, may lead to a development of neoplastic formations. Neoplastic formations may take life threatening forms if the formations are fast developing. Leukemia is a fast developing neoplastic formation. Leukemia is an abnormal proliferation of white blood cells. Because leukemia develops fast, there are concerns that in deep space flights affected astronauts may not be able to return to the Earth where they could receive proper medical treatment.

In order to better plan radiation shielding of spacecrafts carrying the astronauts, and also to better plan duration of deep space flights knowledge of the risk factors, associated with exposure to galactic ray particles, is required. A significant amount of work was started at different laboratories and universities the goal of which was an investigation of the effects of high energy highly charged (HZE) particles on biological systems such as cell cultures and small laboratory animals, and also to determine the probabilities, or risk factors, for a development of observed effects. High energy highly charged particles are the laboratory equivalent to galactic cosmic ray particles.

Without any doubt results of experiments with HZE particles will be very valuable for understanding the effects of galactic cosmic ray particles on live biological systems. There are, however, concerns that application of findings obtained with cell cultures or small laboratory animals to humans may not be as straightforward as it seams because of the drastic differences between cell cultures and laboratory animals and humans.

It was suggested that computer simulations of the passage of galactic cosmic ray particles or high energy highly charged particles through biological media could help with understanding of biological effects of the particles, and could help with a prediction of the risk factors for a development of observed biological effects. Computer simulations could also be useful for a transition of findings obtained with cell cultures and laboratory animals to humans.

If leukemia is taken as one of the effects that can be caused by the galactic cosmic rays, then it is necessary to assess the radiation impact of rays on the blood forming organs, in particular, on the red bone marrow located in cavities of trabecular bone. An assessment of the radiation impact of energetic charged particles on bone marrow in situ is a hard task. It was suggested that computer simulations of the passage of energetic charged particles through bone and bone marrow could help with understanding of the radiation impact of the particles on bone marrow located in cavities of trabecular bone. Computer simulations could provide information on a distribution of doses of radiation in microscopic volumes of bone marrow. The simulations could yield statistics on the physicochemical events which occur around the tracks of individual particles. The simulations could help with understand of the effects of bone on the distribution of doses or given physicochemical events in adjacent bone marrow. And finally, the simulations could be applied for a determination of the risk factors for a development of leukemia in humans exposed

to galactic cosmic ray particles using results of experiments performed with cell cultures or laboratory animals.

Computer programs, used for simulation of the passage of charged particles through matter, use cross sections or probabilities for modeling interactions of incident particles with target matter. In order to perform computer simulations of the passage of high kinetic energy highly charged particles through bone and bone marrow, interaction cross sections of such particles with bone and bone marrow had to be derived.

At the beginning of current work it was decided to consider bone marrow as liquid water, and bone as a mixture of constituent atoms. Such simplification for bone marrow and bone was proposed mainly because of the lack of data on the dielectric or the optical properties of bone marrow and bone needed for a calculation of interaction cross sections.

Current work focused on a calculation of interaction cross sections of charged particles with calcium, one of the constituents of bone. Calcium was selected for an investigation because it is one of the major components of bone, and because it is the heaviest element found in the bone material. It was interesting to see how calcium alters distribution of doses and distribution of other physicochemical events in bone marrow lying adjacent to bone after a passage of a high energy highly charged particle through bone and bone marrow.

The goal of current work was to calculate interaction cross sections of energetic charged particles with calcium. The goal was achieved. Interaction cross sections of electrons, protons, and alpha particles with calcium were successfully calculated. A hypothesis about scaling of interaction cross sections of ions heavier then protons using protons cross sections, was also confirmed by direct calculations.

A number of important results were determined for calcium before it became possible to calculate interaction cross sections of electrons, protons, alpha particles, or ions heavier then alpha particles with calcium. The parameters are the optical and the dielectric properties of calcium, the distribution of electrons between electron shells in atoms of calcium and electron bands in metallic calcium, the mean energy required for an excitation of electrons from the different shells and bands in calcium, the mean energy required for an excitation of electrons in the whole atoms of calcium being in the condensed phase, the photoelectric properties of calcium, the conductive properties of calcium, etc. The current manuscript provides a detailed description of the analysis performed for calcium, and a description of how interaction cross sections of electrons, protons, and alpha particles with calcium were calculated.

A review of the optical and the dielectric properties of calcium

It was known that the dielectric or the optical properties of calcium will be needed for a calculation of interaction cross sections of charged energetic particles with calcium. The current work started with a survey of the optical and the dielectric functions of calcium reported in the literature. The optical functions are the index of refraction n and the extinction coefficient k. The dielectric functions are the real ε_1 and the imaginary ε_2 parts of the complex dielectric response function. The optical and the dielectric functions are related to each other by simple relations:

$$n^2 = \frac{\varepsilon_1 + \sqrt{\varepsilon_1^2 + \varepsilon_2^2}}{2}, \tag{1}$$

$$k^2 = \frac{-\varepsilon_1 + \sqrt{\varepsilon_1^2 + \varepsilon_2^2}}{2}, \tag{2}$$

$$\varepsilon_1 = n^2 - k^2, \tag{3}$$

$$\varepsilon_2 = 2nk. \tag{4}$$

It is necessary to point out that some of the found publications reported only the optical properties of calcium, while the other reported only the dielectric properties. When a particular publication reported only one set of functions, the other set of functions was also calculated using relations (1)-(4).

The optical functions which were compiled for calcium are shown in figure 1. Corresponding dielectric response functions are shown in figure 2. Please see the legends to figures 1 and 2 for references to the data. Also please see particular publications if there is a need for knowing which set of functions, the optical, the dielectric, or both, were originally reported.

The majority of data, shown in figures 1 and 2, were obtained by digitization of graphs shown in found articles or publications. A digitization of the graphs could introduce errors into values of the optical or the dielectric constants. However, it is believed that errors, associated with digitization of the graphs, are small because digitization was always performed at a high resolution of scanned images. The differences between the functions, plotted in figures 1 and 2, are due to the differences in instruments, experimental methods, preparation of samples, or techniques used by the different experimental groups.

Often publications provided data on the optical and the dielectric properties of calcium measured at different conditions. For example, the thickness of samples could vary from one experiment to another, or samples could be annealed in one experiments, but not in the other, etc. In such cases no differentiation between the reported data was made at the time of literature survey because the goal of the survey was to compile any data that could provide information on the optical or the dielectric properties of calcium. At the same time every effort was made to check the consistency of the data. For example, if a publication provided results of calculations performed using measured data, then similar calculations were performed using data obtained by digitization of the graphs shown in the publication, and the results of the calculations were checked against the results reported in the original publication.

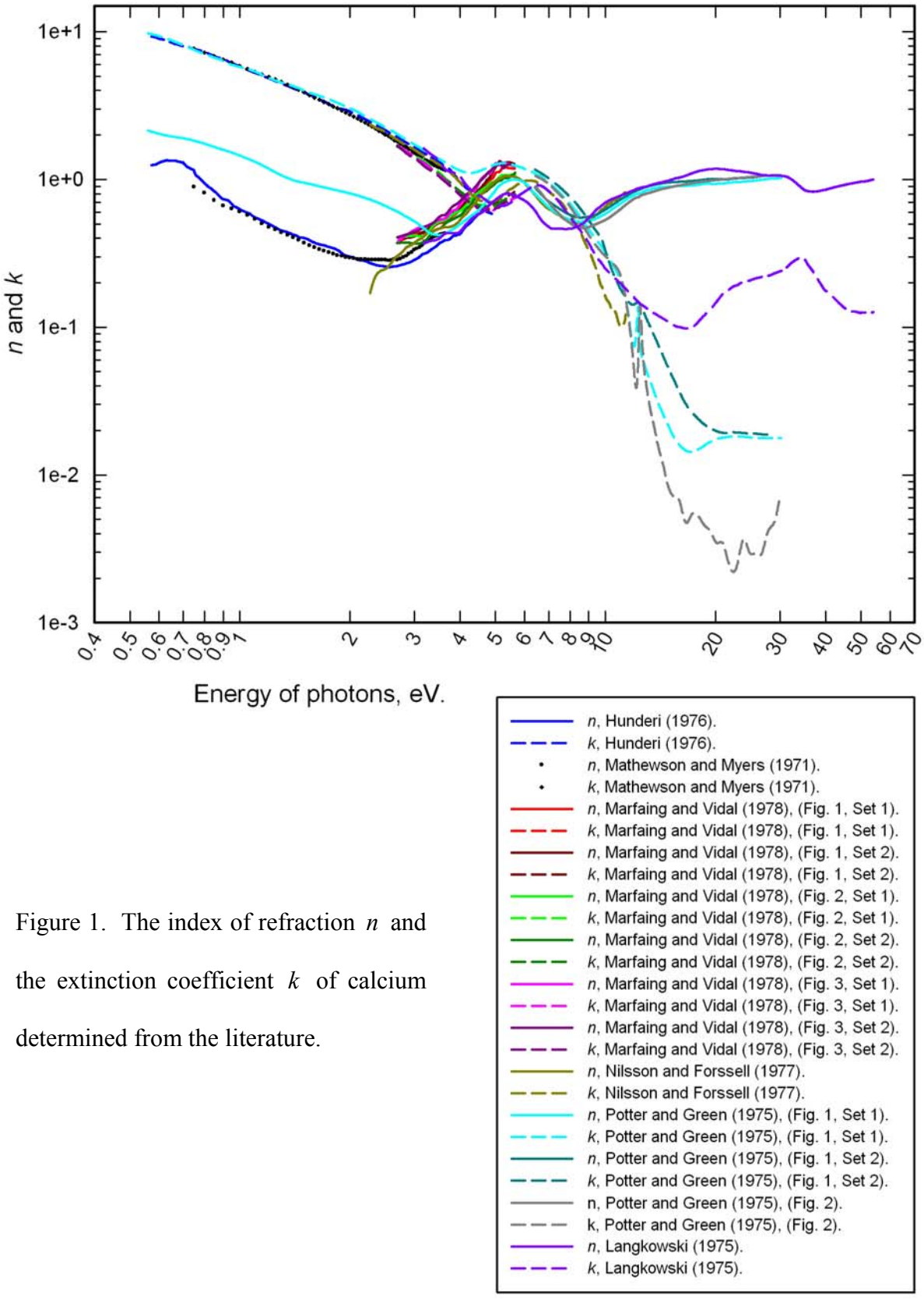

Figure 1. The index of refraction n and the extinction coefficient k of calcium determined from the literature.

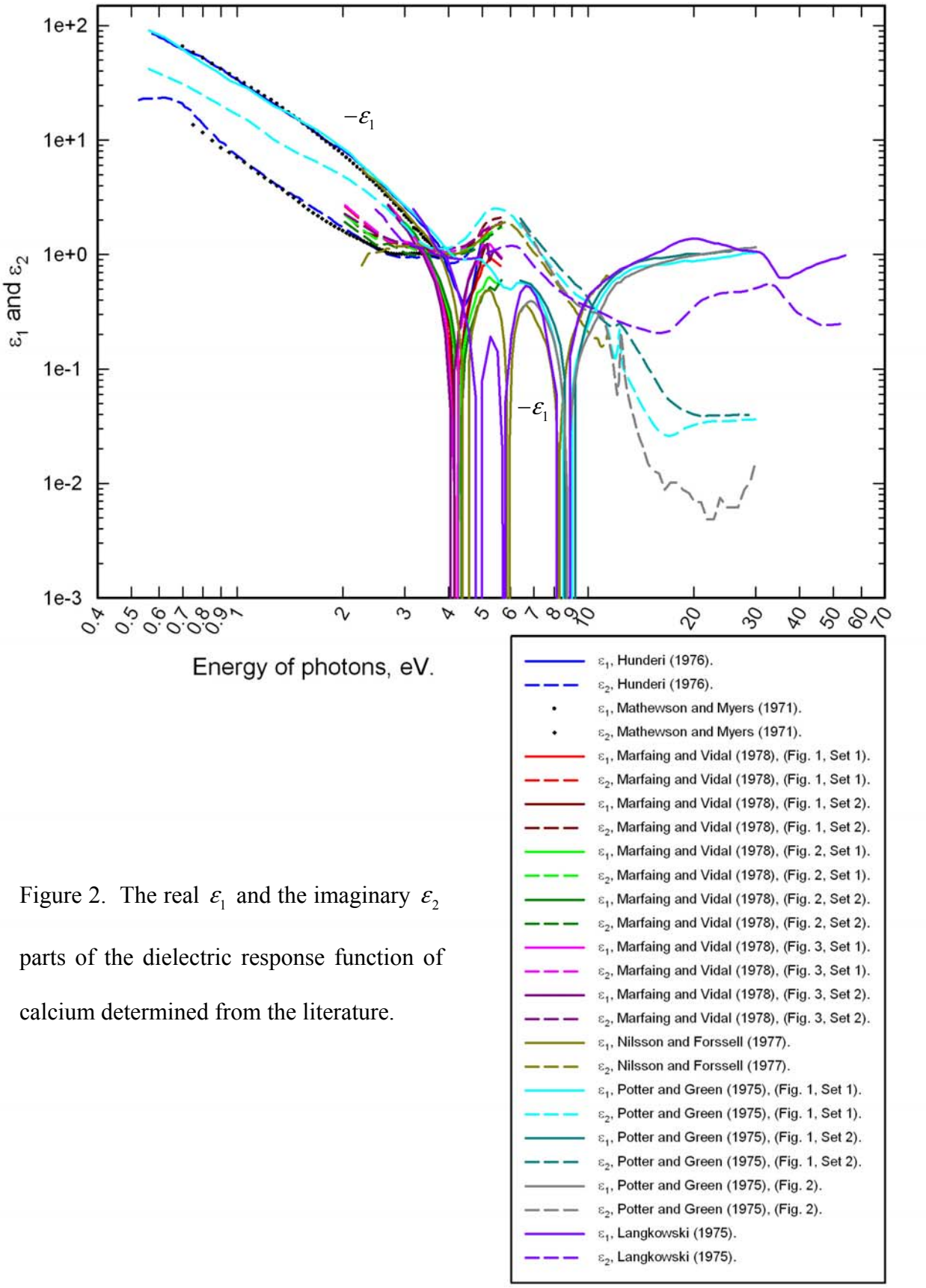

Figure 2. The real ε_1 and the imaginary ε_2 parts of the dielectric response function of calcium determined from the literature.

A literature survey resulted in a determination of the optical and the dielectric response functions of calcium for energy losses ranging from approximately 0.5 to 40 eV. For energy losses larger then 40 eV the extinction coefficient of calcium was calculated from the photoelectric cross sections. For energy losses smaller then 0.5 eV, the dielectric functions were modeled using the Drude theory. The optical functions were then calculated from the dielectric response functions according to equations (1)-(2). Next two sections of the manuscript provide a detailed description of the performed work.

Modeling of the dielectric properties of calcium for low energy losses using the Drude theory

The dielectric properties of metallic calcium were modeled for energy losses less then approximately 0.5 eV using the Drude theory. The Drude theory considers electrons from the conduction band of a metal as a free electron gas, and derives the dielectric properties of such gas. A description of the Drude theory can be found in many texts on optics and electricity. For example, one can check books by Dressel and Grüner (2002) or by Fox (2001) for a description of the theory.

According to the Drude theory the real and the imaginary parts of the dielectric response function due to electrons from the conduction band of a metal can be calculated according to the following two equations:

$$\varepsilon_1(\omega) = 1 - \frac{\omega_p^2 \tau^2}{1 + \omega^2 \tau^2} \tag{5}$$

and

$$\varepsilon_2(\omega) = \frac{\omega_p^2 \tau}{\omega\left(1 + \omega^2 \tau^2\right)}, \tag{6}$$

where τ and ω_p are two parameters descriptive of the system. Parameter τ is called the relaxation time. Parameter ω_p is called the plasma frequency. The relaxation time basically determines the rate with which a system can absorb and dissipate energy. The plasma frequency basically determines the resonant frequency at which the system is most capable of absorbing energy. Variable ω, in equations (5) and (6), is the angular frequency of external electromagnetic perturbations of the system.

The plasma frequency is often substituted by another quantity called the plasma energy. The plasma energy E_p and the plasma frequency ω_p are related to each other by simple relation:

$$E_p = \hbar\omega_p, \tag{7}$$

where $\hbar$ is the Planck constant over two π, the mathematical constant.

The relaxation time τ and the plasma frequency ω_p were determined for calcium using the dielectric properties of calcium found in the literature. A description of the approach, used for a determination of the relaxation time and the plasma frequency of calcium, is provided in the next section of the manuscript.

Determination of the relaxation time and the plasma frequency of electrons from the conduction band of calcium

The real and the imaginary parts of the dielectric response function of a metallic material can be calculated for low energy losses using the Drude theory if the relaxation time and the plasma frequency of the material are known. The relaxation time and the plasma frequency of metallic calcium were determined using a graphical approach as described by Mendlowitz (1960).

Equations (5) and (6) for the real ε_1 and the imaginary ε_2 parts of the dielectric response function can be solved for the relaxation time τ and the plasma frequency ω_p:

$$\tau = \frac{1-\varepsilon_1(\omega)}{\omega\varepsilon_2(\omega)}, \tag{8}$$

$$\omega_p = \omega\sqrt{\frac{\varepsilon_1^2(\omega)+\varepsilon_2^2(\omega)+1-2\varepsilon_1(\omega)}{1-\varepsilon_1(\omega)}}. \tag{9}$$

If the real ε_1 and the imaginary ε_2 parts of the dielectric response function of a material in question are known till sufficiently small energy losses (or angular frequencies ω), then the relaxation time τ and the plasma frequency ω_p can be determined in a graphical way. The relaxation time and the plasma frequency can be determined by an extrapolation of the plots for the time and the frequency to zero energy loss with the same behavior as seen in the plots of the relaxation time and the plasma frequency versus the energy loss.

Figures 3 and 4 show the relaxation time τ and the plasma energy E_p calculated using the real ε_1 and the imaginary ε_2 parts of the dielectric response function of calcium obtained from the literature. Please remember that the plasma frequency and the plasma energy are related to each other by simple relation (7).

From figure 3 it is seen that a plot of the relaxation time versus the energy loss takes a linear format when the time is plotted on the common logarithm scale and the energy loss is plotted on the linear scale. According to the graphical method, an extrapolation of the plot to zero energy loss with the same tendency as seen in the graph should yield the relaxation time. An extrapolation of the plots for the relaxation time of calcium to zero energy loss yielded a value of $5*10^{-15}$ s. It is necessary to point out that an extrapolation of the plots was performed as the best eye-ball estimate, not according to any specific statistical rules. The found number was taken as the relaxation time of electrons from the conduction band of metallic calcium.

Figure 4 shows plots of the plasma energy of electrons from the conduction band of metallic calcium versus the energy loss. From figure 4 it is seen that a plot of the plasma energy levels at a given value for small energy losses. A linear extrapolation of the plots, shown in figure 4, to zero energy loss yielded a value of 6.1 eV for the plasma energy. The found number was taken as the plasma energy of electrons from the conduction band of metallic calcium. It is necessary to point out that an extrapolation of the plots was again performed as the best eye-ball estimate, not according to any specific statistical rules.

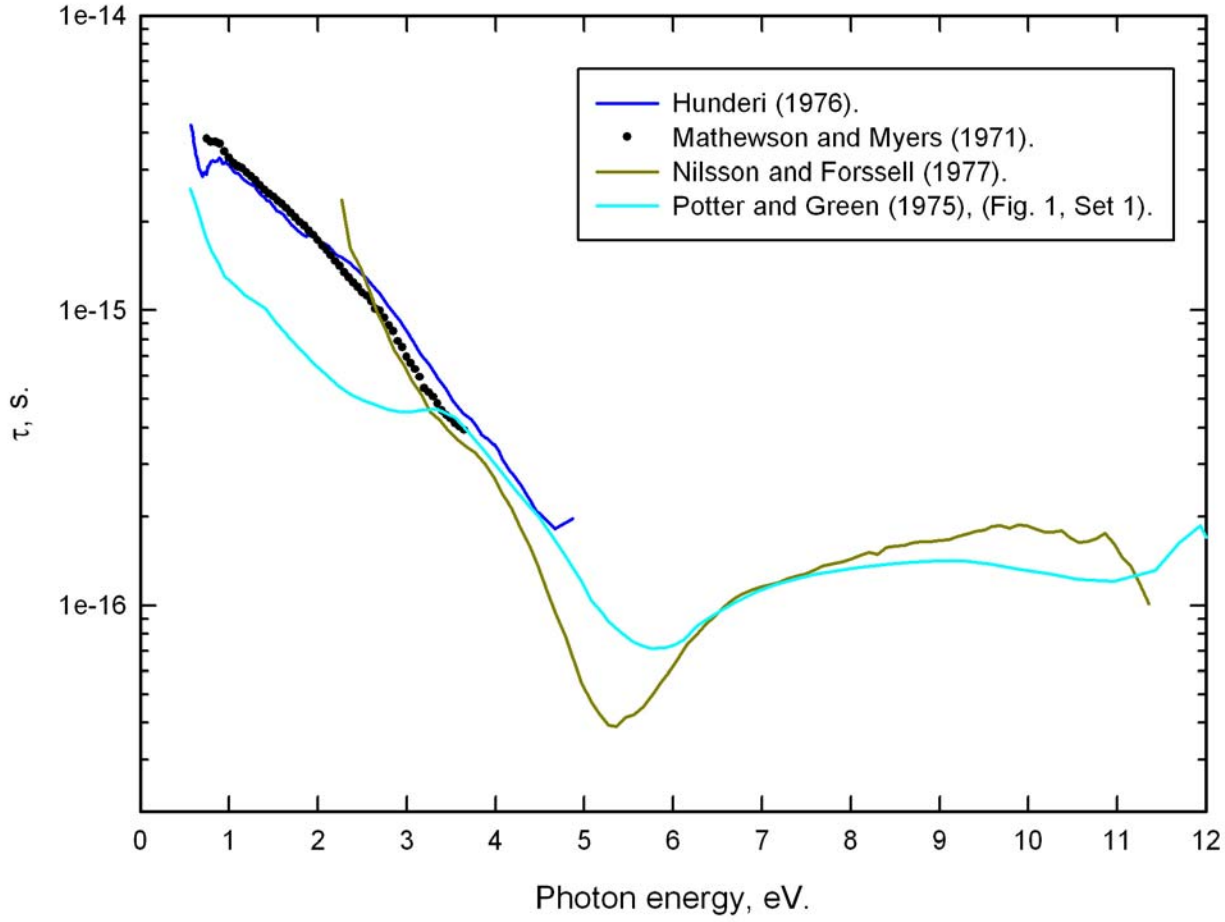

Figure 3. A graphical determination of the relaxation time of electrons from the conduction band of calcium.

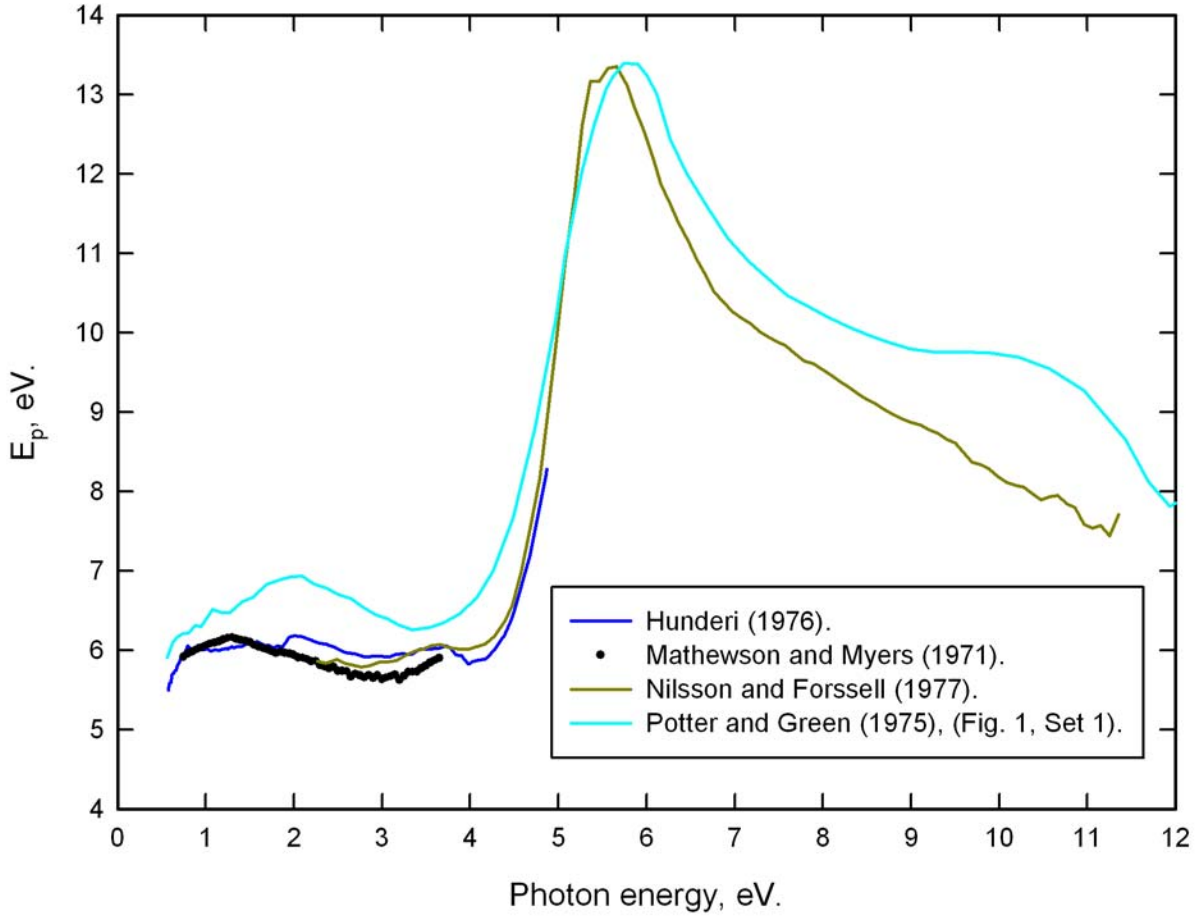

Figure 4. A graphical determination of the plasma energy of electrons from the conduction band of calcium.

The relaxation time and the plasma energy, found for metallic calcium, were used for a calculation of the dielectric response functions of calcium at small energy losses. The relaxation time and the plasma energy were taken equal to $5*10^{-15}$ s and 6.1 eV respectively in the calculations. Calculated dielectric response functions of calcium were compared to the functions found in the literature. Figure 5 shows the real and the imaginary parts of the dielectric response function of calcium calculated using the Drude theory, and the dielectric response functions found in the literature. Figure 5 basically shows how closely calculated dielectric response functions of metallic calcium coincide with the experimental data.

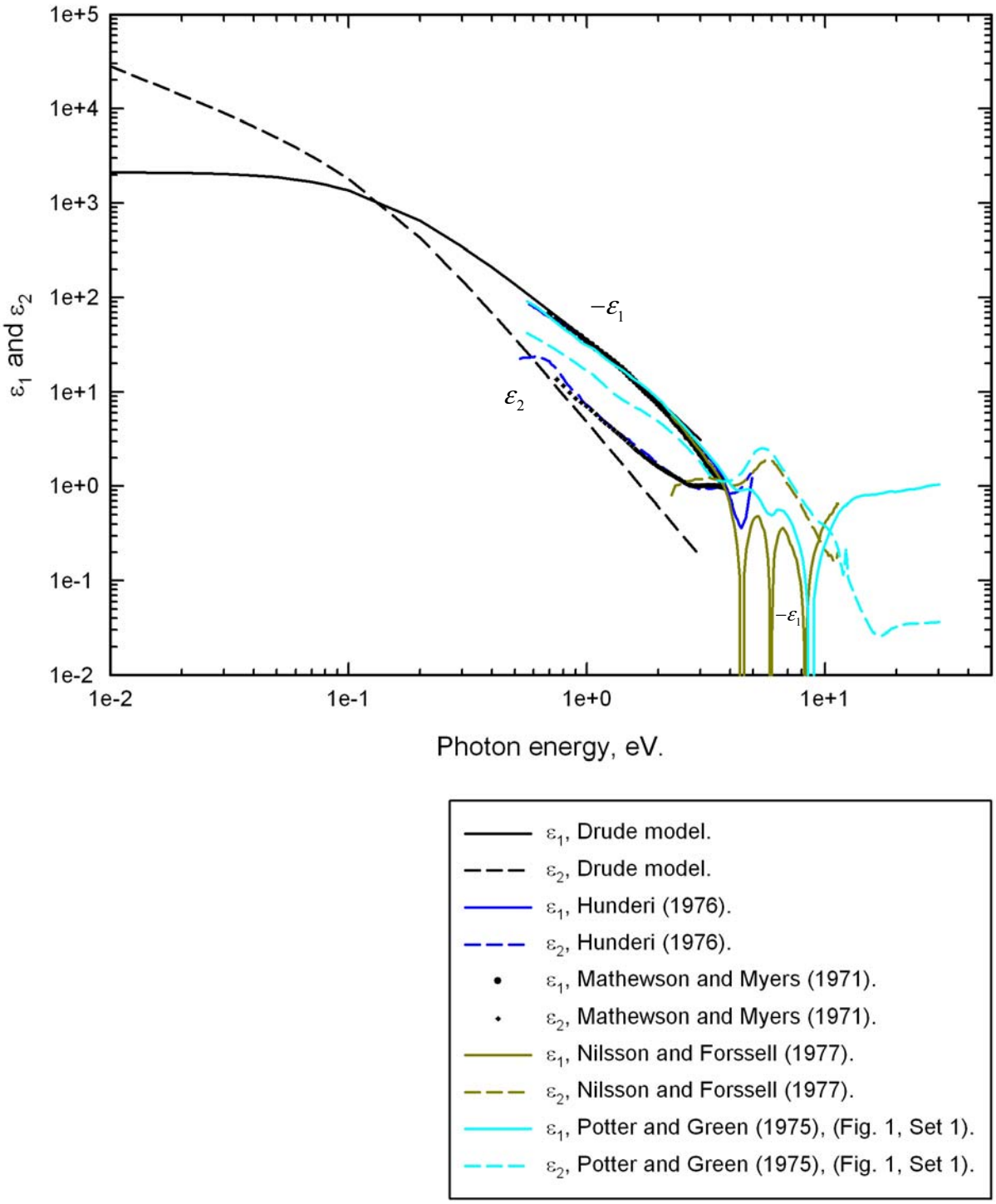

Figure 5. A demonstration of how the dielectric response functions of calcium calculated using the Drude theory coincide with the functions determined from the literature.

Considering figure 5 one may note that the graphs showing calculated dielectric response functions of calcium start to deviate from the graphs showing dielectric response functions of calcium found in the literature at energy losses equal to approximately 0.7 eV and above. The deviation of the graphs is especially noticeable for the imaginary part ε_2 of the dielectric response function of calcium. The deviation of the graphs may be due to the fact that some of the assumptions of the Drude theory, used for a calculation of the dielectric properties of calcium, may be violated for energy losses equal to approximately 0.7 eV and above. The Drude theory is used for modeling the dielectric properties of a material for small energy losses. Energy losses equal to 0.7 eV and above may not be small on a relative scale, and may violate some of the assumptions of the Drude theory in the case of calcium.

Calculation of the extinction coefficient of calcium using the photoelectric cross sections

The literature survey yielded the optical and the dielectric properties of calcium for energy losses up to approximately 45 eV. For energy losses larger then 45 eV, the extinction coefficient of calcium was calculated using the photoelectric cross sections of calcium. The photoelectric cross sections were obtained from two databases, the FFAST and the XCOM databases. Please see the FFAST and XCOM abbreviations in the references section of the manuscript for sources of the two databases. Both databases are available in a printed format. The FFAST database is also available on-line at the National Institute of Standards and Technology website. XCOM is the name of the database, and is also the name of the actual program which is used for a calculation of cross sections. The XCOM program can be downloaded also from the National Institute of Standards and Technology website. Current work used the on-line version of the FFAST

database, and used the XCOM program for a calculation of photoelectric cross sections of calcium.

Figure 6 shows the photoelectric cross sections of calcium obtained from the FFAST and the XCOM databases. The cross sections were used for a calculation of the extinction coefficient of calcium. Calculations of the extinction coefficient of calcium were performed according to the equation:

$$k = \frac{c\hbar}{2}\rho\frac{\mu_{pe}}{E}, \tag{10}$$

where c is the speed of light in vacuum, $\hbar$ is the Planck constant over two π, ρ is the density of the material, μ_{pe} are the photoelectric cross sections, and E is the energy of photons. The extinction coefficient of calcium, calculated using the photoelectric cross sections, are shown in figure 7.

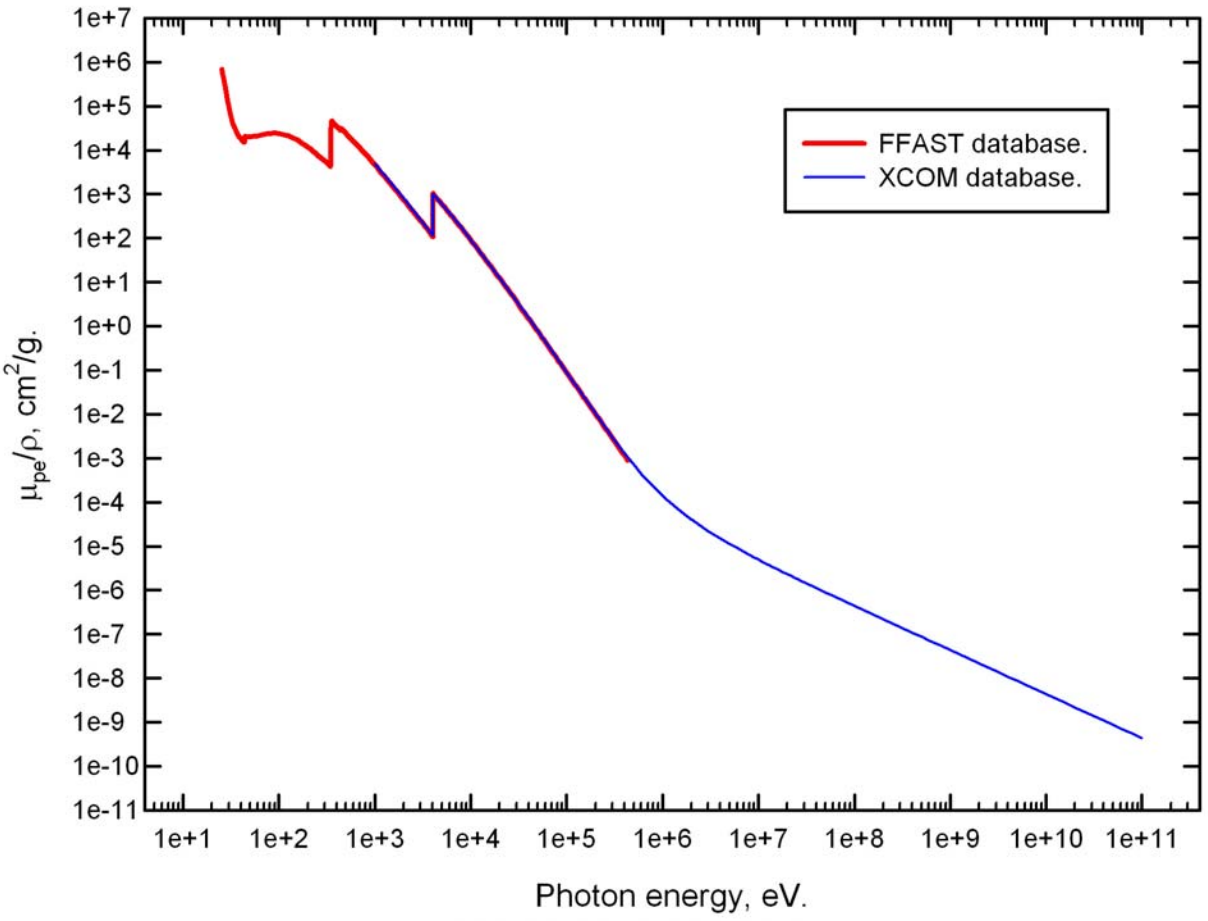

Figure 6. The photoelectric cross sections of calcium determined from the FFAST and the XCOM databases.

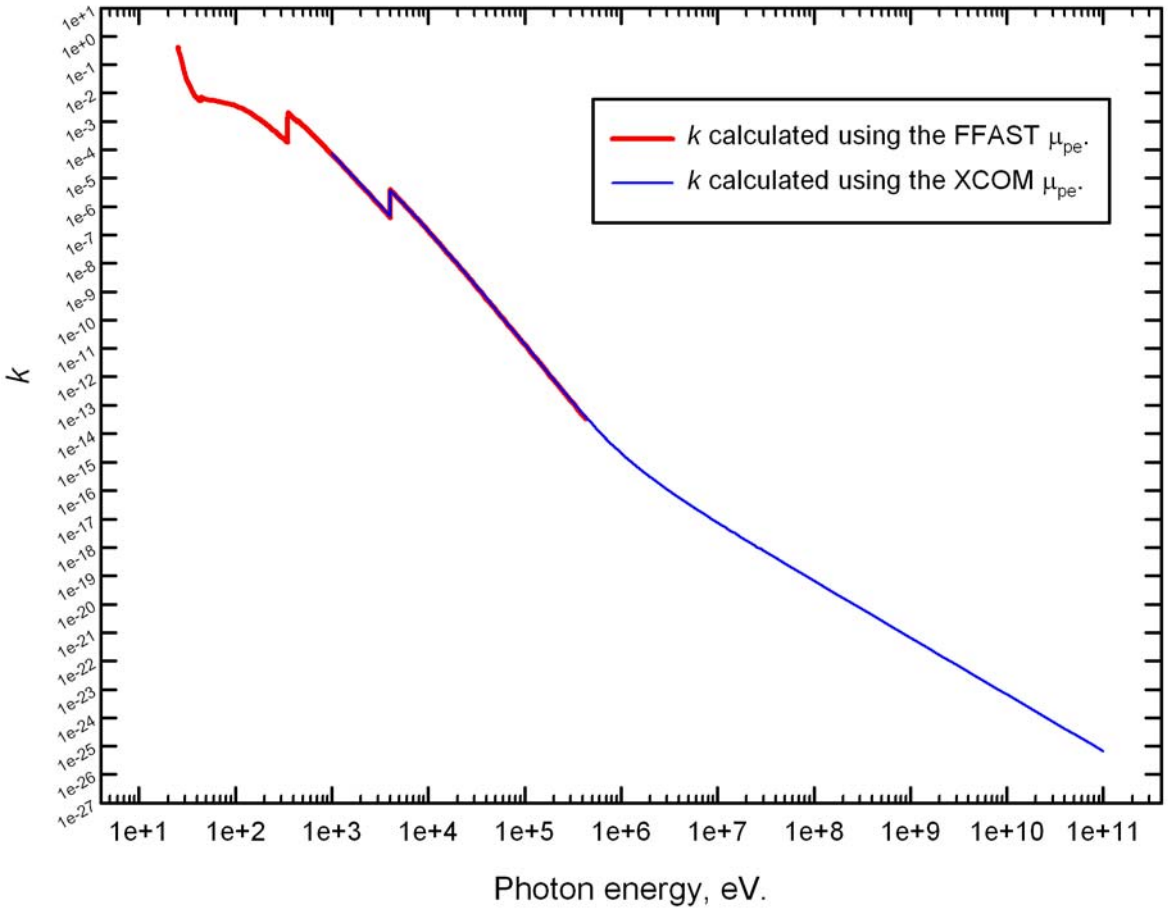

Figure 7. The extinction coefficient of calcium calculated using the photoelectric cross sections obtained from the FFAST and the XCOM databases.

A discussion why the extinction coefficient of calcium was selected for further analysis

It was known that interaction cross sections of energetic charged particles with a material are directly determined by the dielectric properties of the material. The goal of the literature search was a recovery of the dielectric or the optical functions of calcium. The literature search focused on a recovery of the dielectric functions (the real and the imaginary parts of the complex dielectric response function) and the optical functions (the index of refraction and the extinction coefficient) of calcium because the functions are directly related to each other. Knowing, for example, the index of refraction and the extinction coefficient one can recover the real and the imaginary parts of the dielectric response function in a very simple way according to equations (3) and (4). Similarly, one can recover the optical functions from the dielectric functions according to equations (1) and (2).

The optical functions (the index of refraction and the extinction coefficient) and also the dielectric functions (the real and the imaginary parts of the complex dielectric response function) are related to each other through the Kramers-Kronig relations. If, for example, one of the optical functions of a material is known, the other optical function of the material can be recovered from the first optical function by Kramers-Kronig calculations. Similarly, if one of the dielectric response functions of a material is known, the other dielectric response function can be recovered from the first dielectric response functions by Kramers-Kronig calculations. The only requirement which is imposed on the input function is that the function needs to be known within sufficiently broad range of photon energies or photon frequencies. In theory, the input function needs to be known in Kramers-Kronig calculations from zero to infinite photon energies or frequencies.

The Kramers-Kronig relations for the optical functions are (Dressel and Grüner, 2002; Fox, 2001):

$$n(\omega)-1=\frac{2}{\pi}\wp\int_0^\infty \frac{\omega' k(\omega')}{\omega'^2-\omega^2}d\omega' \tag{11}$$

and

$$k(\omega)=\frac{-2}{\pi\omega}\wp\int_0^\infty \frac{\omega'^2\left[n(\omega')-1\right]}{\omega'^2-\omega^2}d\omega', \tag{12}$$

where symbol $\wp$ denotes the principal value of the integral, ω is the angular frequency, $n(\omega)$ is the index of refraction, and $k(\omega)$ is the extinction coefficient.

A survey of the literature, modeling of the dielectric and the optical functions for small energy losses, and also a calculation of the extinction coefficient using the photoelectric cross sections for large energy losses allowed a determination of the extinction coefficient of calcium from a fraction of an electron volt to several hundreds kiloelectron volt. Figure 8 shows the optical functions of calcium obtained by literature survey, modeling, and calculations.

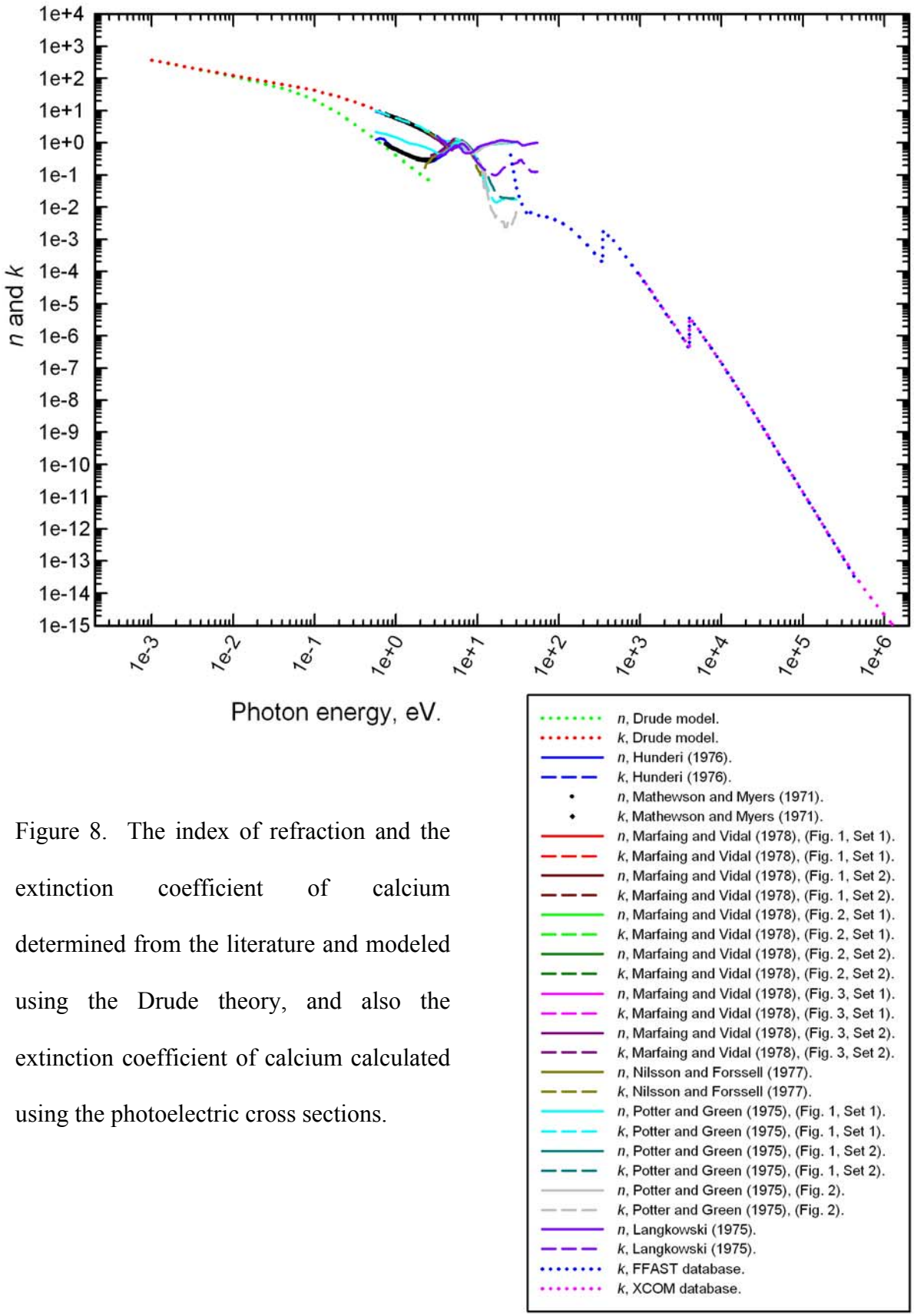

Figure 8. The index of refraction and the extinction coefficient of calcium determined from the literature and modeled using the Drude theory, and also the extinction coefficient of calcium calculated using the photoelectric cross sections.

Because the extinction coefficient of calcium was determined within so large range of energies, it seemed that the coefficient can be used in Kramers-Kronig calculations for a recovery of the index of refraction of calcium. The Kramers-Kronig relations require, as it was just mentioned, knowledge of the input function from zero to infinite energies or frequencies. That is why the extinction coefficient of calcium was selected for further analysis.

In order to perform Kramers-Kronig calculations, it was necessary to derive a single set of data specifying the extinction coefficient of calcium. The derived extinction coefficient had to satisfy a number of requirements. In particular, the coefficient had to be based on all the data compiled for calcium. The coefficient had to satisfy a specific mathematical relation. The derived extinction coefficient had to be suitable for Kramers-Kronig calculations. And finally, the index of refraction, the dielectric functions, and also the energy loss function, determined following the Kramers-Kronig calculations, all had to satisfy corresponding mathematical relations which will be shown later in the manuscript. These four requirements, imposed on the extinction coefficient, had to be satisfied simultaneously.

Introduction to the energy loss function

The energy loss function is defined as the imaginary part of minus one over the complex dielectric response function. In literature the energy loss function is often denoted by the expression $\mathrm{Im}\left(-1/\varepsilon\right)$. The energy loss function is expressed in terms of the real ε_1 and the imaginary ε_2 parts of the complex dielectric response function $\varepsilon = \varepsilon_1 + i\varepsilon_2$ according to equation:

$$\mathrm{Im}\left(\frac{-1}{\varepsilon}\right) = \frac{\varepsilon_2}{\varepsilon_1^2 + \varepsilon_2^2}. \tag{13}$$

The energy loss function is expressed in terms of the index of refraction n and the extinction coefficient k according to equation:

$$\mathrm{Im}\left(\frac{-1}{\varepsilon}\right) = \frac{2nk}{\left(n^2 + k^2\right)^2}. \tag{14}$$

The energy loss function is one of the most important functions determined for calcium. The function was used for a calculation of oscillator strengths and mean excitation energies of electrons from the different shells of calcium atoms, and the bands of metallic calcium. The oscillator strengths and the mean excitation energies were used for modeling of the generalized oscillator strength (GOS) function of calcium. The GOS function, in its turn, was used for a calculation of interaction cross sections of electrons, protons, and alpha particles with calcium.

Sum rule relations applicable to the optical, the dielectric, and the energy loss functions

The optical, the dielectric, and the energy loss functions satisfy some mathematical relations, or sum rules. The relations were used for an analysis of the functions derived for calcium, and also for a calculation of the oscillator strengths and the mean excitation energies of electrons in calcium. A discussion of the analysis performed for calcium, using the sum rule relations, is provided in the following sections of the work.

The extinction coefficient k, the imaginary part of the dielectric response function ε_2, and the energy loss function $\mathrm{Im}\left(-1/\varepsilon\right)$ satisfy the following three very similar relations (Shiles et al, 1980):

$$\int_0^\infty \omega k\left(\omega\right) d\omega = \frac{\pi}{4}\omega_p^2, \tag{15}$$

$$\int_0^\infty \omega \varepsilon_2\left(\omega\right) d\omega = \frac{\pi}{2}\omega_p^2, \tag{16}$$

$$\int_0^\infty \omega \,\mathrm{Im}\left(\frac{-1}{\varepsilon\left(\omega\right)}\right) d\omega = \frac{\pi}{2}\omega_p^2, \tag{17}$$

where ω_p is the plasma frequency. The plasma frequency is determined by the density of electrons in a given material according to the relation:

$$\omega_p^2 = \frac{4\pi e^2 N_{Avog}}{m_e} \cdot \frac{\rho Z}{M_A}, \tag{18}$$

where e is the electron charge, m_e is the electron mass, ρ is the density of the material, Z is the atomic number of elements comprising the material assuming the material is represented by single type atoms, M_A is the atomic weight of the elements, and N_{Avog} is the Avogadro number.

The index of refraction n also satisfies a mathematical relation:

$$\int_0^\infty \left(n(\omega)-1\right)d\omega = 0\,. \tag{19}$$

Relations (15)-(17) and (19) were used extensively in the current work. The relations were used, in particular, for an analysis of the derived optical functions of calcium.

A calculation of the number of electrons per atom participating in absorption of external electromagnetic radiation

Sum rule relations (15)-(17) along with relation (18) for the plasma frequency can be used for a calculation of the number of electrons per one atom of a given target material that participate in absorption of external electromagnetic radiation. The number of electrons per atom that participate in absorption of electromagnetic radiation is calculated according to the expressions (Shiles et al, 1980):

$$n_{eff}^{(k)}(\omega) = \frac{m_e}{\pi^2 e^2 N_{Avog}} \cdot \frac{M_A}{\rho} \cdot \int_0^\omega \omega' k(\omega')\, d\omega'\,, \tag{20}$$

$$n_{eff}^{(\varepsilon_2)}(\omega) = \frac{m_e}{2\pi^2 e^2 N_{Avog}} \cdot \frac{M_A}{\rho} \cdot \int_0^\omega \omega' \varepsilon_2(\omega')\, d\omega'\,, \tag{21}$$

$$n_{eff}^{(\mathrm{Im}(-1/\varepsilon))}(\omega) = \frac{m_e}{2\pi^2 e^2 N_{Avog}} \cdot \frac{M_A}{\rho} \cdot \int_0^\omega \omega' \,\mathrm{Im}\left(\frac{-1}{\varepsilon(\omega')}\right) d\omega'\,. \tag{22}$$

Relations (20)-(22) were obtained by a substitution of relation (18) for the plasma frequency into sum rule relations (15)-(17), and a rearrangement of the resulting expressions.

Please note the new notation. First of all one should not confuse parameters $n_{eff}^{(k,\varepsilon_2,\mathrm{Im}(-1/\varepsilon))}(\omega)$ in relations (20)-(22) with the index of refraction $n(\omega)$ met before. Parameters $n_{eff}^{(k,\varepsilon_2,\mathrm{Im}(-1/\varepsilon))}(\omega)$ in

relations (20)-(22) indicate the number of electrons per atom. Second, one should note the change in the limits of integrals appearing in relations (20)-(22). The integrals in relations (20)-(22) are taken from zero to a given angular frequency of external electromagnetic radiation.

Parameters $n_{eff}^{(k,\varepsilon_2,\mathrm{Im}(-1/\varepsilon))}(\omega)$ in relations (20)-(22) indicate the number of electrons per one atom of a given material that participate in absorption of external electromagnetic radiation angular frequency of which varies from zero to a given value ω. If the integrals in relations (20)-(22) are calculated from zero to infinity, then the total number of electrons per one atom of a given material will be obtained, and the number will be equal to Z, the atomic number of elements of the material in question.

Relations (20)-(22) can be written in terms of the energy of photons of external electromagnetic radiation instead of the angular frequency ω. If done so, the relations will retain their form, only the Planck constant $\hbar$ squared will appear in the denominator on the right hand side of relations (20)-(22). In fact, the majority of calculations performed in the current work were performed in terms of the energy of photons of electromagnetic radiation, and not the angular frequency of photons.

Relations (20)-(22) along with the sum rule relation (19) were used extensively during the analysis of the extinction coefficient of calcium, the recovered index of refraction of calcium, the dielectric functions, and the energy loss function of calcium.

An analysis of the extinction coefficient of calcium

The data compiled for the extinction coefficient of calcium, following the literature survey, using the Drude theory, or using the photoelectric cross sections, existed in a discrete format. In order to proceed with the work, it was necessary to derive a single set of data specifying the extinction coefficient of calcium. The initial set of data, specifying the extinction coefficient of calcium, was obtained by drawing a single curve using the other curves, specifying the coefficient, as a guide. The drawn curve coincided exactly with the curve for the coefficient obtained using the Drude theory. The drawn curve coincided exactly also with the curve for the coefficient calculated using the photoelectric cross sections. At intermediate energies the drawn curve was basically an eyeball estimate of the coefficient based on the data obtained from the literature.

An analysis, performed with the derived extinction coefficient of calcium, demonstrated that the coefficient was significantly underestimated. In particular, the number of electrons per calcium atom, calculated using the derived extinction coefficient, was significantly smaller then the expected number, twenty electrons per atom. Calculations were performed according to equation (20).

In order to fix the problem with the number of electrons per calcium atom, calculated using the extinction coefficient of calcium, the coefficient was increased by a given factor for energy losses smaller then 25 eV. The reason for such increase was the following. The optical and the dielectric properties of calcium were often determined by measurements performed with thin evaporated calcium films. If the density of evaporated calcium films were smaller than the density of bulk metallic calcium, then determined extinction coefficient of calcium would also be smaller. It was hypothesized that an increase of the extinction coefficient would compensate for the smaller density of evaporated films.

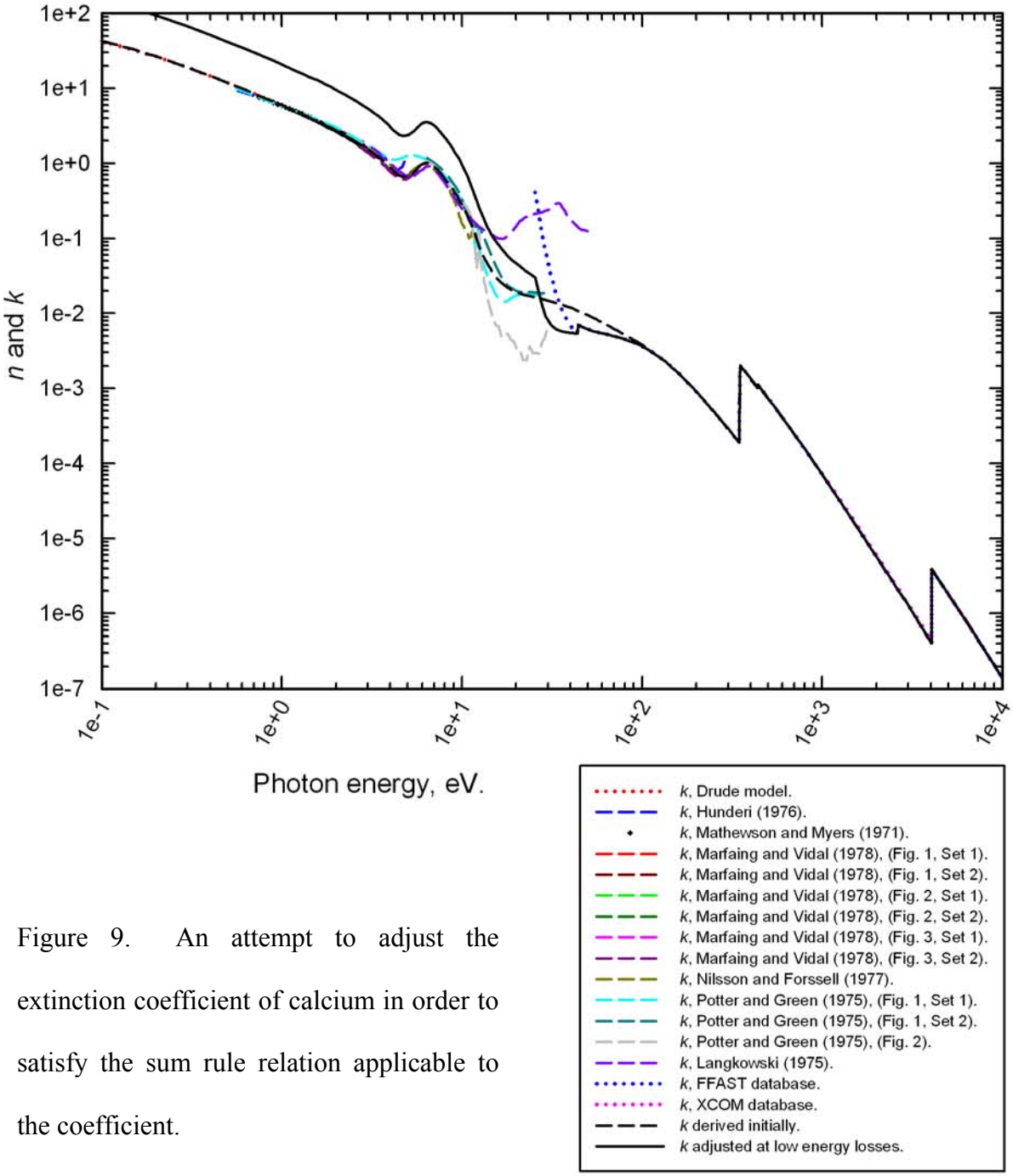

Figure 9. An attempt to adjust the extinction coefficient of calcium in order to satisfy the sum rule relation applicable to the coefficient.

The increase of the extinction coefficient of calcium for energy losses smaller then 25 eV did help to solve the problem with the number of electrons per calcium atom calculated using the coefficient. However, the attempt failed in other aspects. The analysis showed that the extinction coefficient of calcium had to be increased at least three and a half times for energy losses smaller then 25 eV to yield the correct number of electrons per calcium atom calculated using the coefficient. Such large factor, by which the coefficient had to be increased, seemed unrealistic. More importantly, the adjusted extinction coefficient of calcium could not be used in Kramers-Kronig calculations for a recovery of the index of refraction of calcium. The index of refraction of calcium, obtained by Kramers-Kronig calculations, turned negative at some energy losses, a completely unacceptable result.

It is worth mentioning here that the extinction coefficient of calcium could not be modified at energy losses larger then approximately 25 eV. The coefficient could not be modified because it was calculated specifically at the density of metallic calcium. The extinction coefficient of calcium was calculated using the photoelectric cross sections provided by the FFAST and the XCOM databases for energy losses larger then 25 eV. Both databases specified the exact density at which the cross sections were provided. The density, specified by the FFAST and the XCOM databases, was that of metallic calcium.

The extinction coefficient of calcium was adjusted only after an analysis of the distribution of electrons between individual electron shells in calcium atoms and individual electron bands in metallic calcium. The following section provides a detailed description of performed work.

An adjustment of the extinction coefficient of calcium to account for the M shell electrons

An analysis of the distribution of electrons between shells in calcium atoms and bands in metallic calcium clearly indicated that the extinction coefficient of calcium, prepared by drawing a single curve between all the curves representing the extinction coefficient of calcium, omitted electrons from the *p* state of the M shell. The analysis involved a calculation of the number of electrons that occupy individual electron shells in calcium atoms and electron bands in metallic calcium.

In order to account for missing electrons, an additional peak was introduced into the curve for the extinction coefficient of calcium. The peak was centered at 25 eV, the energy given by the FFAST database as the binding energy of electrons from the *3p* state of calcium atoms. The height and the width of the peak were adjusted to account for the correct number of electrons calculated per calcium atom.

Figure 10 shows the peak which was introduced into the curve for the extinction coefficient of calcium. As it is seen from the figure, the peak is located within the most questionable area for the extinction coefficient. According to the data by Potter and Green (1975) there is no indication for a peak at energy losses equal to about 25 eV. However, the peak merges well with the data obtained by Langkowski (1975), and also with the extinction coefficient of calcium calculated using the theoretical photoelectric cross sections provided by the FFAST database.

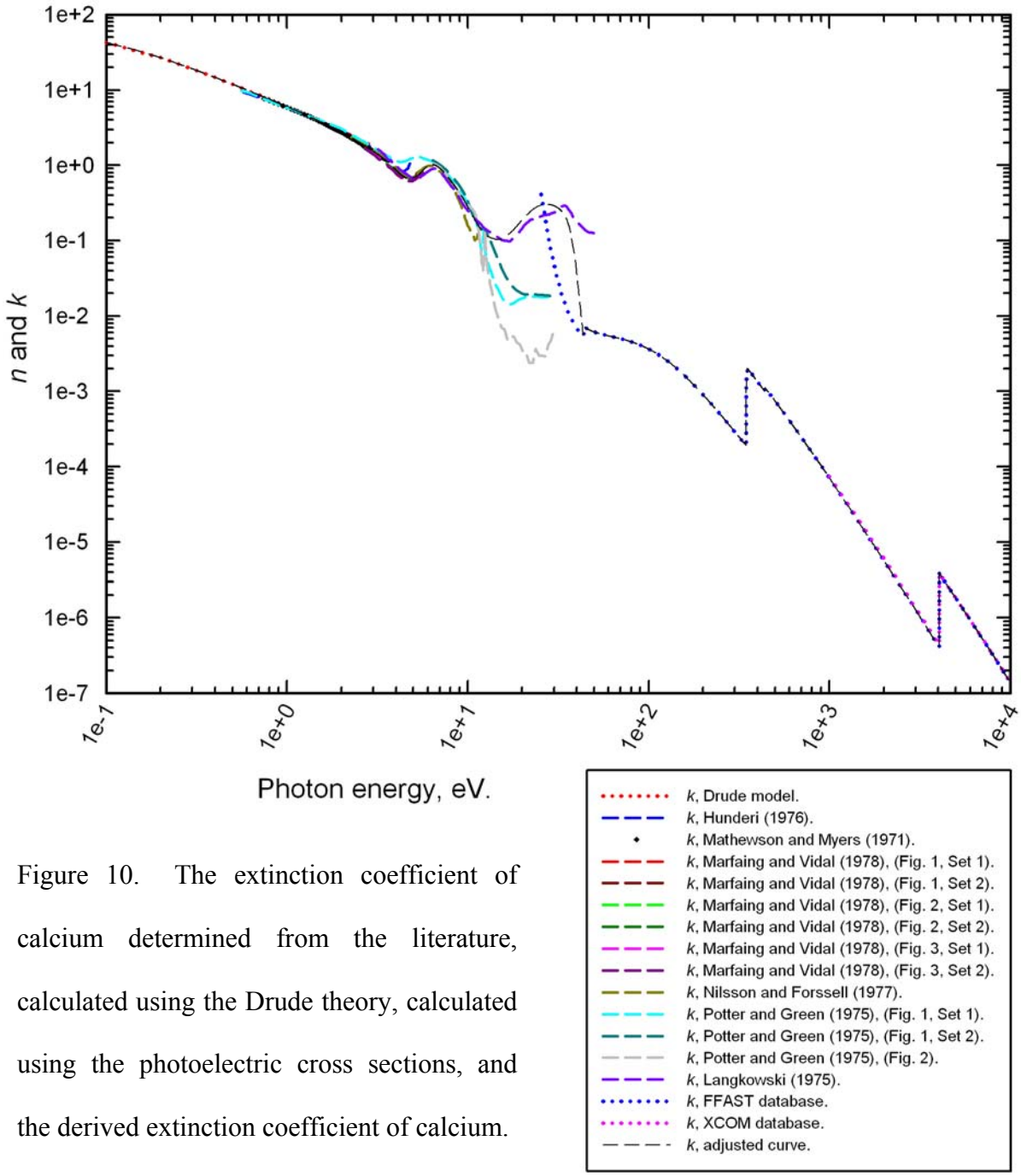

Figure 10. The extinction coefficient of calcium determined from the literature, calculated using the Drude theory, calculated using the photoelectric cross sections, and the derived extinction coefficient of calcium.

The extinction coefficient of calcium, which was adjusted in order to satisfy sum rule relation (15), is shown by the short dashed black curve in the figure.

The number of electrons per calcium atom, calculated using the extinction coefficient of calcium, is shown in figure 11. As it is seen in figure 11, more and more electrons in calcium atoms start to participate in absorption of external electromagnetic radiation as the energy of radiation increases until all twenty electrons per calcium atom become involved in absorption and dissipation of energy.

The curve for the number of electrons per calcium atom, calculated using the extinction coefficient of calcium, will be repeated in other figures shown later in the work. As it was shown before, the number of electrons per atom can be calculated using the extinction coefficient, the imaginary part of the dielectric response function, or the energy loss function of a given material. Calculations of the number of electrons per calcium atom were performed using all three functions for calcium once they were determined. Results of the calculations will be compared later in the work.

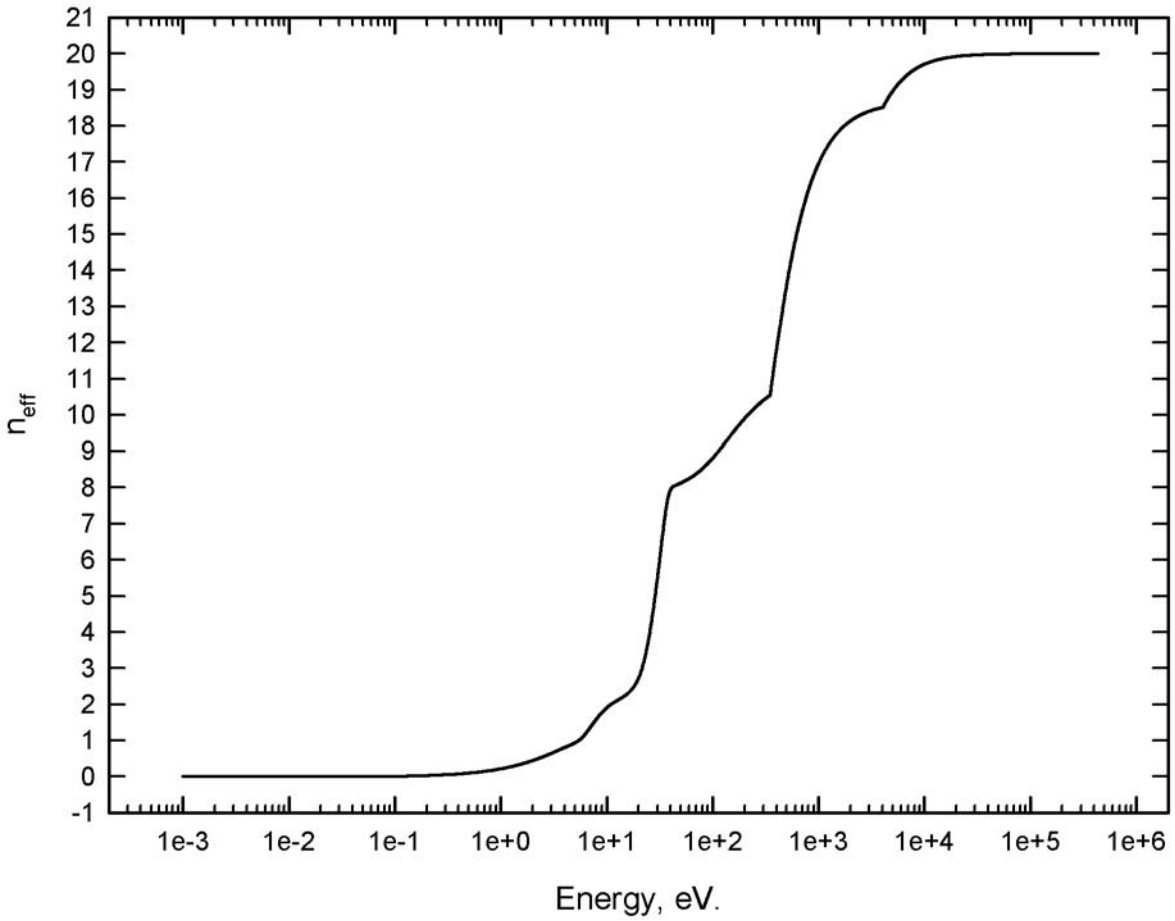

Figure 11. The number of electrons per calcium atom which participate in absorption of external electromagnetic radiation calculated using the extinction coefficient of calcium.

Recovery of the index of refraction of calcium

The index of refraction of calcium was recovered from the adjusted extinction coefficient of calcium by Kramers-Kronig calculations. Calculations were performed according to equation (11). Obtained index of refraction of calcium, and also the extinction coefficient of calcium are shown in figure 12. Figure 13 shows the recovered index of refraction of calcium, the adjusted extinction coefficient of calcium, and the optical functions determined from the literature, obtained using the Drude theory, or calculated using the photoelectric cross sections of calcium. A closer look at the index of refraction and the extinction coefficient of calcium is provided in figure 14. Figures 13 and 14 allow one to compare how close the index of refraction of calcium, recovered by Kramers-Kronig calculations, coincides with the index of refraction determined from the literature, or obtained using the Drude theory. The index of refraction of calcium, recovered by Kramers-Kronig calculations, is shown by a solid black curve in figures 12-14. The adjusted extinction coefficient of calcium is shown by a short dashed black curve in the figures.

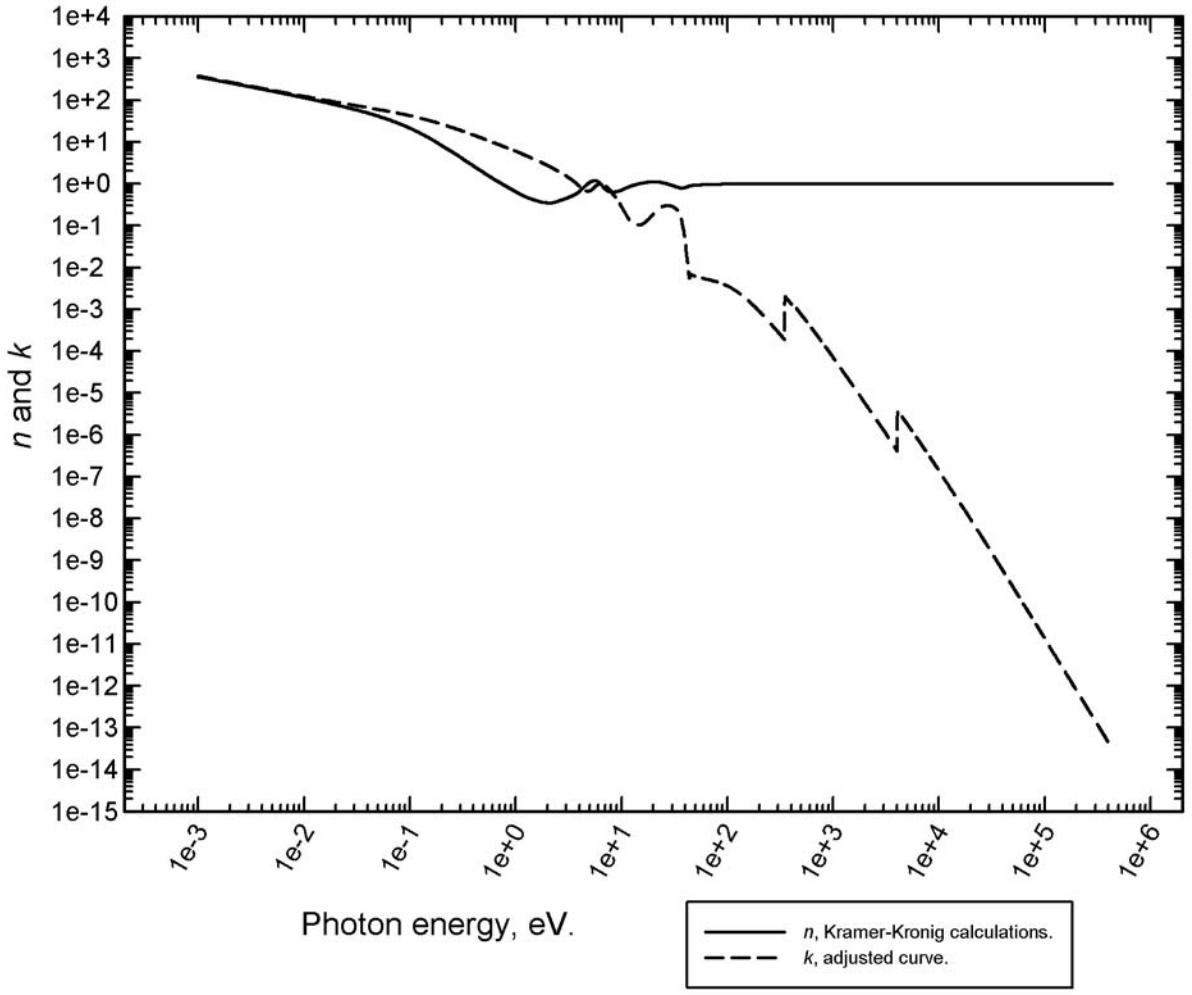

Figure 12. The extinction coefficient of calcium, adjusted in order to satisfy the sum rule relation for the coefficient, and the index of refraction of calcium obtained by Kramers-Kronig calculations.

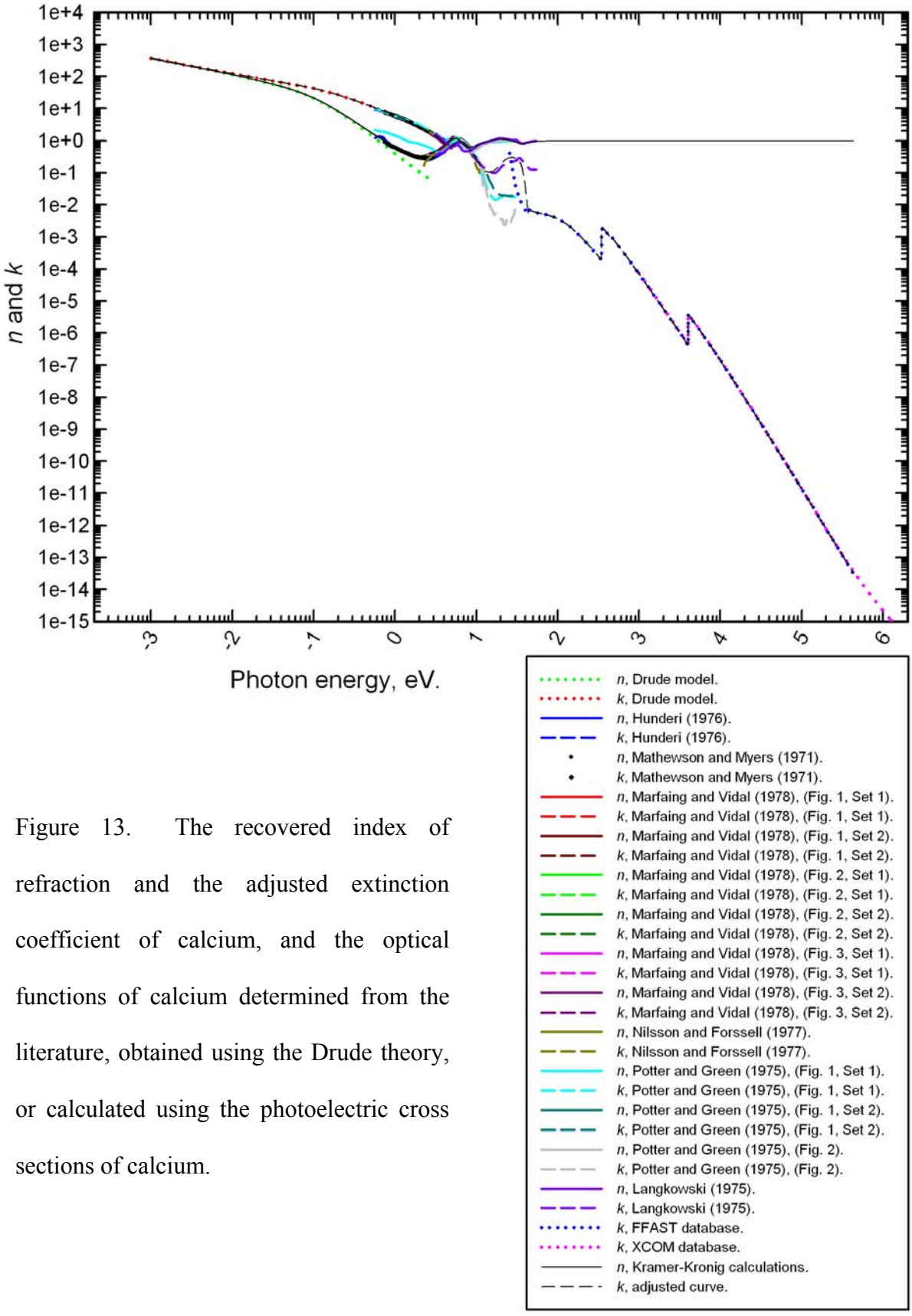

Figure 13. The recovered index of refraction and the adjusted extinction coefficient of calcium, and the optical functions of calcium determined from the literature, obtained using the Drude theory, or calculated using the photoelectric cross sections of calcium.

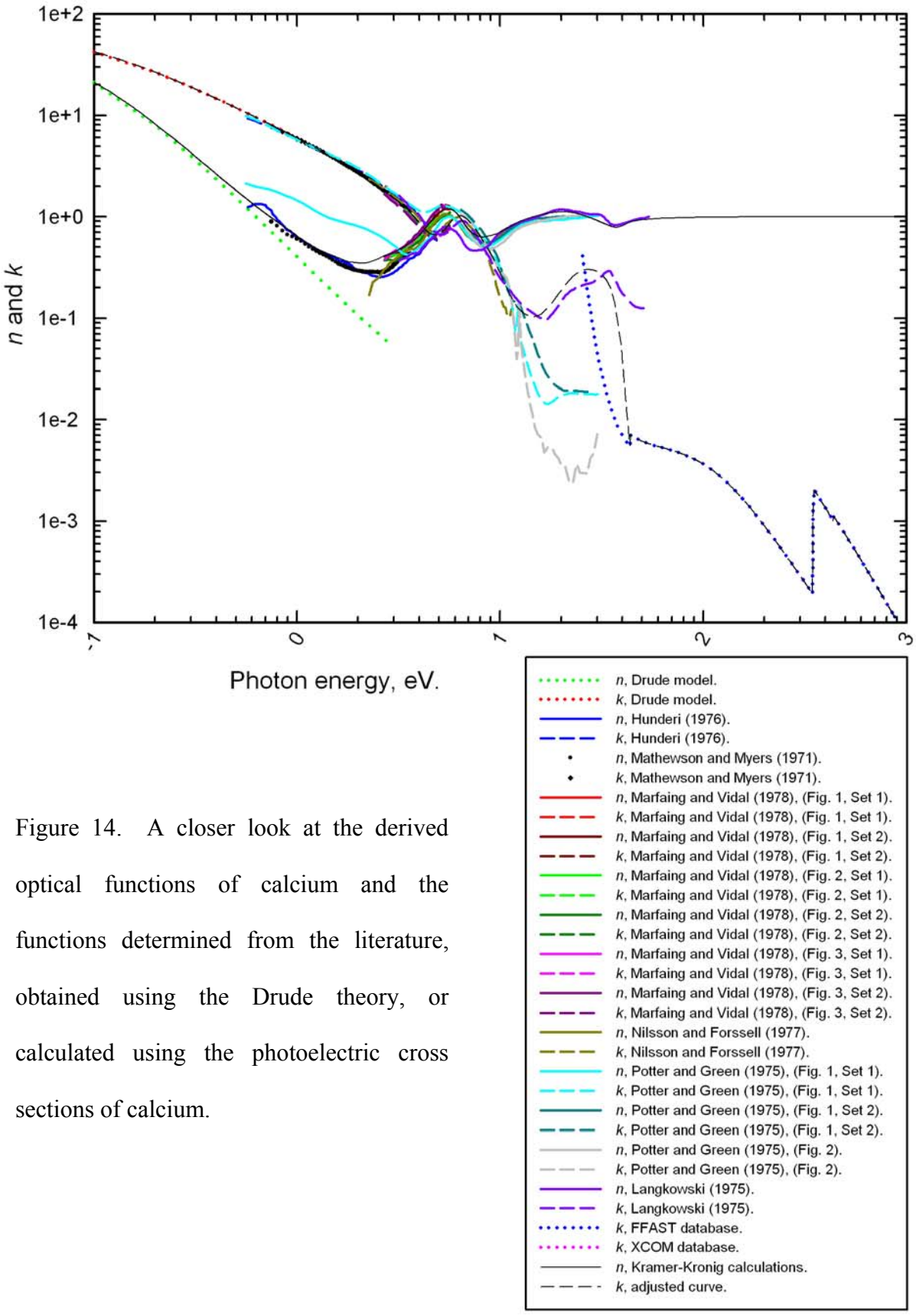

Figure 14. A closer look at the derived optical functions of calcium and the functions determined from the literature, obtained using the Drude theory, or calculated using the photoelectric cross sections of calcium.

A check of the recovered index of refraction of calcium

The accuracy of the index of refraction of calcium, recovered from the adjusted extinction coefficient of calcium by Kramers-Kronig calculations, was checked by a calculation of the sum rule relation applicable to the index. According to sum rule relation (19) an integral over expression $n(\omega)-1$ taken from zero to infinite angular frequency should yield zero if the index of refraction $n(\omega)$ is determined accurately.

A slightly modified version of sum rule relation (19) was used in calculations performed using the recovered index of refraction of calcium. The energy W of external electromagnetic radiation was used in place of the angular frequency ω in calculations of the sum rule relation applicable to the index of refraction. The switch from the angular frequency ω to the energy W of external electromagnetic radiation affected only the units in which the results of integration over $n(W)-1$ were expressed. Figure 15 shows the results of integration over expression $n(W)-1$ calculated from zero to a given energy of external electromagnetic radiation up to infinite energy.

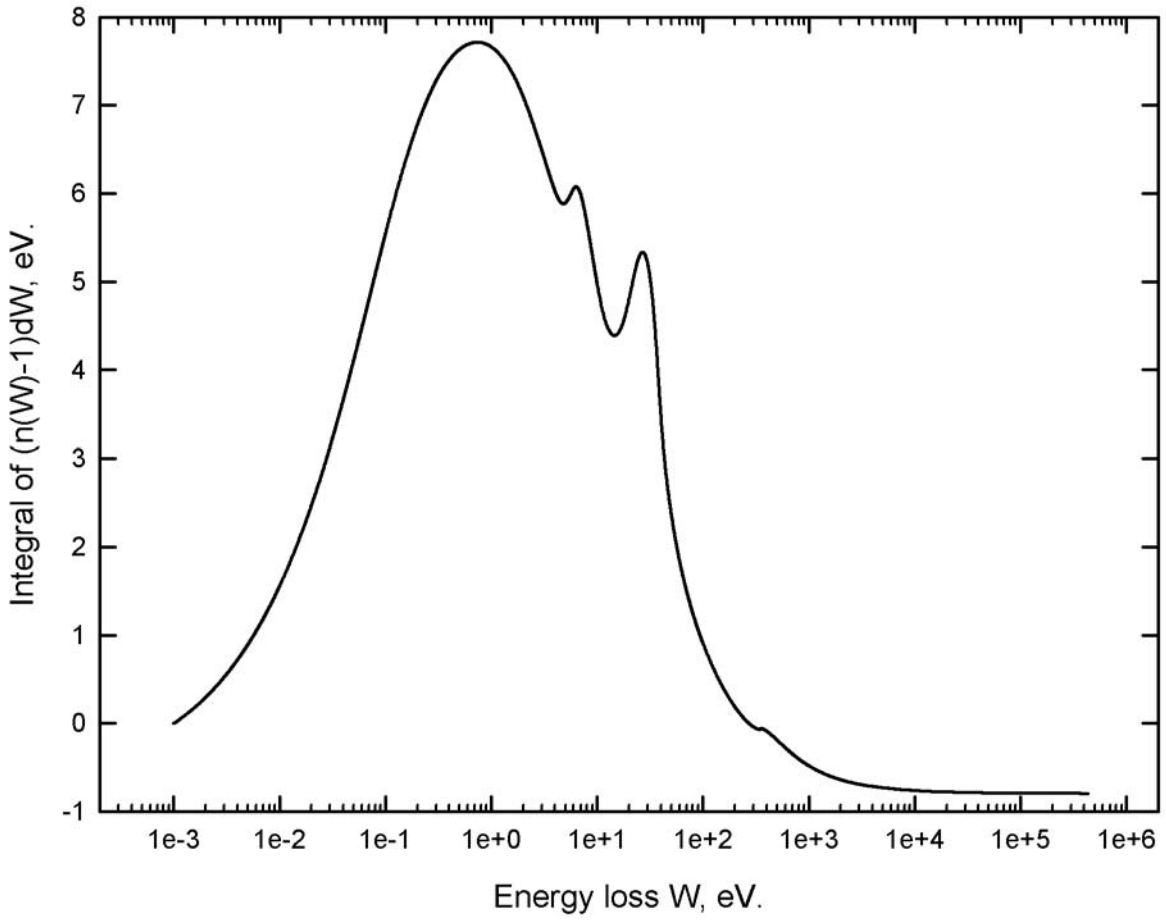

Figure 15. Result obtained for the sum rule relation calculated using the recovered index of refraction of calcium.

As it is seen in figure 15, an integral over expression $n(W)-1$ taken from zero to infinite energy of external electromagnetic radiation dropped below expected zero. The drop of the integral below zero indicated that the recovered index of refraction of calcium lacked some accuracy. In order to come up with a more accurate index of refraction of calcium it was necessary to return to the extinction coefficient of calcium, adjust the coefficient, check the sum rule relation for the coefficient, perform Kramers-Kronig calculations, and finally check the sum rule relation applicable to the index of refraction. Such work seemed not very productive. In addition there

was no guaranty that the optical functions, derived after all the iterative adjustments, would be any closer to the true optical functions of calcium. The work proceed with the derived optical functions of calcium regardless the fact that the sum rule relation, calculated for the index of refraction of calcium, yielded a result slightly different from the desired one.

The optical, the dielectric, and the energy loss functions of calcium

The real ε_1 and the imaginary ε_2 parts of the complex dielectric response function of calcium and also the energy loss function $\mathrm{Im}\left(-1/\varepsilon\right)$ of calcium were calculated in a trivial way once the index of refraction n and the extinction coefficient k of calcium were determined. The functions were calculated according to equations (3), (4), and (14). The optical, the dielectric, and the energy loss functions of calcium are shown in figure 16. The functions, shown in figure 16, were adopted for calcium. All further calculations performed for calcium were performed using the optical, the dielectric, and the energy loss functions shown in figure 16.

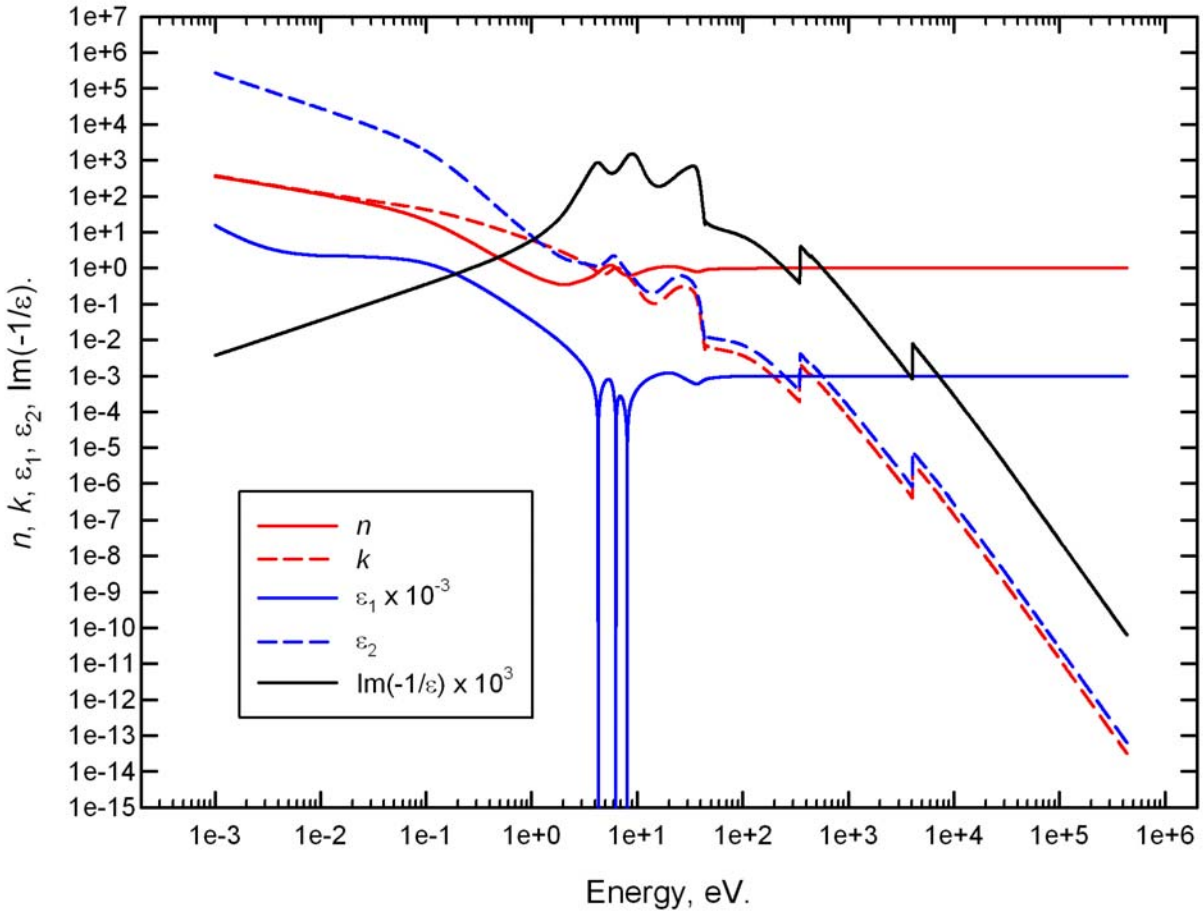

Figure 16. The optical, the dielectric, and the energy loss functions adopted for calcium.

Calculation of the number of electrons per calcium atom using k, ε_2, and $\mathrm{Im}(-1/\varepsilon)$ functions

The extinction coefficient k, the imaginary part of the complex dielectric response function ε_2, and the energy loss function $\mathrm{Im}(-1/\varepsilon)$ of calcium were used for a calculation of the number of electrons in calcium atoms that participate in absorption of external electromagnetic radiation. Calculations were performed for the three functions because it was interesting to see if the k, ε_2, and $\mathrm{Im}(-1/\varepsilon)$ functions will yield the same distribution of electrons between the *K*, *L*, and *M* shells of calcium atoms, and the bands of metallic calcium. It was also interesting to see if the total number of electrons, calculated per calcium atom, will be the same for all three functions of calcium. Calculations of the number of electrons per atom were performed according to equations (20)-(22).

The extinction coefficient k, the imaginary part of the complex dielectric response function ε_2, and the energy loss function $\mathrm{Im}(-1/\varepsilon)$ of calcium are shown in figure 17. The results of calculations of the number of electrons per calcium atom using the k, ε_2, and $\mathrm{Im}(-1/\varepsilon)$ functions of calcium are shown in figure 18.

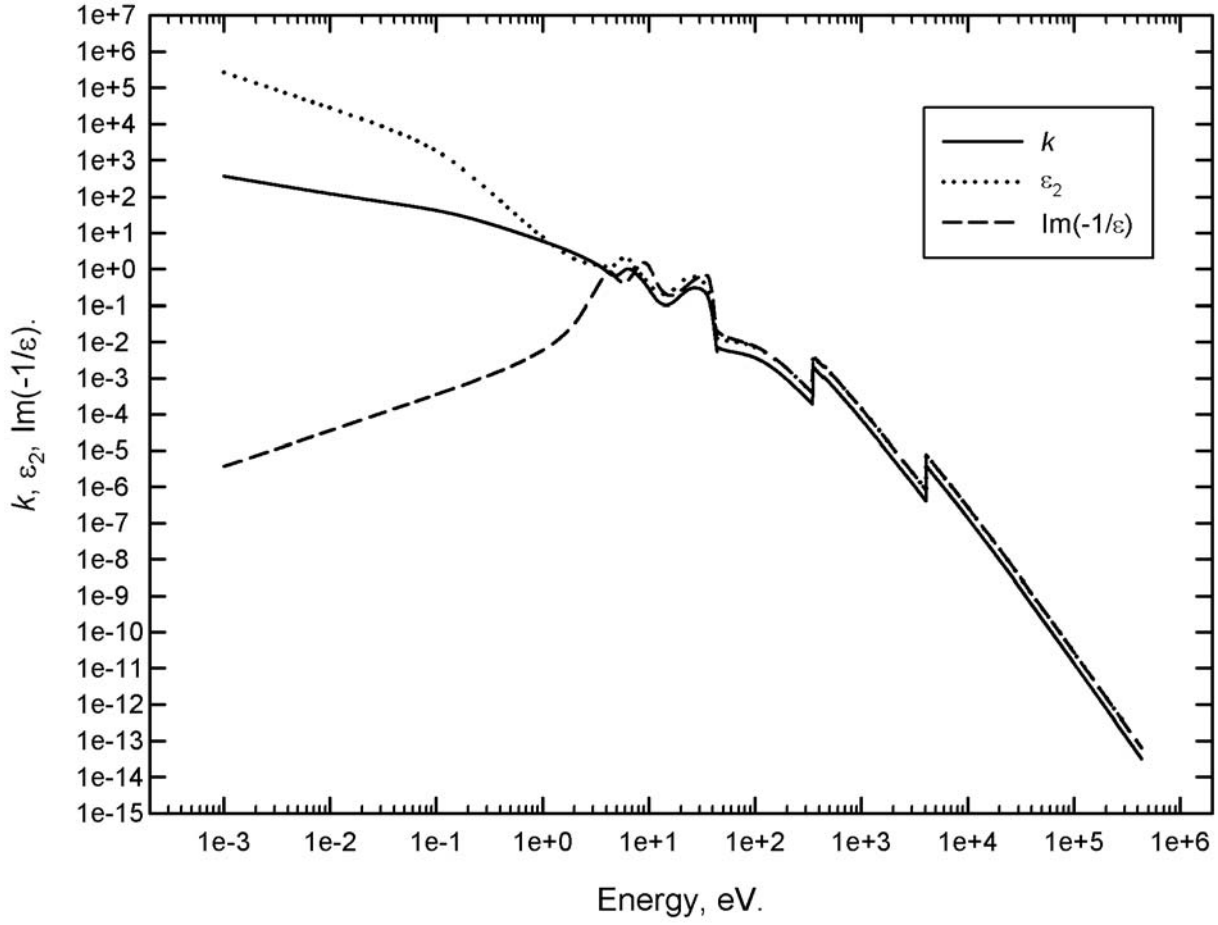

Figure 17. The extinction coefficient, the imaginary part of the complex dielectric response function, and the energy loss function of calcium.

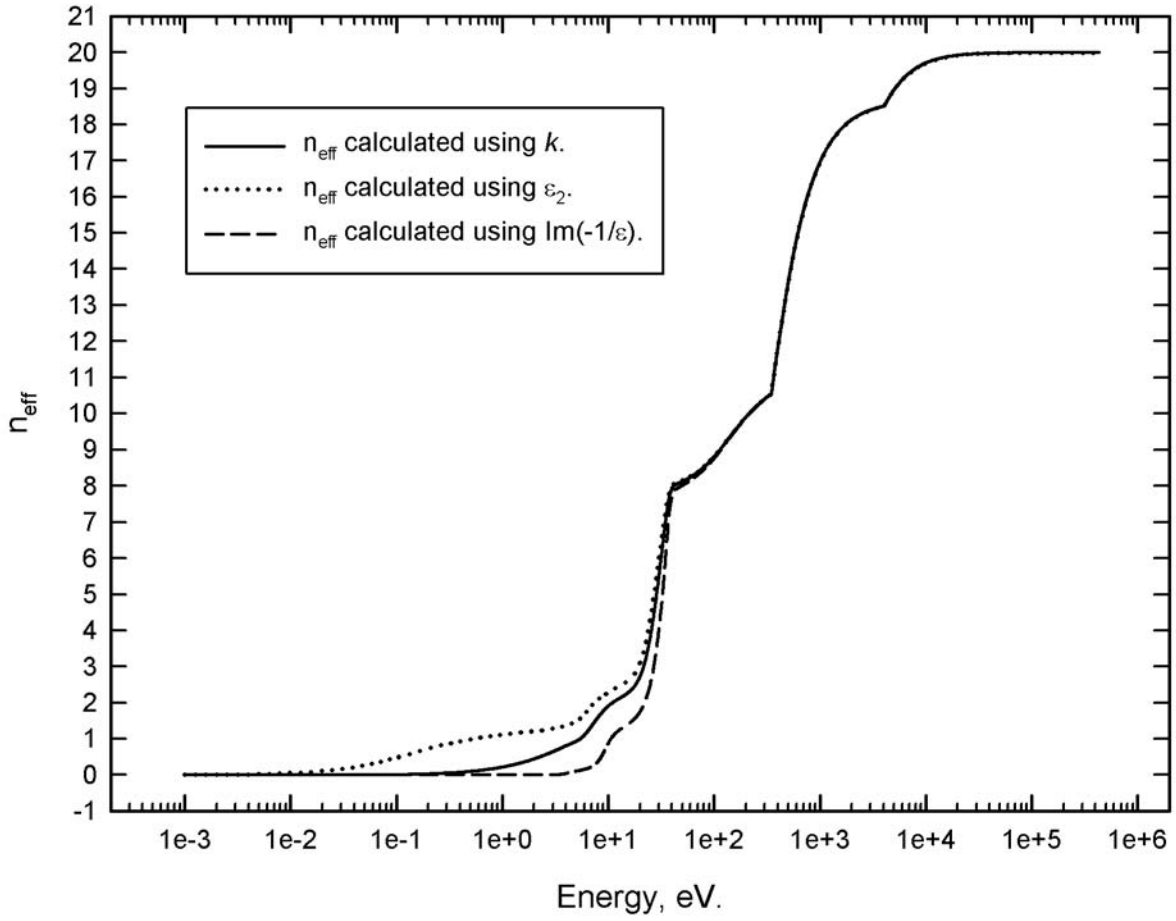

Figure 18. The number of electrons per calcium atom participating in absorption of external electromagnetic radiation.

Figure 18 shows three curves each of which represents the number of electrons per calcium atom calculated using the extinction coefficient k, the imaginary part ε_2 of the complex dielectric response function, and the energy loss function $\mathrm{Im}(-1/\varepsilon)$ adopted for calcium. One can see that the curves, shown in the figure, separate from each other in the limit of small energy losses, but merge together in the limit of large energy losses. It is possible that the curves for the number of electrons calculated per calcium atom separate from each other in the limit of small energy losses because the adopted k, ε_2, and $\mathrm{Im}(-1/\varepsilon)$ functions of calcium slightly differ from

the true k, ε_2, and $\mathrm{Im}(-1/\varepsilon)$ functions of calcium. At the same time, the adopted k, ε_2, and $\mathrm{Im}(-1/\varepsilon)$ functions of calcium are consistent and satisfy corresponding sum rule relations. That is why the adopted k, ε_2, and $\mathrm{Im}(-1/\varepsilon)$ functions yield exactly twenty electrons per calcium atom.

Calculation of the mean excitation energy of electrons in metallic calcium

The energy loss function of metallic calcium was used for a calculation of the mean excitation energy of electrons in calcium. In literature another very similar term, the mean ionization potential, can often be met. The preference is given to the mean excitation energy term in the current work. The preference is given to the mean excitation energy term because current work does not differentiate between ionization and excitation events which occur in metallic calcium following absorption of external electromagnetic radiation.

As the name suggests, the mean excitation energy has something to do with the mean energy required for an excitation of atomic electrons. Coupled with the density of electrons in a given material, the parameter can be used for a calculation of the stopping power of the material to energetic charged particles. In reverse, results of stopping power measurements can be used for a determination of the mean excitation energy (or the mean ionization potential) of electrons in a given material.

Because the mean excitation energy can be calculated theoretically and also can be determined from results of stopping power measurements, the parameter can be considered as a bridge between theory and experiment. The parameter can be used, for example, for testing the

accuracy of theories used for a description of the loss of energy by energetic charged particles passing through a given material.

The mean excitation energy I of electrons in metallic calcium was calculated according to equation (Shiles et al, 1980):

$$\ln(I) = \frac{\int_0^\infty \omega \ln(\hbar\omega)\,\mathrm{Im}\left(\frac{-1}{\varepsilon}\right) d\omega}{\int_0^\infty \omega\,\mathrm{Im}\left(\frac{-1}{\varepsilon}\right) d\omega}, \tag{23}$$

where $\mathrm{Im}(-1/\varepsilon)$ is the energy loss function of the material, and $\hbar$ is the reduced Planck constant.

The mean excitation energy of electrons in calcium was found equal to 172 eV. The found value is somewhat smaller then the suggested value of 191±8 eV (ICRU report 37).

Calculating the mean excitation energy, the integrals in relation (23) need to be calculated from zero to infinite angular frequency or energy. However, as with the sum rule relations encountered before, integrals in relation (23) can be calculated from zero to a given angular frequency or energy yielding the mean excitation energy of electrons that participate in absorption of external electromagnetic radiation the frequency or the energy of which changes from zero up to a given value. Figure 19 shows the variation of the mean excitation energy of electrons in metallic calcium as a function of the energy of external electromagnetic radiation. In the limit of large energy losses, the curve in figure 19 reaches 172 eV, the found mean excitation energy of electrons in metallic calcium.

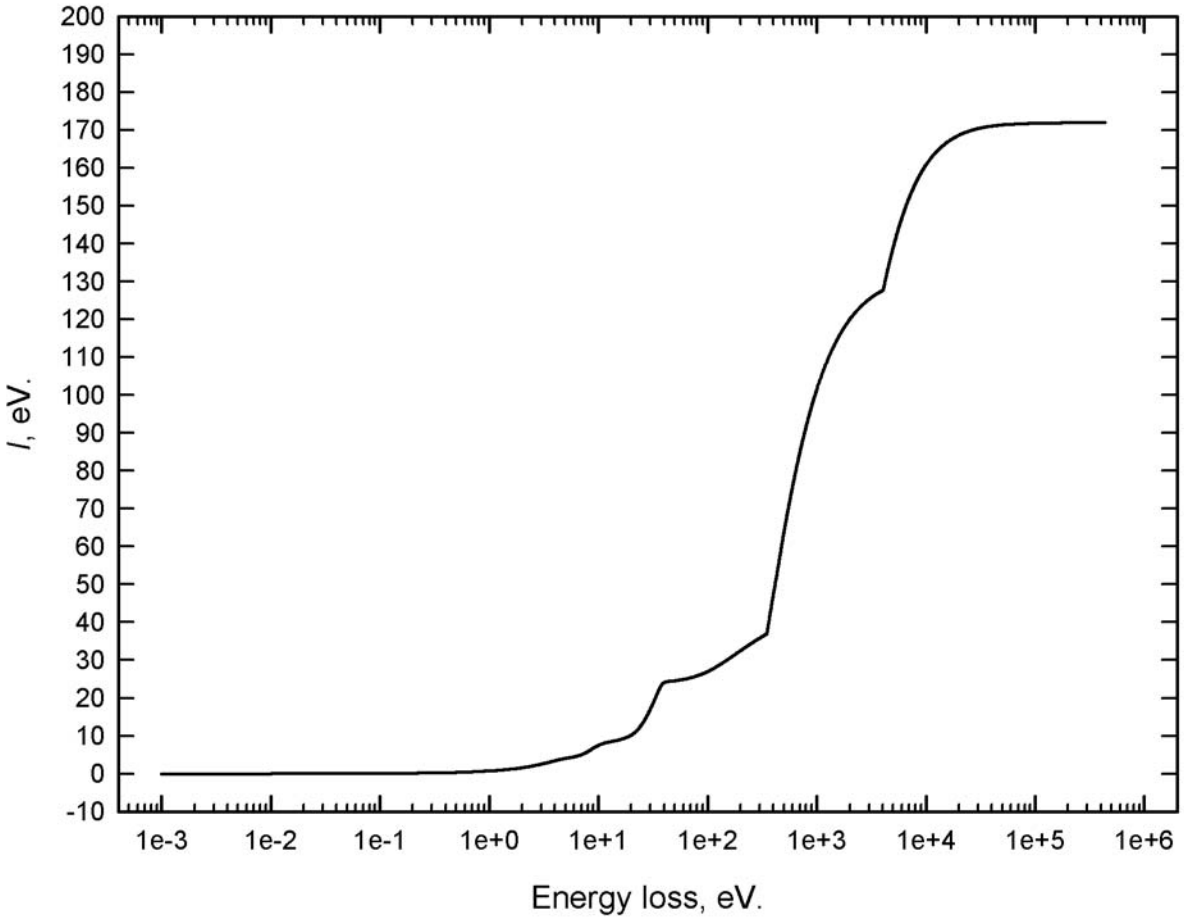

Figure 19. Variation of the mean excitation energy of electrons in metallic calcium as a function of the energy of external electromagnetic radiation.

Determination of contributions of electron shells and electron bands to the energy loss function of calcium

The energy loss function of metallic calcium was shown in figures 16 and 17. The function, shown in figures 16 and 17, is the total energy loss function arising due to all electrons of calcium. The work, however, required knowledge of the energy loss functions arising due to electrons from individual electron shells of atoms of calcium and individual electron bands of metallic calcium. Contributions of electrons from individual shells and individual bands of calcium to the energy loss function of calcium were determined in a graphical way. Please take a look at figures 20 and 21. It is believed that an examination of the figures prior to reading the following description will help with understanding of the approach used for a determination of contributions of electrons shells of atoms of calcium and electron bands of metallic calcium to the energy loss function of calcium.

Electrons of calcium were formally divided between six groups. The groups included electrons from the *K* shell of calcium atoms, electrons from the *L* shell of calcium atoms, electrons from the *s* state of the *M* shell of calcium atoms, electrons from the *p* state of the *M* shell of calcium atoms, electrons responsible for the peak in the energy loss function of calcium centered at about 9 eV, and finally electrons responsible for the peak in the energy loss function of calcium centered at about 4 eV.

The following procedure was performed for a determination of contributions of individual electron shells of calcium atoms and electrons bands of metallic calcium to the energy loss function of calcium. Each peak, seen in the graph of the energy loss function of calcium, was extrapolated to infinite energy losses. The slopes, with which the graphs were extrapolated, were based on the slopes of the original energy loss function of calcium. Figure 20 shows how the

peaks, seen in the graph of the energy loss function of calcium, were extrapolated. Contributions of electrons from the individual shells of atoms of calcium and the bands of metallic calcium to the energy loss function of calcium were determined by a subsequent subtraction of the extrapolated curves. Determined contributions were taken as the energy loss functions arising due to electrons from the given electron shells and the given electron bands of calcium. Figure 21 shows the determined energy loss functions.

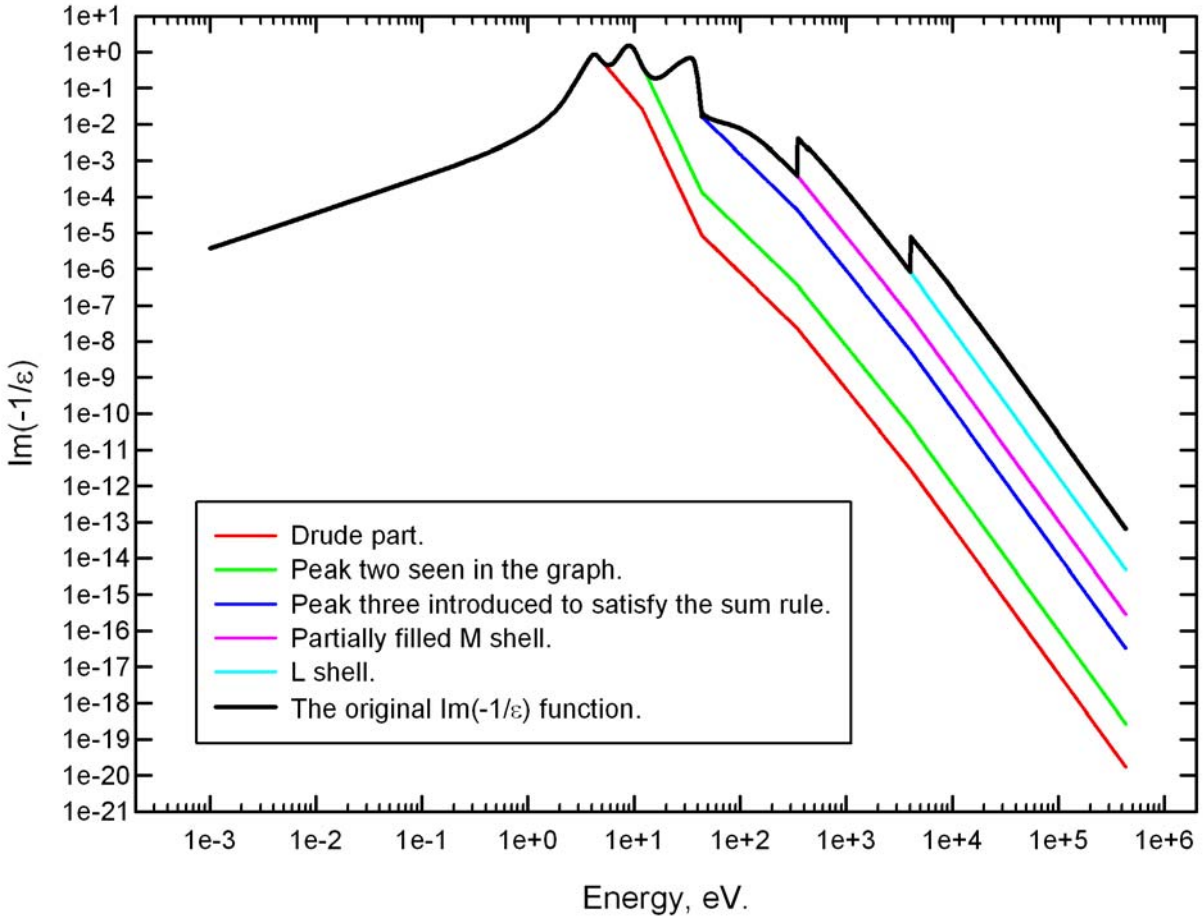

Figure 20. An extrapolation of the peaks, seen in the graph of the energy loss function of calcium, to infinite energy losses.

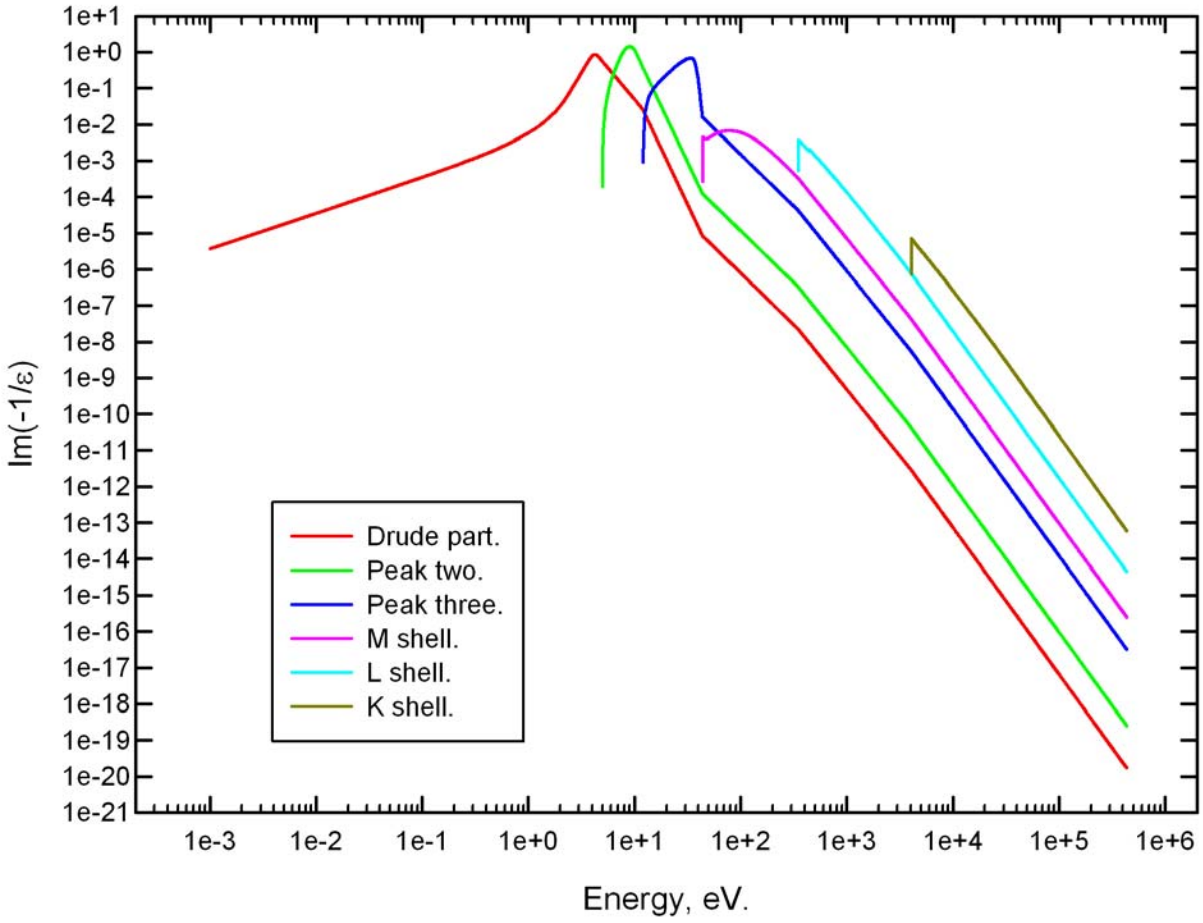

Figure 21. The energy loss functions arising due to electrons from the individual shells and the individual bands of calcium.

Calculation of oscillator strengths and mean excitation energies of electrons from the individual shells and bands of calcium

Speaking of the number of electrons in an atomic state, one expects the number to be an integer one. The number of electrons in an atomic state will be integer only in the case of a completely isolated atom. In the case of a condensed matter, i.e. an aggregation of atoms, electrons in atoms of the matter distribute in some way between different states, and their number in any particular state can be any real number. A special term is used in the condensed matter physics for a specification of the number of electrons in a state. The term is the oscillator strength.

The terminology used so far had the goal to provide a simple and clear definition of used parameters. The number of electrons in an atom is probably much more understandable concept rather then the oscillator strength of an atom, even though the two terms are equivalent in their meaning. In order to comply with the terminology used in the condensed matter physics and also in the atomic collision physics, the new term, the oscillator strength, will be used from this point onward for a specification of the number of electrons in an atomic state.

The energy loss functions, arising due to electrons from the shells and the bands of calcium, were used for a calculation of oscillator strengths of electrons from the shells and the bands. Calculations of the oscillator strengths were performed according to already familiar equation (22).

In order to examine the variation of the oscillator strengths as a function of the energy loss, the upper limit of integral relation (22) was varied from zero to infinity. The lower limit of the relation was always kept equal to zero in calculations. Figure 22 shows results of calculations of

oscillator strengths of electrons from the different shells and bands of calcium. The figure shows results for all six electron groups defined for calcium.

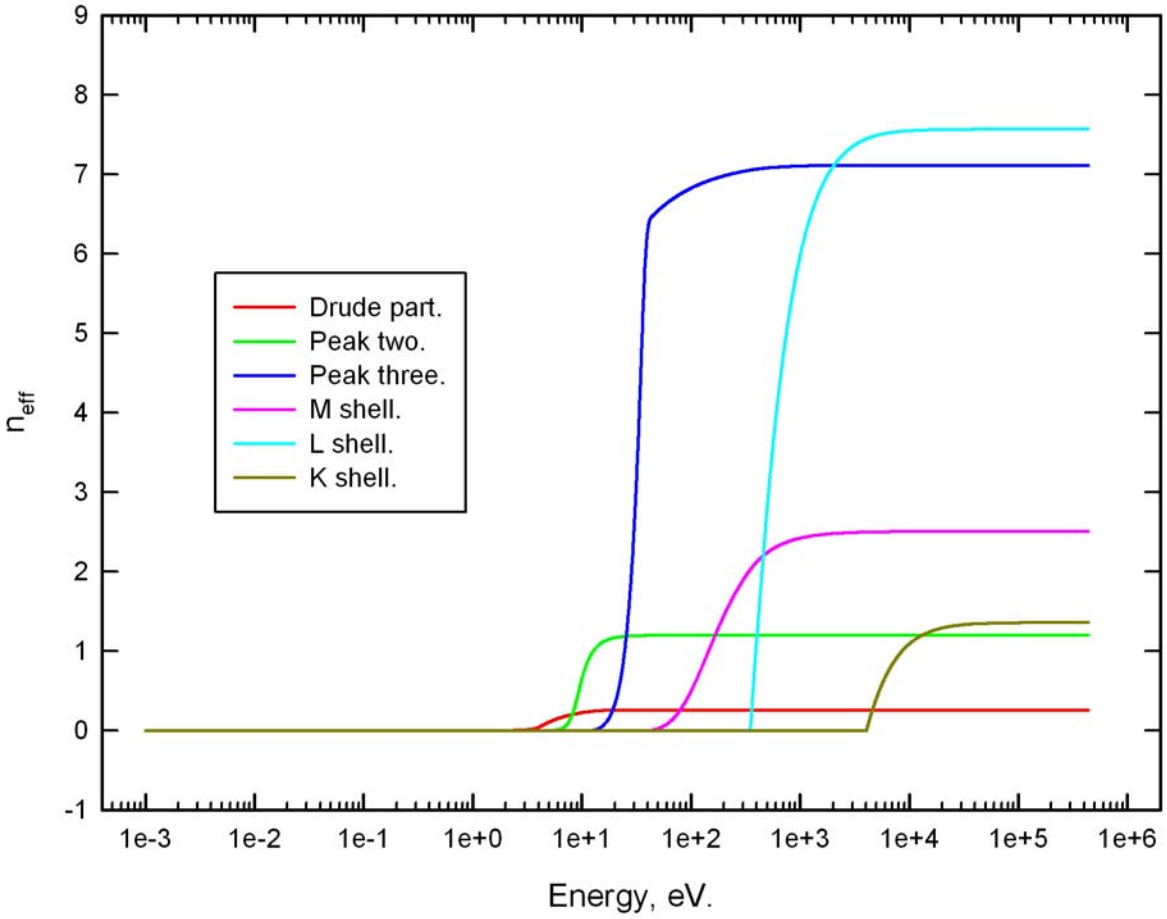

Figure 22. The oscillator strengths of electrons from the shells and the bands of calcium calculated using the individual energy loss functions of calcium.

The energy loss functions, arising due to electrons from the individual electron shells and bands of calcium, were also used for a calculation of partial mean excitation energies of electrons from the shells and the bands. Word "partial" is introduced here to differentiate mean excitation energy of electrons from a particular shell or band of calcium from the mean excitation energy of electrons from the whole atom of calcium. Calculations of the partial mean excitation energies were performed according to equation (23).

The variation of partial mean excitation energies of electrons in calcium atoms as a function of the energy loss was studied by varying the upper limit of integral relation (23) from zero to a given value. The lower limit of integral relation (23) was always kept equal to zero. The variation of the partial mean excitation energies of electrons in calcium atoms as a function of the energy loss is shown in figure 23.

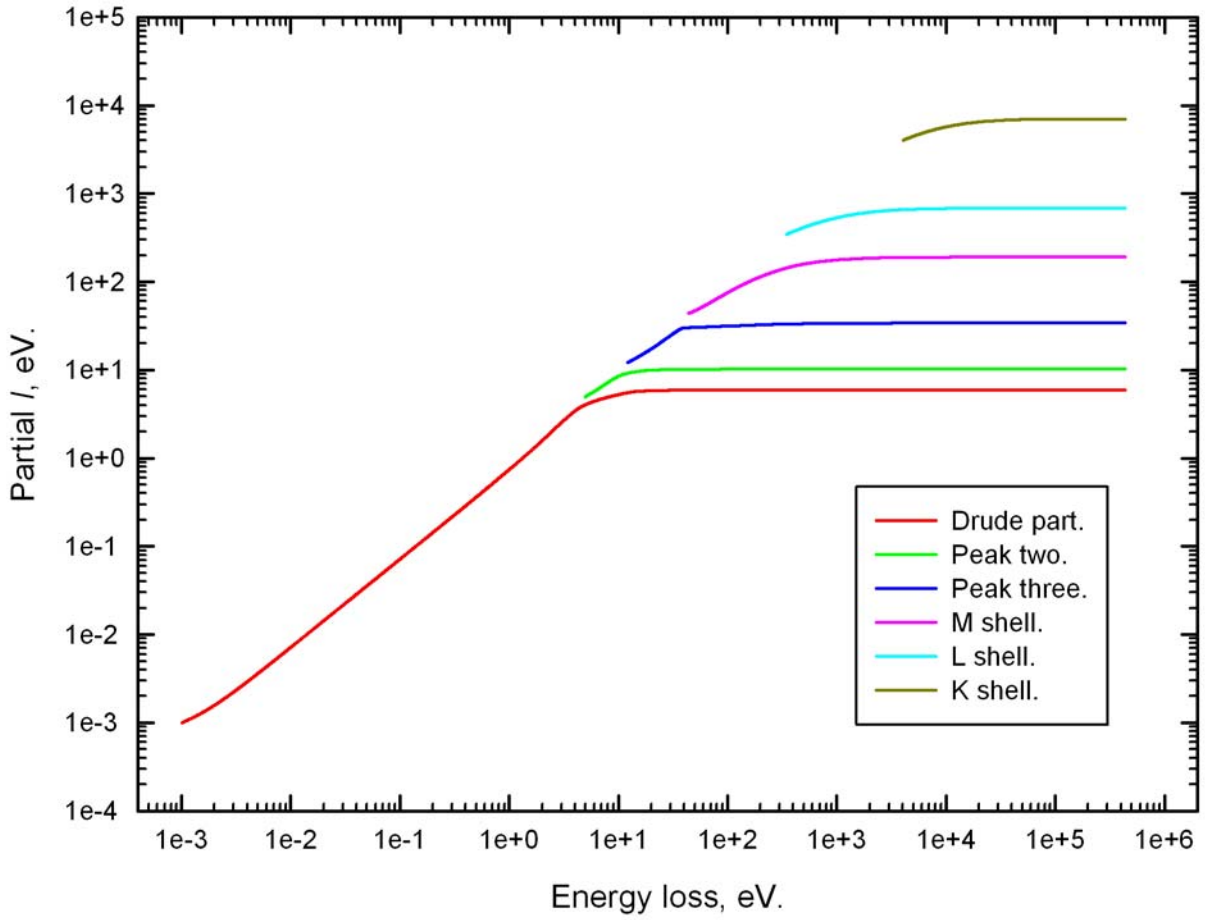

Figure 23. The partial mean excitation energies of electrons from the different shells and bands of calcium calculated using the individual energy loss functions of calcium.

Calculated oscillator strengths and partial mean excitation energies of electrons from the different shells and bands of calcium are summarized in table 1.

Electron group	**Oscillator strength**	**Partial mean excitation energy, eV**
Peak at 4 eV of $\mathrm{Im}(-1/\varepsilon)$	0.26	5.92
Peak at 9 eV of $\mathrm{Im}(-1/\varepsilon)$	1.20	10.29
p state of the *M* shell	7.11	34
s state of the *M* shell	2.50	191
The *L* shell	7.57	684
The *K* shell	1.36	7050

Table 1. The oscillator strengths and the partial mean excitation energies of electrons from the shells of atoms of calcium and the bands of metallic calcium.

The oscillator strengths and the mean excitation energies of electrons from the shells and the bands of calcium were used for modeling the generalized oscillator strength function of calcium. A discussion of how the generalized oscillator strength function of calcium was modeled is provided in the following several sections of the manuscript.

An introduction to the generalized oscillator strength function

The generalized oscillator strength (GOS) function describes the ability of a material to absorb and dissipate energy. The function, however, provides very little or no information at all about the processes which occur in the target material following absorption of energy. Neither the function provides any information about the kinetic energy or the angle at which secondary electrons are ejected from atoms of a given target material in the case of ionizations. Despite the fact that the generalized oscillator strength function yields very little information about the processes which occur in a target material following absorption of energy by the material, the function finds many uses. In particular, the generalized oscillator strength function is used in calculations of interaction cross sections of charged particles with electrons of atoms of a given target material. That is why one of the goals of the current work was a derivation of the generalized oscillator strength function of calcium. The function was used for a calculation of interaction cross sections of electrons, protons, and alpha particles with calcium.

The generalized oscillator strength function is dependent on two variables: the energy loss and, depending on methodology, the scattering angle, the momentum transfer, or the recoil energy. The three variables, the scattering angle, the momentum transfer, and the recoil energy, are directly related to each other as it will be shown in the next section of the manuscript. The choice between the three variables is dictated mostly by the adopted methodology. In current work the generalized oscillator strength function is considered as a function of the energy loss and the recoil energy.

Kinematics of inelastic collisions

Consider a particle initial momentum and kinetic energy of which are $\overline{p}$ and E_K. The rest energy of the particle is $E_0 = M_0 c^2$. The particle experiences an inelastic collision. The momentum and the kinetic energy of the particle after the collision are $\overline{p}'$ and E_K'. The energy lost by the particle in the collision is $W = E_K - E_K'$. The particle deviates by angle θ from its initial direction of motion.

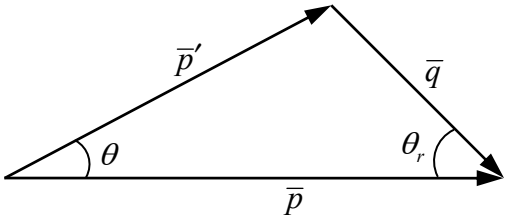

Figure 24. A schematic representation of an inelastic collision.

The deviation of the particle from its initial direction of motion can be described by the scattering angle θ, the momentum transfer $\overline{q} = \overline{p} - \overline{p}'$, or the recoil energy Q which is defined below.

According to the relativistic mechanics the following relations hold for p and E_K, and p' and E_K':

$$(cp)^2 = E_K\left(E_K + 2E_0\right), \tag{24}$$

$$(cp')^2 = E_K'\left(E_K' + 2E_0\right), \tag{25}$$

where p and p' are the absolute values of vectors $\overline{p}$ and $\overline{p}'$.

The magnitude of the momentum transfer is found according to equation:

$$(cq)^2 = c^2\left(p^2 + p'^2 - 2pp'\cos\theta\right), \tag{26}$$

where θ is the scattering angle.

The recoil energy Q is introduced in an analogy to equations (24), (25), and (26):

$$(cq)^2 = Q(Q + 2E_0). \tag{27}$$

From equations (26) and (27) it should be clear that the scattering angle θ, the momentum transfer q, and the recoil energy Q are directly related to each other, and basically describe the same event in the scattering history of an incident particle. The choice between the three parameters, θ, q, or Q, is made depending on the methodology which is used for a description of inelastic collisions. Current work uses the recoil energy Q for a description of the deviation of an incident particle from its initial direction of motion following an inelastic collision. Similarly many other parameters, used or derived in the current work, are expressed in terms of the recoil energy Q. For example, the generalized oscillator strength function of calcium was modeled in terms of the energy loss W and the recoil energy Q. Interaction cross sections of electrons, protons, or alpha particles with calcium were calculated in terms of the energy loss W and the recoil energy Q.

Please note angle θ_r depicted in figure 24. Angle θ_r is called the recoil angle. Angle θ_r will be met again in calculations of the energy loss and recoil energy differential interaction cross sections arising due to the transverse interactions between an incident particle and atomic electrons.

Modeling of the generalized oscillator strength function of calcium

using the Dirac's delta functions

The initial method, used for modeling the generalized oscillator strength function of calcium, relied on the Dirac's delta functions. The method was similar to the one described by Liljequist (1983).

The Dirac's delta function $\delta(x-a)$, where x is the variable and a is a constant, is an abstract mathematical function equal to zero everywhere except point a, called pole, at which the function is infinite. An integral over the pole of a delta function equals to one:

$$\int_{a-\tau}^{a+\tau} \delta(x-a)\,dx = 1, \tag{28}$$

where $\tau > 0$.

Modeling of the generalized oscillator strength function of a material using the Dirac's delta functions is based on the following three assumptions.

a) Collisions of incident particles with atomic electrons are considered as binary encounter collisions when energy, lost by incident particles in individual collisions, is larger then the mean excitation energy of electrons from a given atomic shell or electron band.
b) When the energy loss, experienced by an incident particle, equals to the mean excitation energy of electrons from a given atomic shell or electron band all electrons from the shell or the band participate in absorption of energy. Collective absorption of energy results in stochastic values of the recoil energy. In such collisions the recoil energy can take any value from zero to the maximal energy loss which can be experienced by a given incident particle.
c) At energy losses less then the mean excitation energy of electrons from a given atomic shell or electron band no transfer of energy from an incident particle to atomic electrons occurs.

Mathematically the generalized oscillator strength function, modeled with the Dirac's delta functions, is written as (Liljequist, 1983, Liljequist, 1985):

$$\frac{df(Q,W)}{dW} = \sum_i f_i \frac{dg_i(Q,W)}{dW}, \tag{29}$$

where

$$\frac{dg_i(Q,W)}{dW} = \begin{cases} \delta(W - W_i) & Q < W_i \\ \delta(W - Q) & Q > W_i. \end{cases} \tag{30}$$

Parameters f_i and W_i in equations (29) and (30) are the oscillator strengths and the partial mean excitation energies of electrons from atomic shells or electron bands of a given target material.

Figure 25 shows the generalized oscillator strength function of calcium modeled using the Dirac's delta functions. The black lines, shown in the figure, represent the Dirac's delta functions. The green surfaces are projections of the black lines on the energy loss and recoil energy plane. The elevation of the black lines above the energy loss and recoil energy plane corresponds to the oscillator strength of electrons from a given atomic shell or electron band of calcium.

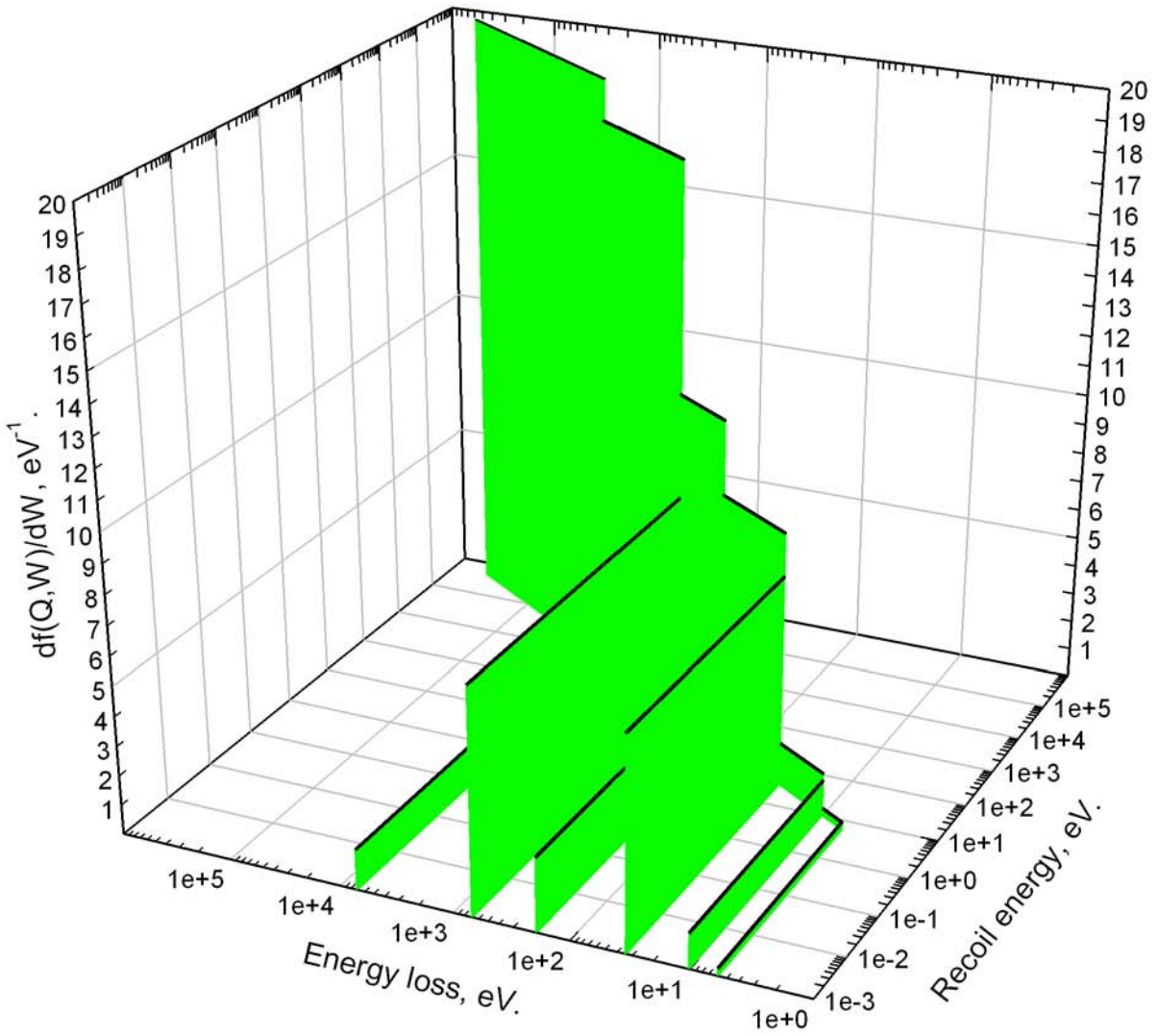

Figure 25. The generalized oscillator strength function of calcium modeled with the Dirac's delta functions.

A representation of the generalized oscillator strength function by means of the Dirac's delta functions is acceptable only for a description of isolated atoms or simple molecules. In the case of complex molecules or condensed matter the representation becomes less and less accurate. The representation fails in description of energy losses less then the mean excitation energy of electrons from given atomic shells or electron bands. The representation also fails in description

of variations in the recoil energy when incident particles experience a given energy loss. In order to create a more realistic model for the generalized oscillator strength function of calcium, the Dirac's delta functions were substituted by Gaussian functions.

Modeling of the generalized oscillator strength function of calcium using Gaussian functions

The Dirac's delta functions are suitable for modeling the generalized oscillator strength function of isolated atoms or isolated simple molecules. Isolated atoms and simple molecules often exhibit sharp energy absorption or energy emission lines characteristic to the atoms or the molecules. The Dirac's delta functions turn very suitable for a description of such sharp energy absorption or emission lines.

In the case of complex molecules and especially in the case of condensed matter energy absorption and energy emission lines, characteristic of atoms making the molecules or the matter, broaden. Broadening of the lines happens because of a degeneration of electronic states of atoms making the molecules or the matter. The larger broadening of the lines, the less the Dirac's delta functions become suitable for a description of the lines.

Current work considered metallic calcium. Metallic calcium is an example of a complex condensed phase material. It was expected that an aggregation of atoms of calcium in the metallic phase would alter the states of electrons in atoms of calcium, and would lead to broadening of energy absorption or emission lines of calcium. It seamed that functions other then the Dirac's delta functions had to be used for an accurate description of the energy absorption properties of metallic calcium. Gaussian functions were chosen in place of the Dirac's delta functions for a description of the energy absorption properties of metallic calcium.

In order to improve the model for the generalized oscillator strength function of calcium, the Dirac's delta functions, used in the model, were replaced by Gaussian functions. Gaussian functions allowed to "spread" the Dirac's delta functions over the energy loss and recoil energy plane. The new model for the generalized oscillator strength function of calcium permitted description of energy losses less then the mean excitation energy of electrons from given shells in calcium atoms and bands in metallic calcium. The new model also permitted description of stochastic variations in the recoil energy when incident particles experience given energy losses.

Gaussian functions are defined according to equation:

$$f\left(x\right) = ae^{-\frac{(x-b)^2}{2c^2}}, \tag{31}$$

where x is the variable, a, b, and c are constants, and e is the base of the natural logarithm. Constants a, b, and c have the following meaning. Constant a determines the magnitude or the height of a Gaussian function. Constant b determines the position of the function along the x axis. Constant c determines the width of the function. In probability theory and in statistics constant c is known as the variance.

Current work considered normalized Gaussian functions for which:

$$\int_{-\infty}^{+\infty} ae^{-\frac{(x-b)^2}{2c^2}} dx \equiv 1. \tag{32}$$

Condition (32) is satisfied only when constants a and c are related to each other as:

$$a = \frac{1}{c\sqrt{2\pi}}. \tag{33}$$

Gaussian functions were used in place of the Dirac's delta functions for modeling the generalized oscillator strength function of calcium. Gaussian functions were centered at the same energies as

the Dirac's delta functions. Gaussian functions were centered at the partial mean excitation energy of electrons from a given group when the recoil energy, experienced by an incident particle, was less then or equal to the partial mean excitation energy of electrons from the group. Gaussian functions were centered at a given energy loss when the recoil energy, experienced by an incident particle, was larger then the partial mean excitation energy of electrons from a given group.

Initially it was planned that magnitudes a and variances c of Gaussian functions, used for modeling the generalized oscillator strength function of calcium, will be determined empirically. The analysis revealed, however, that the parameters of empirically selected Gaussian functions more or less satisfy the following mathematical relations:

$$a \cdot b = 1 \tag{34}$$

and

$$c = \frac{b}{\sqrt{2\pi}}. \tag{35}$$

Relations (34) and (35) were used in all further calculations of the parameters of Gaussian functions used for modeling of the generalized oscillator strength function of calcium. A detailed description of the analysis, performed with Gaussian functions, and an explanation of how relations (34) and (35) were determined will be provided in the next section of the manuscript.

Figure 26 shows the generalized oscillator strength function of calcium modeled using Gaussian functions. The functions were positioned on the energy loss and recoil energy plane according to the two rules stated above. The magnitude and the variance of the functions were calculated according to relations (34) and (35) respectively. The functions, shown

in the figure, are scaled by the oscillator strengths of electrons from the different electron bands and electron shells of calcium.

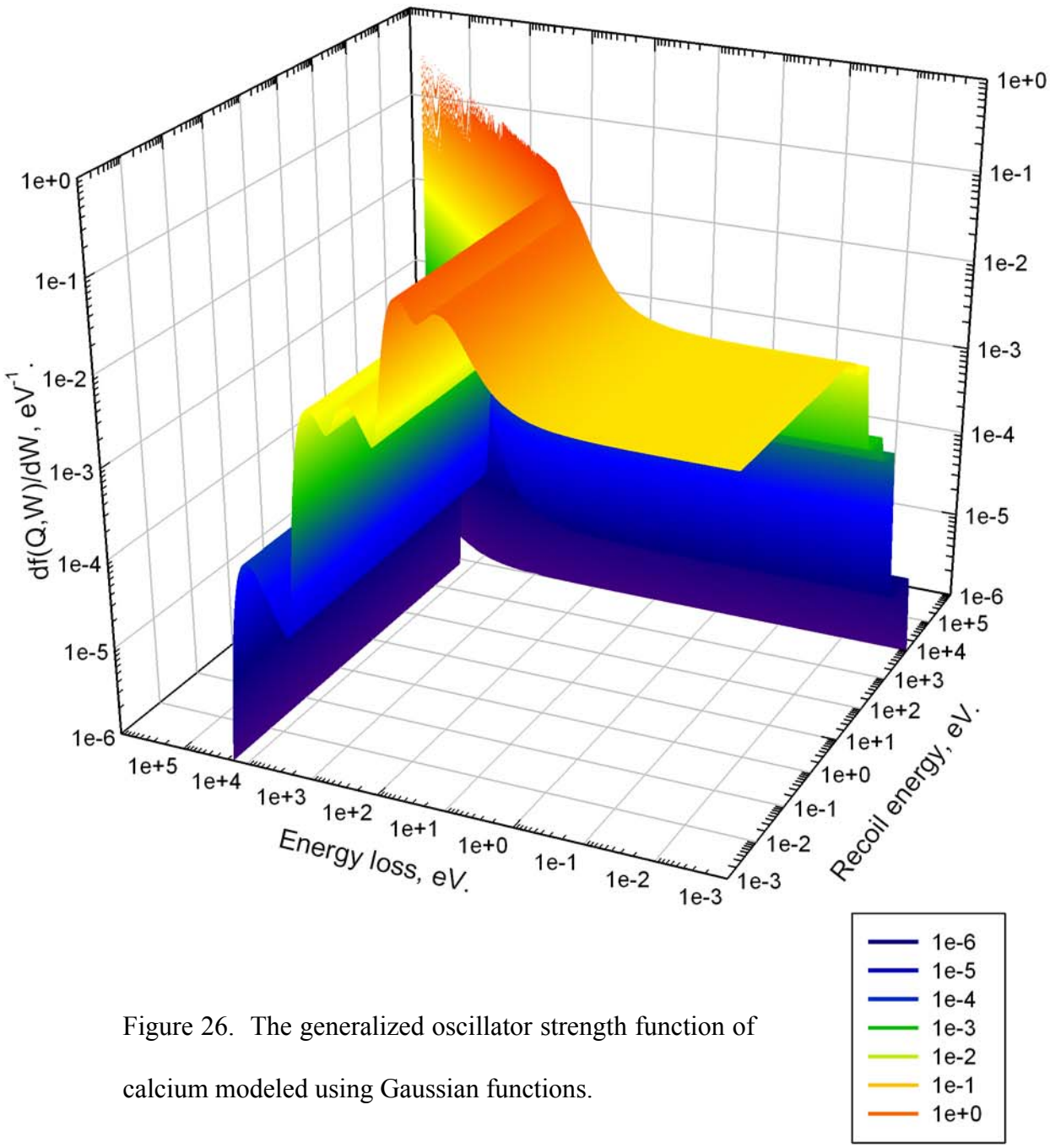

Figure 26. The generalized oscillator strength function of calcium modeled using Gaussian functions.

Considering figure 26 one may note a prominent elevation of the generalized oscillator strength function along the line at which the recoil energy is equal to the energy loss. The elevation is called the Bethe ridge. Initially variances of Gaussian functions centered at the Bethe ridge were the same as the variances of Gaussian functions centered at partial mean excitation energies of electrons from a given band or shell of calcium. In a later model of the generalized oscillator strength function of calcium variances of Gaussian functions, centered at the Bethe ridge, were determined by the actual energy loss at which the functions were centered.

Determination of variances of Gaussian functions

The approach, used for an empirical determination of variances of Gaussian functions, was based on a comparison of results of calculations of the number of electrons in calcium atoms obtained with Gaussian functions and with the energy loss functions determined for calcium. The generalized oscillator strength function $\frac{df(Q,W)}{dW}$ and the energy loss function $\mathrm{Im}\left(\frac{-1}{\varepsilon(Q,W)}\right)$ are related to each other as (Fernández-Varea, 2005):

$$\frac{df(Q,W)}{dW} = W\frac{2n_{eff}}{\pi E_p^2}\mathrm{Im}\left(\frac{-1}{\varepsilon(Q,W)}\right), \tag{36}$$

where n_{eff} is the oscillator strength or the number of electrons in a particular band or shell, and E_p is the plasma energy of corresponding electrons.

Either of the functions (the generalized oscillator strength function or the energy loss function) can be used for a calculation of the number of electrons in a particular electron band, atomic shell, or whole atoms of a given material. In fact, examples of calculations of the number of electrons using the energy loss functions of calcium have already been shown. The energy loss

function of calcium and the energy loss functions, arising due to electrons from individual bands of metallic calcium and shells of atoms of calcium, were used for a calculation of the number of electrons in the whole atoms of calcium and in individual bands of metallic calcium and shells of atoms of calcium. Figure 22 showed the effective number of electrons that participate in absorption of external electromagnetic radiation as a function of the energy of radiation, while Table 1 listed the determined oscillator strengths of electrons in metallic calcium.

A determination of variances of Gaussian functions, used for modeling the generalized oscillator strength function of calcium, was performed the following way. Several Gaussian functions, each having a slightly different variance, were used for a calculation of the number of electrons in a particular band of metallic calcium, or in a particular shell in atoms of calcium. Results of the calculations were compared to the result of an equivalent calculation performed using the energy loss functions determined for calcium. Gaussian function, which yielded the closest representation of the number of electrons, was selected for modeling of the generalized oscillator strength function of calcium.

Soon after a set of Gaussian functions was empirically selected for modeling of the generalized oscillator strength function of calcium it was realized that parameters a and b (magnitude and position) of selected Gaussian functions approximately satisfied the relation $a \cdot b = 1$. Relation $a \cdot b = 1$ together with expression (33) yielded the relation $c = b/\sqrt{2\pi}$ for variance c of Gaussian functions.

Use of relations (34) and (35) seamed very attractive for a calculation of magnitudes and variances of Gaussian functions, used for modeling of the generalized oscillator strength function of calcium. First of all, the relations would eliminate the ambiguity about values of variances of

Gaussian functions. Second, the relations would permit to relate variances of Gaussian functions, positioned along the line at which the recoil energy is equal to the energy loss, to the actual energy losses at which the functions are positioned. As a reminder, the elevation of the generalized oscillator strength function along the line at which the recoil energy is equal to the energy loss is called the Bethe ridge. Linkage of variances of Gaussian functions, centered at the Bethe ridge, to the actual energy losses at which the functions are positioned would permit to spread the Bethe ridge even more over the energy loss and recoil energy plane. It was important to spread the Bethe ridge over the energy loss and recoil energy plane for a more realistic representation of the generalized oscillator strength function of calcium.

An additional analysis was performed in order to test the acceptance of relations (34) and (35) for a calculation of magnitudes and variances of Gaussian functions used for modeling of the generalized oscillator strength function of calcium. In order to test relations (34) and (35) a set of Gaussian functions was created. One of Gaussian functions from the set had a magnitude and a variance calculated according to relations (34) and (35). The function was considered as the reference one. The other Gaussian functions had variances larger or smaller then the variance of the reference function. All the functions from the set were normalized. Gaussian functions were used for a calculation of the number of electrons in a given band of metallic calcium, or shell of atoms of calcium. Results of the calculations were compared with the result of an equivalent calculation performed with a corresponding energy loss function determined for calcium. The calculations were performed for all six electron groups defined for calcium.

The following figures show Gaussian functions, the optical oscillator strength functions, and results of calculations of the number of electrons in given electron groups of calcium. There are six pairs of figures. Each pair shows results for a particular band or shell of calcium. The upper

figure of each pair shows Gaussian functions which were tested, and the optical oscillator strength function determined for electrons from a given electron group of calcium. The optical oscillator strength functions were calculated from the energy loss functions according to equation (36). The lower figure of each pair of figures shows results of calculations of the number of electrons in a given band or shell of calcium obtained with Gaussian functions and with the energy loss function determined for electrons from the given band or shell of calcium.

The analysis confirmed that relations (34) and (35) can be used for a calculation of the magnitude and the variance of Gaussian functions used for modeling of the generalized oscillator strength function of calcium. The relations removed the ambiguity about values of variances of Gaussian functions. The relations permitted automation of calculations. And finally, the relations permitted to additionally spread the Bethe ridge over the energy loss and recoil energy plane.

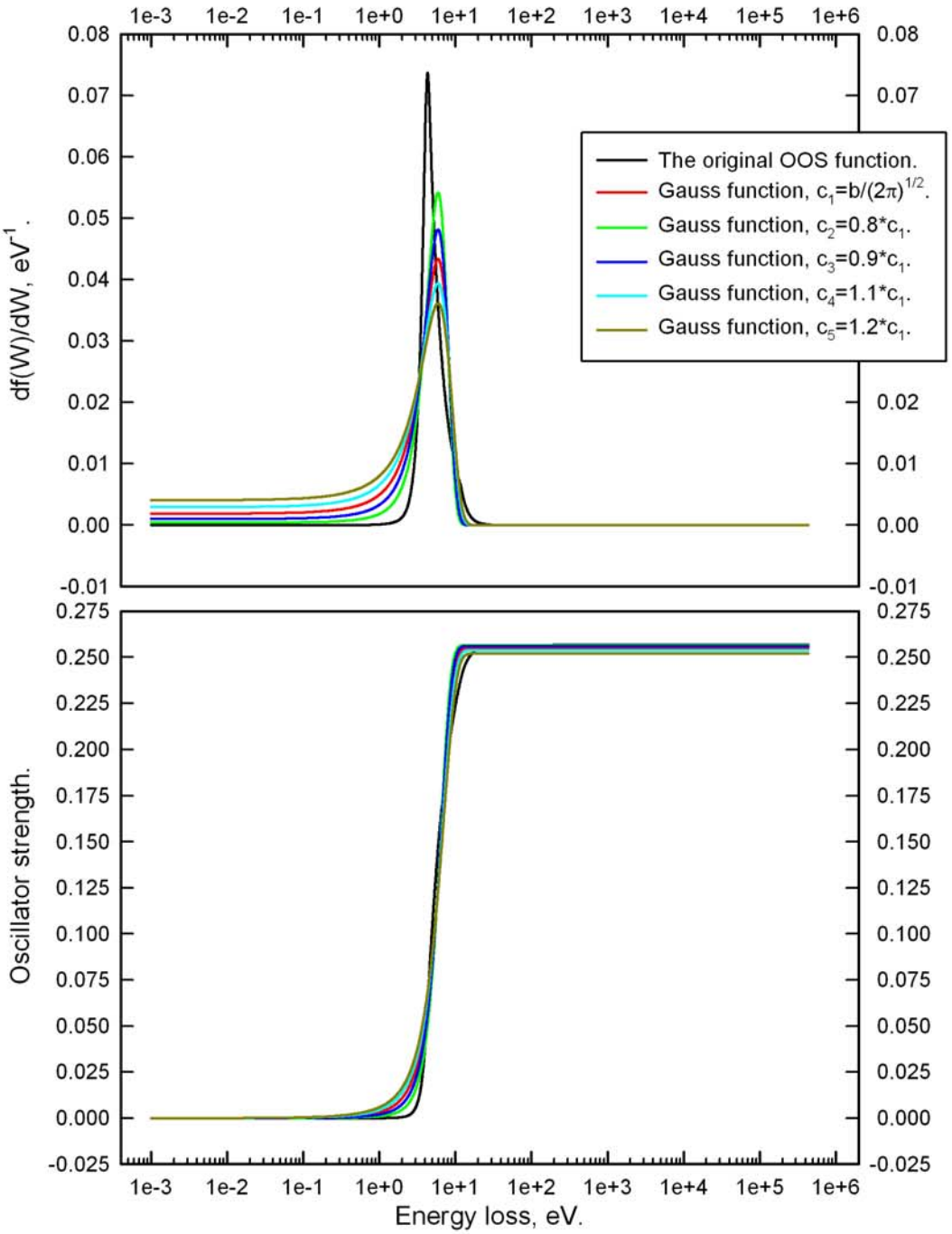

Figure 27. Gaussian functions which were tested and the optical oscillator strength function determined for electrons from a given group of calcium (top), and the oscillator strengths obtained (bottom) during an analysis performed for electrons responsible for the peak at 4 eV of the energy loss function of calcium.

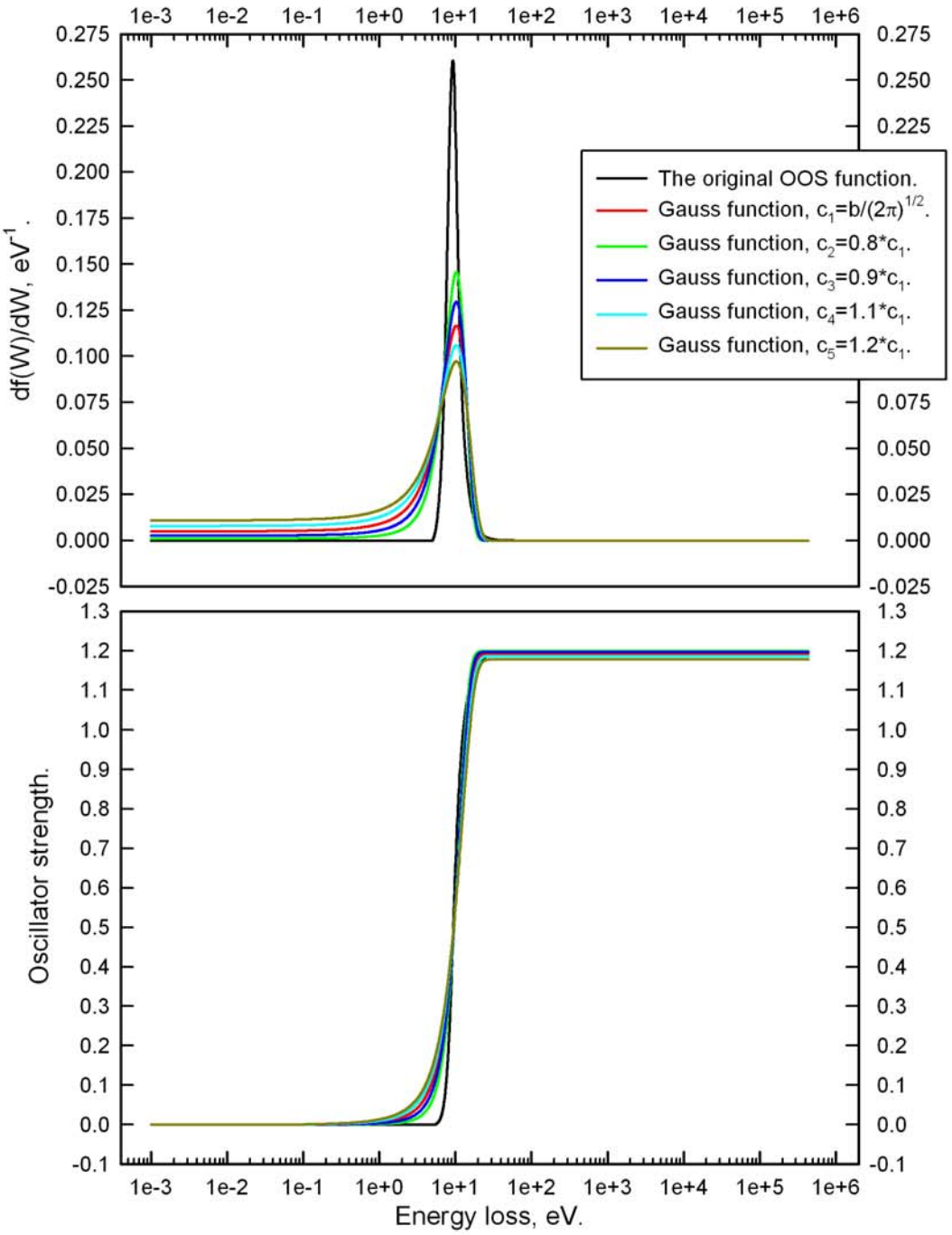

Figure 28. Gaussian functions which were tested and the optical oscillator strength function determined for electrons from a given group of calcium (top), and the oscillator strengths obtained (bottom) during an analysis performed for electrons responsible for the peak at 9 eV of the energy loss function of calcium.

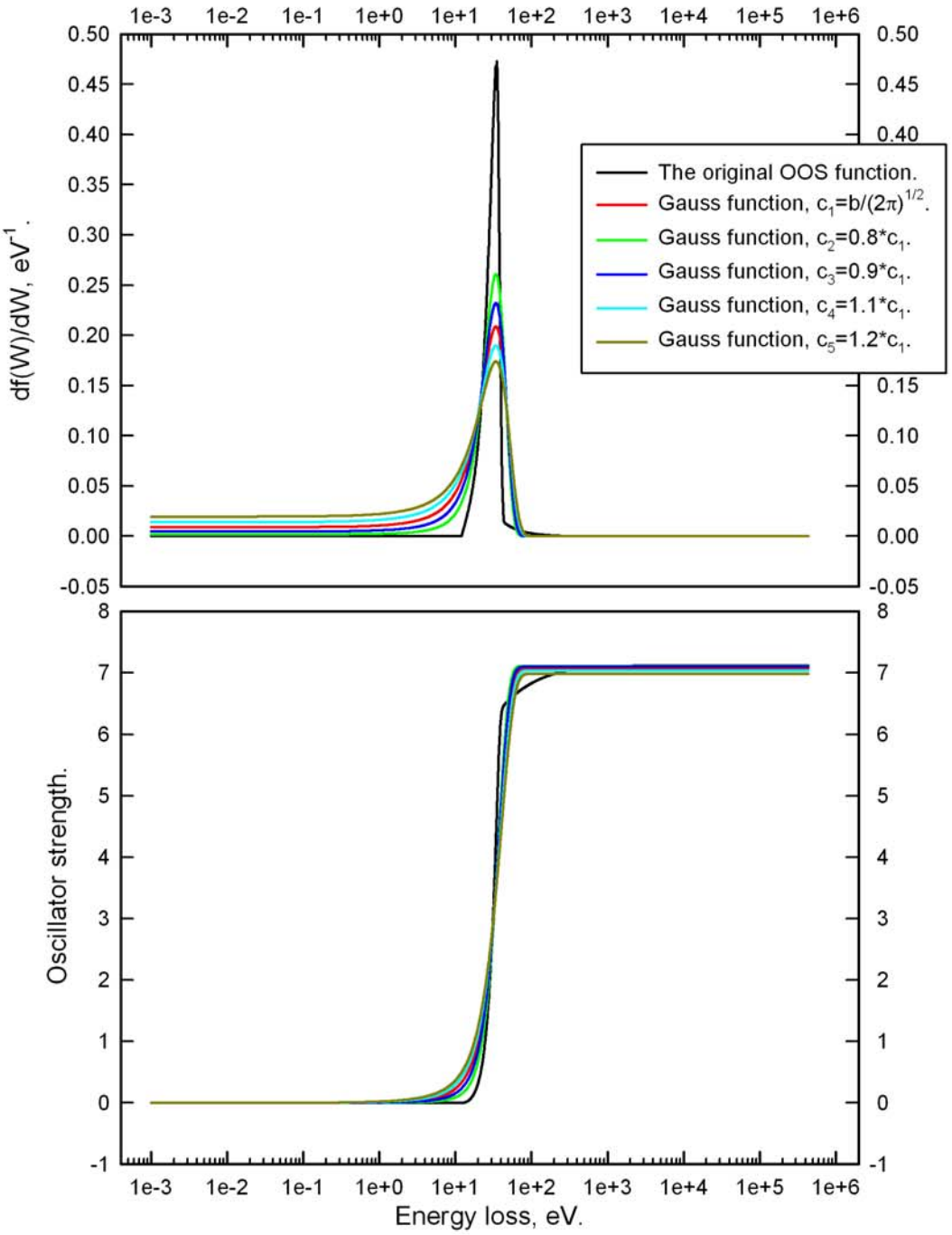

Figure 29. Gaussian functions which were tested and the optical oscillator strength function determined for electrons from a given group of calcium (top), and the oscillator strengths obtained (bottom) during an analysis performed for electrons from the *p* state of the *M* shell of calcium.

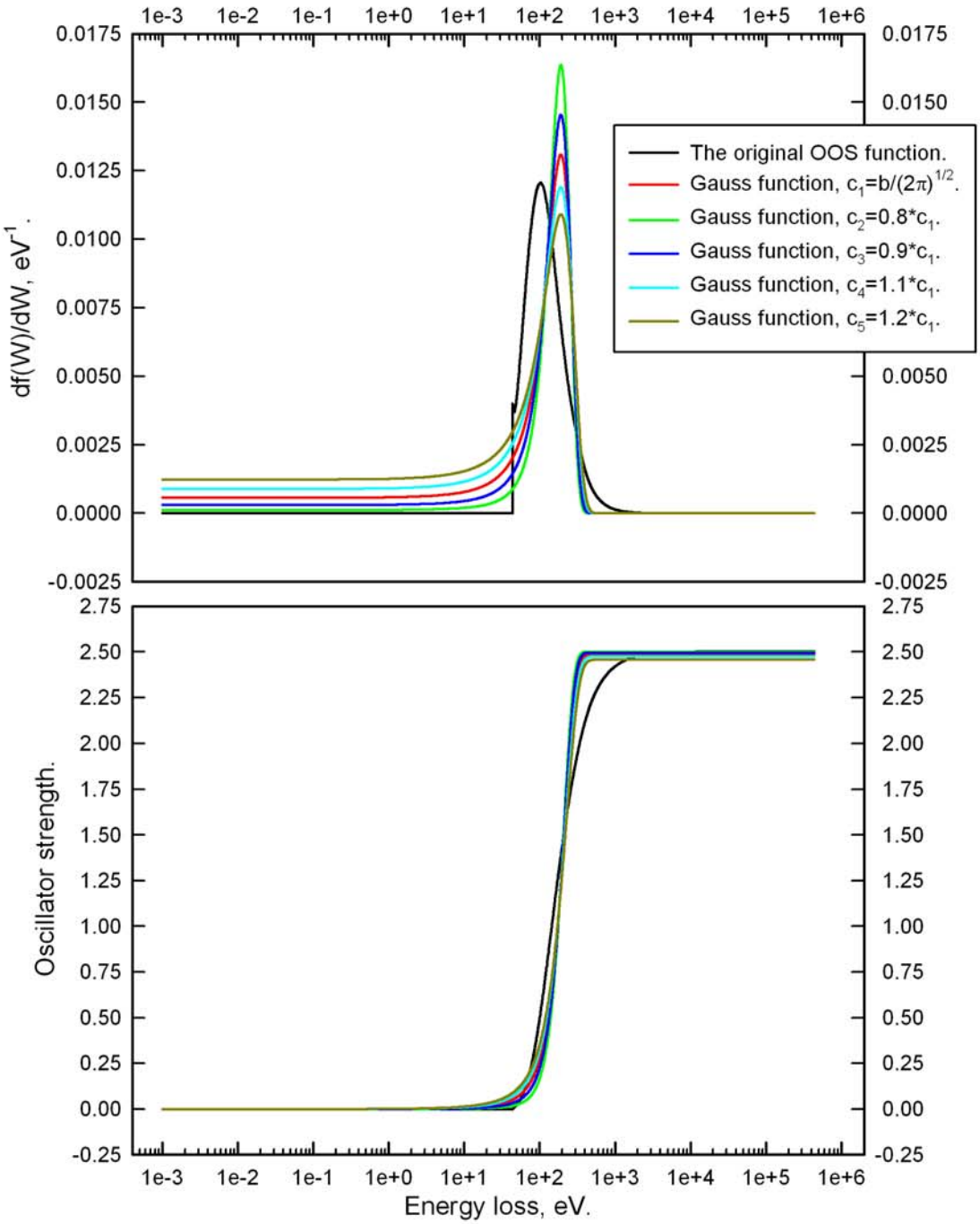

Figure 30. Gaussian functions which were tested and the optical oscillator strength function determined for electrons from a given group of calcium (top), and the oscillator strengths obtained (bottom) during an analysis performed for electrons from the *s* state of the *M* shell of calcium.

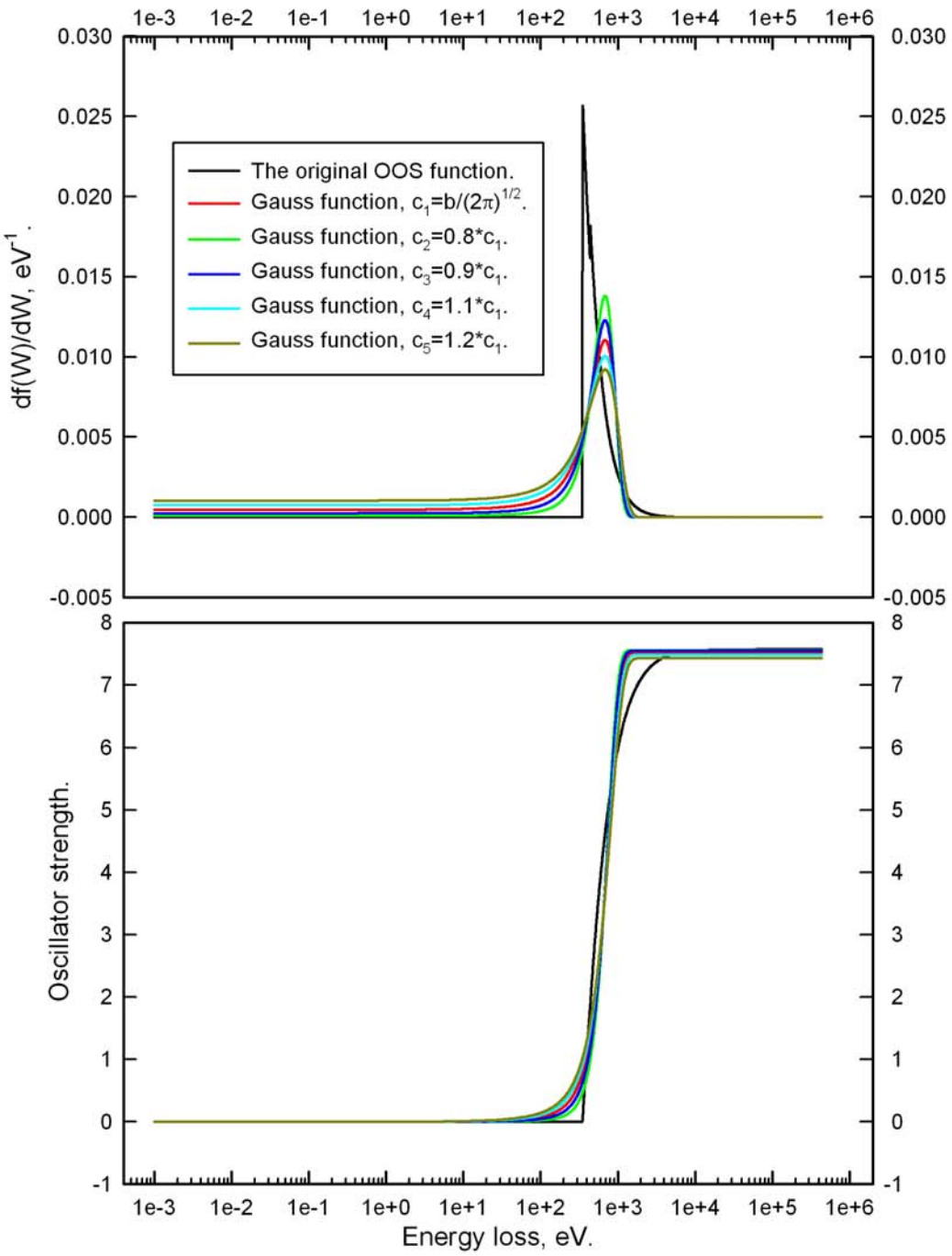

Figure 31. Gaussian functions which were tested and the optical oscillator strength function determined for electrons from a given group of calcium (top), and the oscillator strengths obtained (bottom) during an analysis performed for electrons from the *L* shell of calcium.

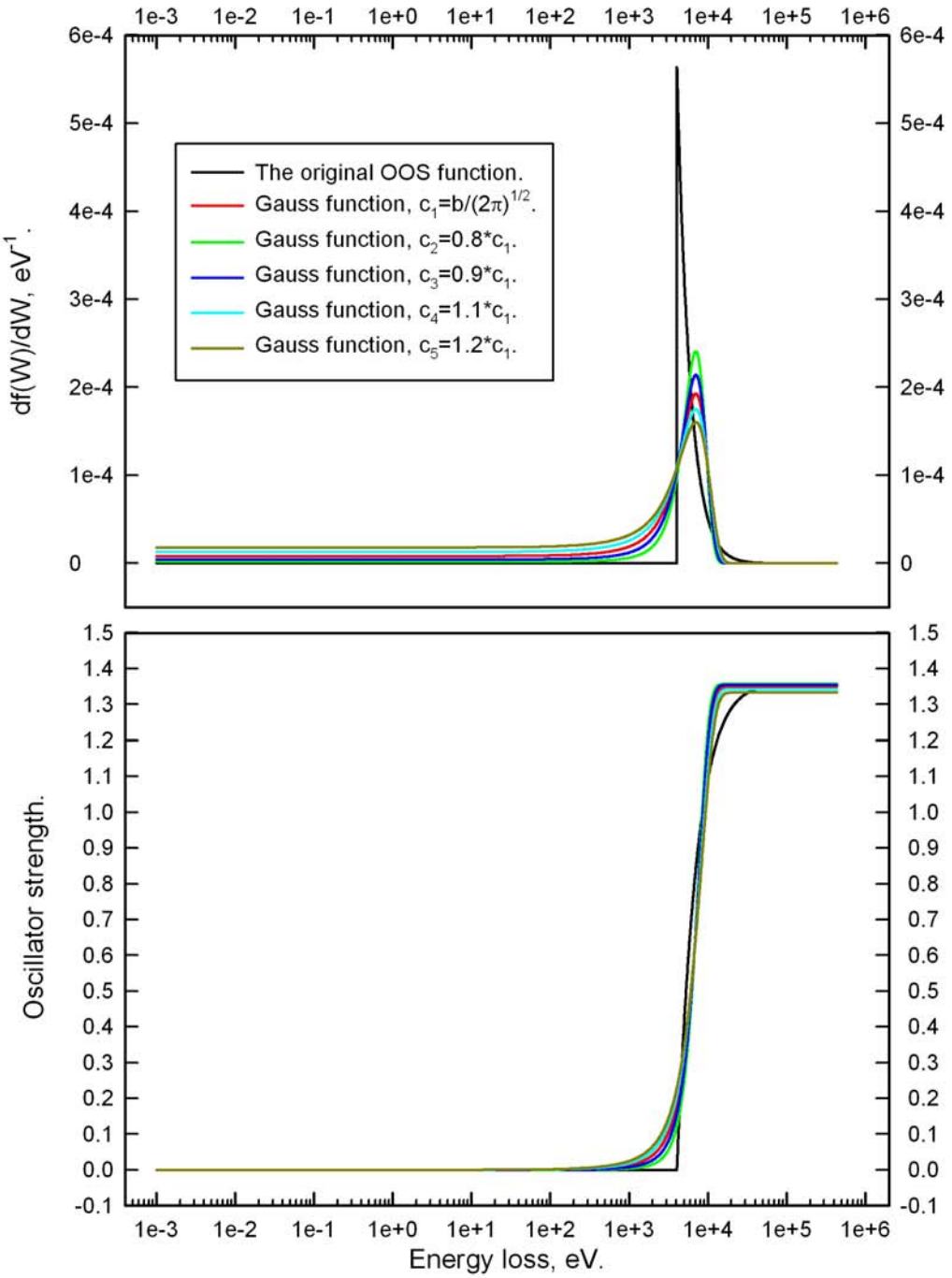

Figure 32. Gaussian functions which were tested and the optical oscillator strength function determined for electrons from a given group of calcium (top), and the oscillator strengths obtained (bottom) during an analysis performed for electrons from the *K* shell of calcium.

Extrapolation of Gaussian functions at small and at large energy losses for an accurate representation of the optical oscillator strength function of calcium

The accuracy with which Gaussian functions approximated the generalized oscillator strength function of calcium was assessed for one particular case, at zero recoil energy. The generalized oscillator strength function is a function of two variables, the energy loss and the recoil energy. At zero recoil energy the generalized oscillator strength (GOS) function reduces to the optical oscillator strength (OOS) function. An analysis of the optical, the dielectric, and the photoelectric properties of calcium permitted to derive the energy loss function of calcium in the optical limit, i.e. for cases in which the recoil energy is equal to zero. The derived energy loss function of calcium was shown in figure 16. The derived energy loss function was used for a calculation of the OOS function of calcium.

The OOS function of calcium, modeled with Gaussian functions, was compared to the OOS function calculated using the derived energy loss function of calcium. A comparison of the functions revealed that the OOS function, modeled with Gaussian functions, dropped in its magnitude much faster in the limit of large energy losses, and much slower in the limit of small energy losses then the OOS function calculated using the derived energy loss function of calcium. In order to figure out the cause for the observed behavior of the modeled OOS function of calcium, an analysis was performed using each of the six Gaussian functions used for modeling the OOS function of calcium.

The energy loss function derived for calcium was represented as a sum of six functions. Each of the six functions was due to electrons from one of the bands of metallic calcium, or one of the shells of atoms of calcium. An explanation of how the derived energy loss function of calcium

was split into six functions was provided before in the manuscript. Figure 21 showed the energy loss functions arising due to electrons from the bands and the shells defined for calcium. The six energy loss functions were used for a calculation of the optical oscillator strength functions of calcium. A calculation of the OOS functions was performed according to equation (36). The calculated OOS functions were used in comparisons with Gaussian functions.

Each of the six Gaussian functions was compared to a corresponding OOS function of calcium calculated using one of the derived energy loss functions of calcium. A comparison of Gaussian functions to the OOS functions demonstrated that in all six cases Gaussian functions dropped in their magnitude much faster in the limit of large energy losses, and much slower in the limit of small energy losses then the calculated OOS functions. The results of a comparison of the modeled to the calculated OOS functions of calcium are shown in figure 33.

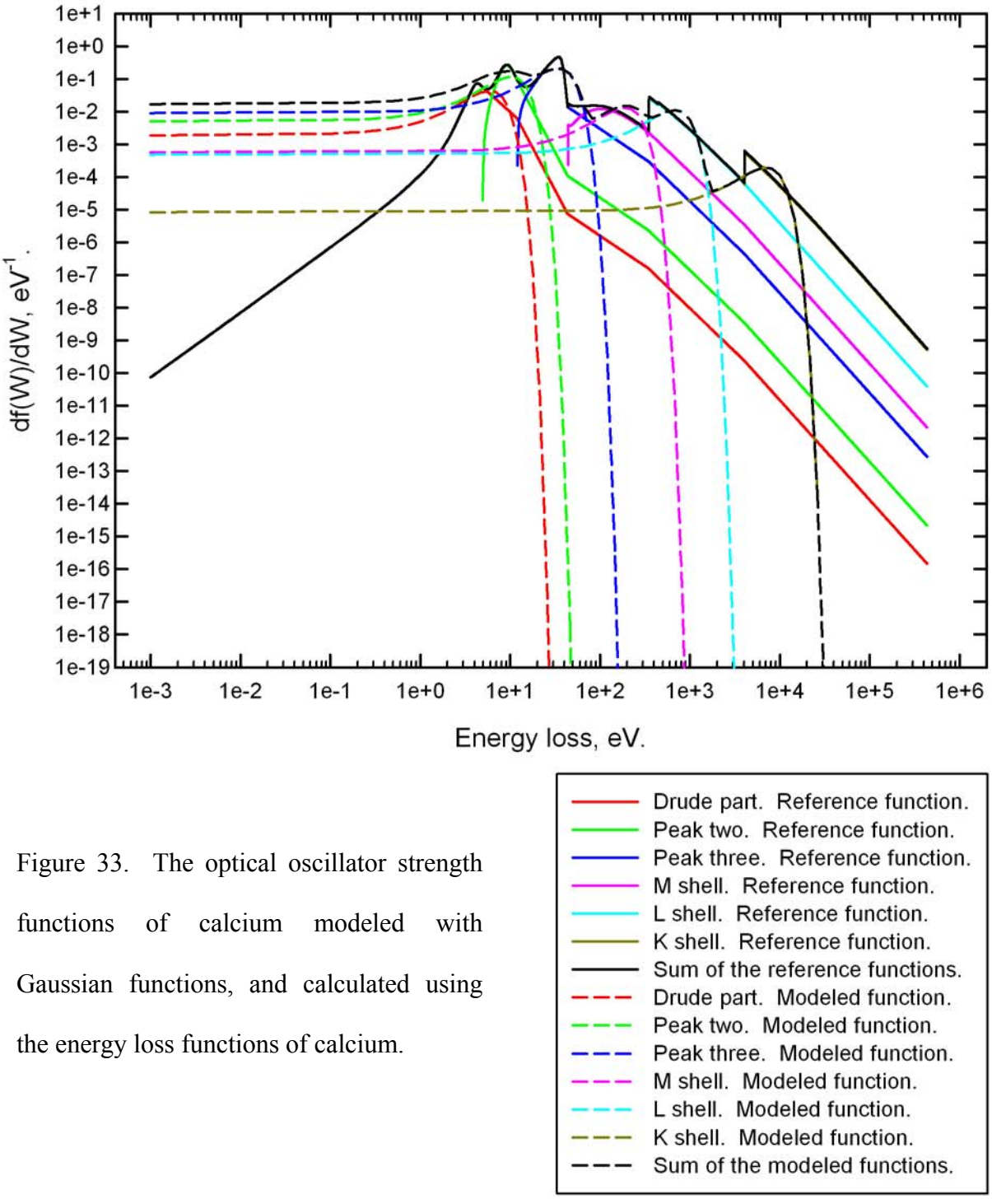

Figure 33. The optical oscillator strength functions of calcium modeled with Gaussian functions, and calculated using the energy loss functions of calcium.

Considering figure 33 one may note that the OOS functions, calculated using the energy loss functions of calcium, decrease at small and at large energy losses practically linearly when the OOS functions and the energy losses are plotted on a log-log scale. In order to create a more

accurate model for the optical oscillator strength function of calcium, Gaussian functions, used for modeling the OOS function, were extrapolated at small and at large energy losses with the same inclination as the inclination of the calculated OOS functions of calcium.

Each of the six Gaussian functions was compared to a corresponding optical oscillator strength function of calcium calculated using one of the derived energy loss functions of calcium. Each of the six Gaussian functions was extrapolated at small and at large energy losses with the inclination of a corresponding OOS function. Gaussian functions were renormalized following extrapolation to ensure proper oscillator strengths of electrons from the different bands and shells of calcium.

Extrapolation of Gaussian functions was performed from the energy loss at which inclination of Gaussian functions turned equal to the inclination of corresponding OOS functions of calcium. In the limit of small energy losses inclination of Gaussian functions turned equal to the inclination of corresponding OOS functions of calcium at two energy losses. The larger of the two energy losses was taken as the energy loss starting from which Gaussian functions were extrapolated. By taking the larger of the two energy losses, one eliminated a creation of a shoulder in the graphs of the OOS functions. In the limit of large energy losses inclination of Gaussian functions turned equal to the inclination of corresponding calculated OOS functions of calcium only at one energy loss. The determined energy loss was taken as the energy loss starting from which an extrapolation of Gaussian functions was performed.

The optical oscillator strength functions of calcium, modeled with extrapolated Gaussian functions, and also calculated using the derived energy loss functions of calcium are shown in

figure 34. The figure shows the OOS functions arising due to each electron group of calcium. The figure also shows the total OOS functions.

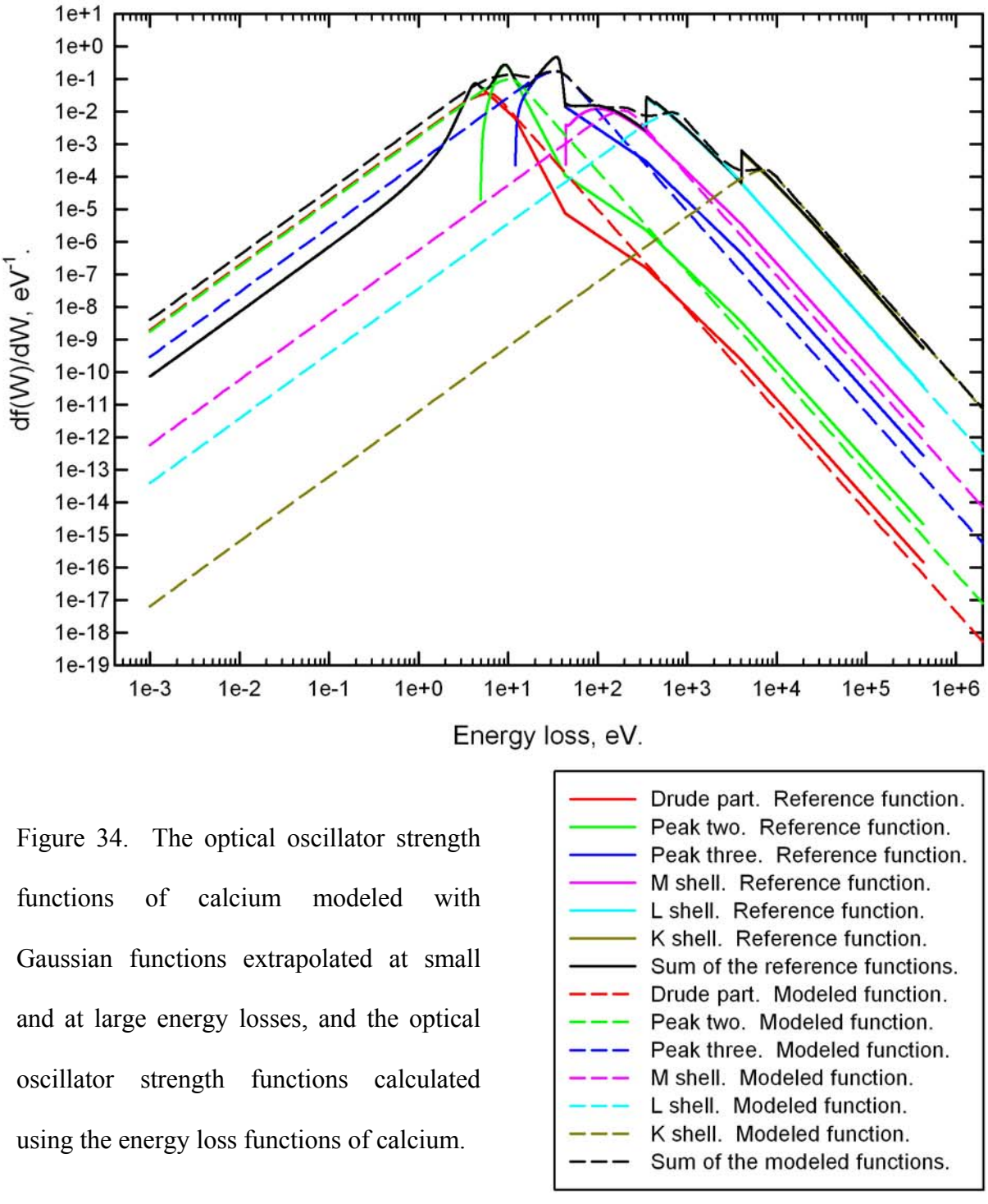

Figure 34. The optical oscillator strength functions of calcium modeled with Gaussian functions extrapolated at small and at large energy losses, and the optical oscillator strength functions calculated using the energy loss functions of calcium.

Modeling of the generalized oscillator strength function of calcium using Gaussian functions extrapolated at small and at large energy losses

Once it was observed that Gaussian functions had to be extrapolated at small and at large energy losses for an accurate representation of the optical oscillator strength function of calcium, it was assumed that the functions had to be extrapolated also during modeling of the generalized oscillator strength function of calcium for an accurate representation of the latter function. The approach, used for modeling of the generalized oscillator strength function of calcium, was adjusted following the observations.

The generalized oscillator strength function (GOS) of calcium was represented as a sum of six functions. Each of the six functions arose due to electrons from a particular band of metallic calcium or shell of atoms of calcium. The GOS functions, arising due to electrons from the individual bands and shells of calcium, were modeled with Gaussian functions extrapolated at small and at large energy losses. Extrapolation of the functions was performed with the inclination of corresponding optical oscillator strength functions of calcium. Gaussian functions were, at the same time, renormalized to ensure proper oscillator strengths of electrons from the individual bands and shells of calcium.

In the latest model of the generalized oscillator strength function of calcium variances of Gaussian functions, used for modeling the individual GOS functions, were determined by the actual energy loss at which Gaussian functions were centered. Determination of variances of Gaussian functions by the actual energy loss at which the functions were centered permitted to broaden Gaussian functions centered at energy losses equal to the recoil energy. In other words, determination of variances of Gaussian functions by the actual energy loss at which the functions were centered permitted to broaden Gaussian functions which made the Bethe ridge. Spreading

of the Bethe ridge over the energy loss and recoil energy plane seemed important for a realistic representation of the distribution of momentums of electrons in atoms. Spreading of the Bethe ridge seemed important also for an accurate numerical integration over the ridge.

The generalized oscillator strength function of calcium, modeled with Gaussian functions extrapolated at small and at large energy losses, is shown in figure 35. The figure shows the total GOS function of calcium. The total GOS function was obtained by a summation of the GOS functions arising due to electrons from the three electron bands of metallic calcium and the three electron shells of atoms of calcium.

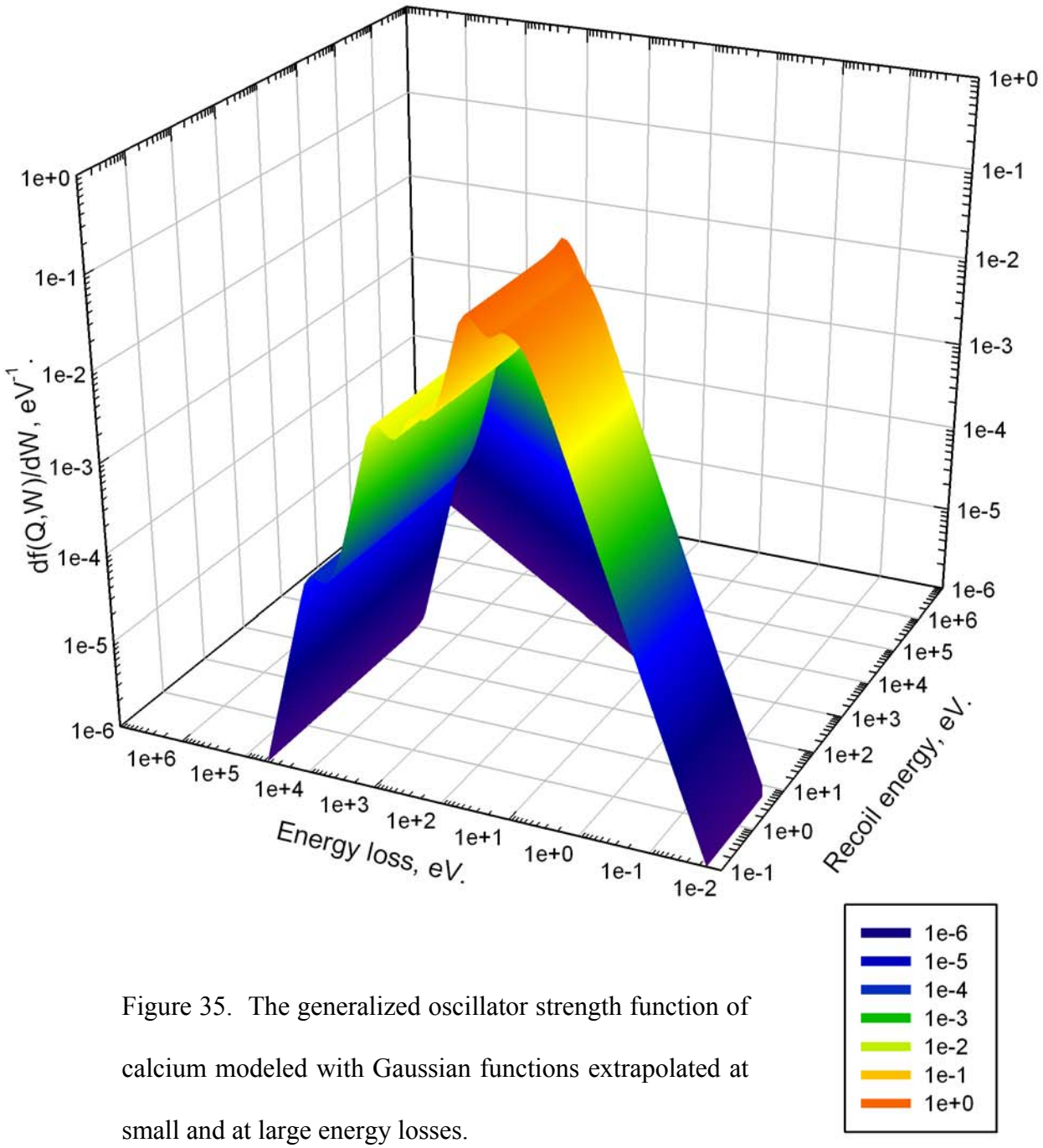

Figure 35. The generalized oscillator strength function of calcium modeled with Gaussian functions extrapolated at small and at large energy losses.

The total GOS function of calcium, shown in figure 35, is provided for illustration purposes only. The total GOS function of calcium was not used directly in any calculations. The constituent GOS functions, arising due to electrons from the three bands and the three shells of calcium, were used in calculations of interaction cross sections of electrons, protons, and alpha particles with electrons of metallic calcium. Calculated interaction cross sections and also integrated cross sections obtained for electrons, protons, and alpha particles will be presented and discussed in the following several sections of the manuscript.

Calculation of the energy loss and recoil energy differential interaction cross sections of energetic charged particles

The energy loss and recoil energy differential interaction cross sections of electrons, protons, and alpha particles with electrons of calcium were calculated following the approach described by Segui et al (2002) and Fernández-Varea et al (2005). The interaction cross sections were calculated within a fully relativistic plane wave Born approximation framework. Current work used the equations for the energy loss and recoil energy differential interaction cross sections, provided in the two articles, for a calculation of interaction cross sections of electrons, protons, and alpha particles with electrons of calcium.

It was specified in articles by Segui et al (2002) and by Fernández-Varea et al (2005) that the equations for the cross sections were derived for spin ½ charged particles. Electrons and protons are spin ½ particles, but alpha particles are not. Calculations of the cross sections were performed for alpha particles too in order to test a hypothesis about scaling of interaction cross sections. A discussion of the hypothesis will be provided later in the manuscript.

A calculation of the energy loss and the recoil energy differential interaction cross sections was performed using equations (Segui et al, 2002; Fernández-Varea et al, 2005):

$$\frac{d^2\sigma_L}{dWdQ} = \frac{2\pi Z_0^2 e^4}{m_e c^2 \beta^2} \frac{1}{WQ\left(1+Q/2m_e c^2\right)} \frac{df\left(Q,W\right)}{dW} \tag{37}$$

and

$$\frac{d^2\sigma_T}{dWdQ} = \frac{2\pi Z_0^2 e^4}{m_e c^2 \beta^2} \frac{\beta_t^2 W/2m_e c^2}{\left[Q\left(1+Q/2m_e c^2\right)-W^2/2m_e c^2\right]^2} \frac{df\left(Q,W\right)}{dW}, \tag{38}$$

where Z_0 is the charge of the incident particle expressed in terms of the elementary charge, e is the elementary charge, m_e is the mass of an electron, β is the speed of the incident particle expressed in terms of the speed of light in vacuum, W is the energy loss experienced by the incident particle in an individual collision with atomic electrons, Q is the recoil energy experienced by the particle, and factor $df(Q,W)/dW$ is the generalized oscillator strength function of the target material.

Parameter β_t, seen in equation (38), is the component of $\vec{\beta} = \vec{v}/c$ perpendicular to $\vec{q}$, the momentum transfer. Please see figure 24 for the schematics of inelastic collisions. Parameter β_t is calculated according to equation (Segui et al, 2002):

$$\beta_t^2 = \beta^2 - \frac{W^2}{Q\left(Q + 2m_e c^2\right)}\left(1 + \frac{Q\left(Q + 2m_e c^2\right) - W^2}{2W\left(E + Mc^2\right)}\right)^2, \tag{39}$$

where E is the kinetic energy of the incident particle, and M is the mass of the particle.

Incident particles experience two types of interactions with target atomic electrons, the longitudinal and the transverse interactions. The longitudinal interactions arise due to the instantaneous Coulomb field, while the transverse interactions arise due to an exchange with virtual photons between an incident particle and target electrons. Equation (37) is for a calculation of interaction cross sections which arise due to the longitudinal interactions between an incident particle and atomic electrons. Equation (38) is for a calculation of interaction cross sections which arise due to the transverse interactions.

The generalized oscillator strength function of calcium was represented as a sum of six functions each of which arose due to electrons from one of the six electron groups of calcium.

Calculations of the energy loss and recoil energy differential interaction cross sections of electrons, protons, and alpha particles with electrons of calcium were performed for all six electron groups of calcium. In total twelve sets of interaction cross sections were obtained and operated at any particular time. The six electron groups and the two types of interactions yielded twelve sets of interaction cross sections. The total interaction cross sections could be obtained by a simple summation of the cross sections calculated for each electron group of calcium and for each type of interactions. The cross sections, however, were kept separate in most calculations performed over the course of the work. The cross sections were kept separate in order to keep as much information about the details of collisions of incident particles with atomic electrons as possible. Only the results for the stopping power and the mean free path were summed over the six electron groups of calcium and the two types of interactions.

Calculation of the energy loss differential interaction cross sections

Equations (37) and (38) are for a calculation of the energy loss and recoil energy differential interaction cross sections. The energy loss differential interaction cross sections $d\sigma_{L,T}/dW$ were obtained by an integration of the double differential interaction cross sections by the recoil energy. An integration of the cross sections was performed from the minimal Q_- to the maximal Q_+ recoil energy permitted by the collision kinematics.

$$\frac{d\sigma_{L,T}}{dW} = \int_{Q_-}^{Q_+} \frac{d^2\sigma_{L,T}}{dWdQ} dQ . \tag{40}$$

The minimal Q_- and the maximal Q_+ recoil energies, which an incident particle can experience in a collision with an electron, are determined using the initial p and the final p' momentums of the particle according to equation (Fernández-Varea et al, 2005):

$$Q_{\pm} = \sqrt{\left(cp \pm cp'\right)^2 + m_e^2 c^4} - m_e c^2 , \tag{41}$$

where $m_e c^2$ is the electron rest energy.

If the initial and the final momentums of an incident particle are expressed in terms of the kinetic energy E of the particle before an inelastic collision, the rest energy Mc^2 of the particle, and the energy loss W, then equation (41) converts to (Segui et al, 2002; Fernández-Varea et al, 2005):

$$Q_{\pm} = \sqrt{\left(\sqrt{E\left(E+2Mc^2\right)} \pm \sqrt{\left(E-W\right)\left(E-W+2Mc^2\right)}\right)^2 + m_e^2 c^4} - m_e c^2 . \tag{42}$$

A calculation of the minimal recoil energy involved a subtraction of two very close values in the limit of small energy losses. Often calculated minimal recoil energy turned equal to zero because of numerical errors. A more accurate relation was used for a calculation of the minimal recoil energy that electrons can experience in collisions with other electrons (Fernández-Varea et al, 2005):

$$Q_{-} \approx m_e c^2 \left(x - \frac{x^2}{2} + \frac{x^3}{2} \right), \tag{43}$$

where $x = \frac{1}{2}\left(\frac{cp - cp'}{m_e c^2} \right)^2 \approx \frac{W^2}{2\beta^2 m_e^2 c^4}\left(1 + \frac{1}{2\gamma\left(\gamma+1\right)}\frac{W}{E} + \frac{1}{2\left(\gamma+1\right)^2}\left(\frac{W}{E}\right)^2 \right)^2$, and $\gamma = \sqrt{\frac{1}{1-\beta^2}}$.

Relation (43) was obtained from relation (41) in two steps. First, an approximation $\sqrt{2x+1} - 1 \approx x - x^2/2 + x^3/2$ was used. Then, the change in the momentum $p - p'$ was expanded into Taylor series, and the series were limited to the first three terms. Please see Appendix A of Fernández-Varea et al (2005) article for details on derivation of relation (43).

Calculation of the integrated cross sections

The energy loss differential interaction cross sections $d\sigma/dW$ were used for a calculation of the integrated cross sections:

$$\sigma^{(n)} = \int_0^{W_{\max}} W^n \frac{d\sigma}{dW} dW \,, \tag{44}$$

where n can be zero or an integer number, and $W_{\max}$ is the maximal energy loss that incident particles can experience in inelastic collisions with atomic electrons.

The maximal energy loss that incident particles could experience in collisions with target electrons was calculated according to equation (Podgoršak, 2006):

$$W_{\max} = \frac{2(\gamma+1)m_p m_e}{m_p^2 + m_e^2 + 2\gamma m_p m_e} E \,, \tag{45}$$

where m_p is the rest mass of the projectile particle, m_e is the rest mass of an electron, $\gamma = \left(1 - \upsilon^2/c^2\right)^{-1/2}$, and E is the kinetic energy of the incident particle before an inelastic collision.

Please note that equation (45) does not take into account the indistinguishability principle for incident and target electrons, or the binding energy of target electrons. Nevertheless equation (45) was used for a calculation of the maximal energy loss that electrons, protons, and alpha particles could experience in collisions with electrons of calcium.

The integrated cross sections $\sigma^{(0)}$, $\sigma^{(1)}$, and $\sigma^{(2)}$ are known as the total inelastic cross section, the stopping cross section, and the energy straggling cross section, respectively. The mean free path λ of incident particles in a given target material, the stopping power S of the material to

the particles, and the energy straggling Ω^2 of the particles are calculated using the integrated cross sections according to equations:

$$\lambda^{-1} = N\sigma^{(0)}, \tag{46}$$

$$S = N\sigma^{(1)}, \tag{47}$$

and

$$\Omega^2 = N\sigma^{(2)}, \tag{48}$$

where N is the number of atoms per unit volume of the target material.

Interaction cross sections of electrons, protons, and alpha particles with electrons of calcium were calculated for the six electron groups of calcium, and for the longitudinal and the transverse interactions. Calculated interaction cross sections were always kept separate. By keeping calculated interaction cross sections separate, it was possible to determine contributions of the individual electron groups of calcium and the two types of interactions to the integrated cross sections. Contributions of the individual electron groups and the two types of interactions were determined by using corresponding energy loss differential interaction cross sections in equation (44). For example, if there was a need for knowing how much electrons from the *L* shell of calcium atoms contributed to stopping of protons in calcium due to the longitudinal interactions between incident protons and target electrons, then the energy loss differential interaction cross sections $d\sigma_{\text{p, L shell, longitudinal}}/dW$ of protons with electrons from the *L* shell of calcium atoms arising due to the longitudinal interactions between protons and atomic electrons were used for a calculation of the integrated cross section $\sigma^{(1)}_{\text{p, L shell, longitudinal}}$. Calculations were performed using equation (44). The calculated integrated cross section was used for a calculation of the stopping power $S_{\text{p, L shell, longitudinal}}$. The latter calculation was performed using simple relation (47). The

subscript *p, L shell, longitudinal*, which just appeared, simply indicates that protons experience a collision with electrons from the *L* shell, and only longitudinal interactions between protons and atomic electrons are considered.

Interaction cross sections of 100 keV electrons with electrons of calcium

Calculations of interaction cross sections and also of the mean free path and the stopping power were performed for 100 keV electrons passing through calcium. The energy loss and recoil energy differential interaction cross sections of electrons with electrons of calcium were calculated according to equations (37) and (38). The exchange effect between incident and target electrons was not considered during calculations of interaction cross sections. Equations (37) and (38) were used alone for a calculation of interaction cross sections of incident electrons with electrons of calcium.

The cross sections which arose due to the longitudinal interactions between incident 100 keV electrons and electrons of calcium are shown in figure 36. The cross sections which arose due to the transverse interactions between incident and target electrons are shown in figure 37. Please note that both figures show the total longitudinal and the total transverse interaction cross sections obtained by a summation of the cross sections calculated for each electron group of calcium. Also please note that the figures show the most prominent features of the double differential interaction cross sections. The cross sections were calculated over much larger area of the energy loss and the recoil energy plane than it is shown in figures 36 and 37.

Figure 38 shows the energy loss and recoil energy differential interaction cross sections of 100 keV electrons colliding with electrons from group three of calcium, and experiencing 20 eV energy loss. The figure is presented here for a demonstration purpose only. One may get a

better understanding of the graphs for the energy loss and recoil energy differential interaction cross sections by considering the figure.

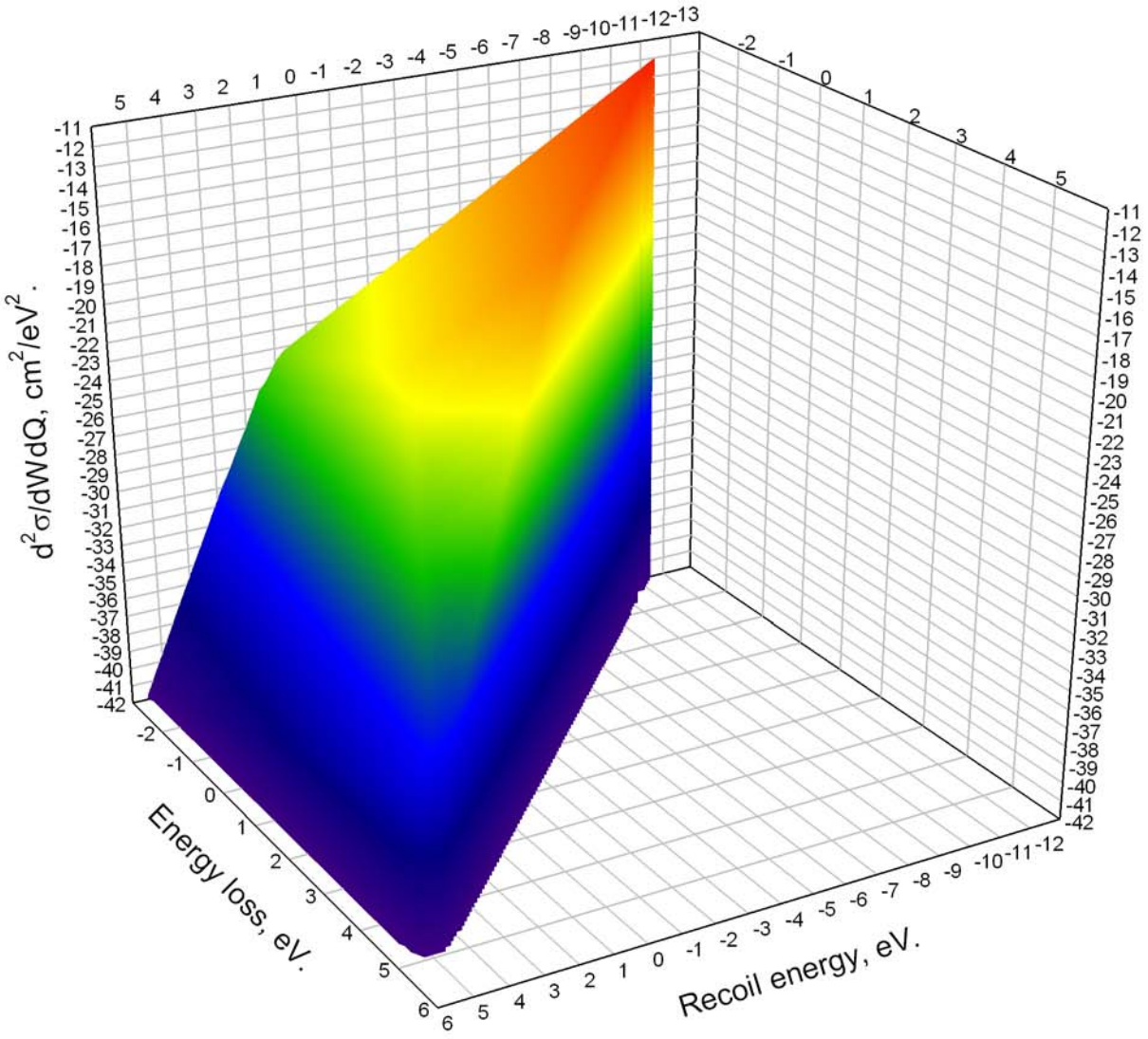

Figure 36. The energy loss and recoil energy differential interaction cross sections of 100 keV electrons with electrons of calcium arising due to the longitudinal interactions between incident and target electrons.

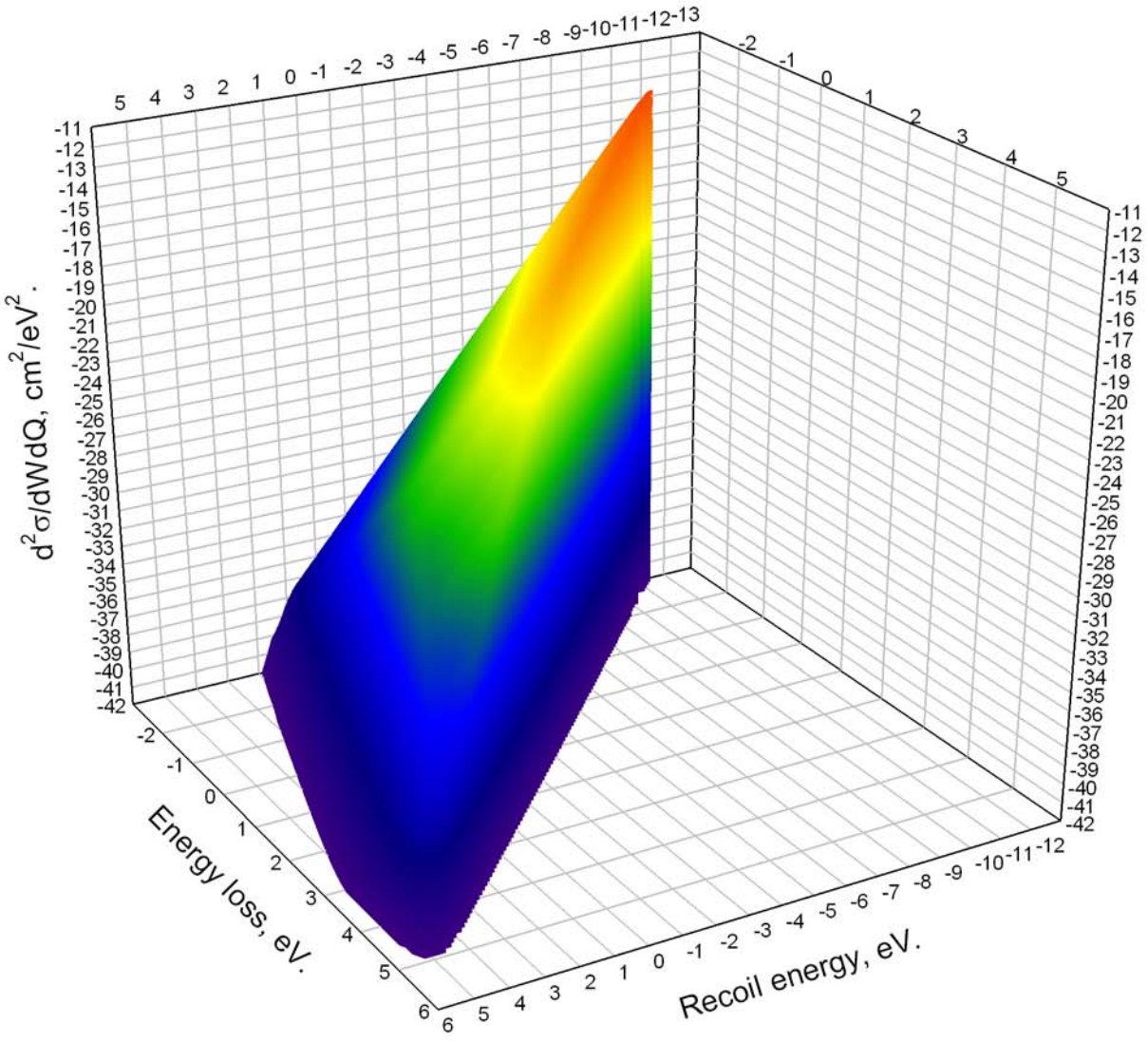

Figure 37. The energy loss and recoil energy differential interaction cross sections of 100 keV electrons with electrons of calcium arising due to the transverse interactions between incident and target electrons.

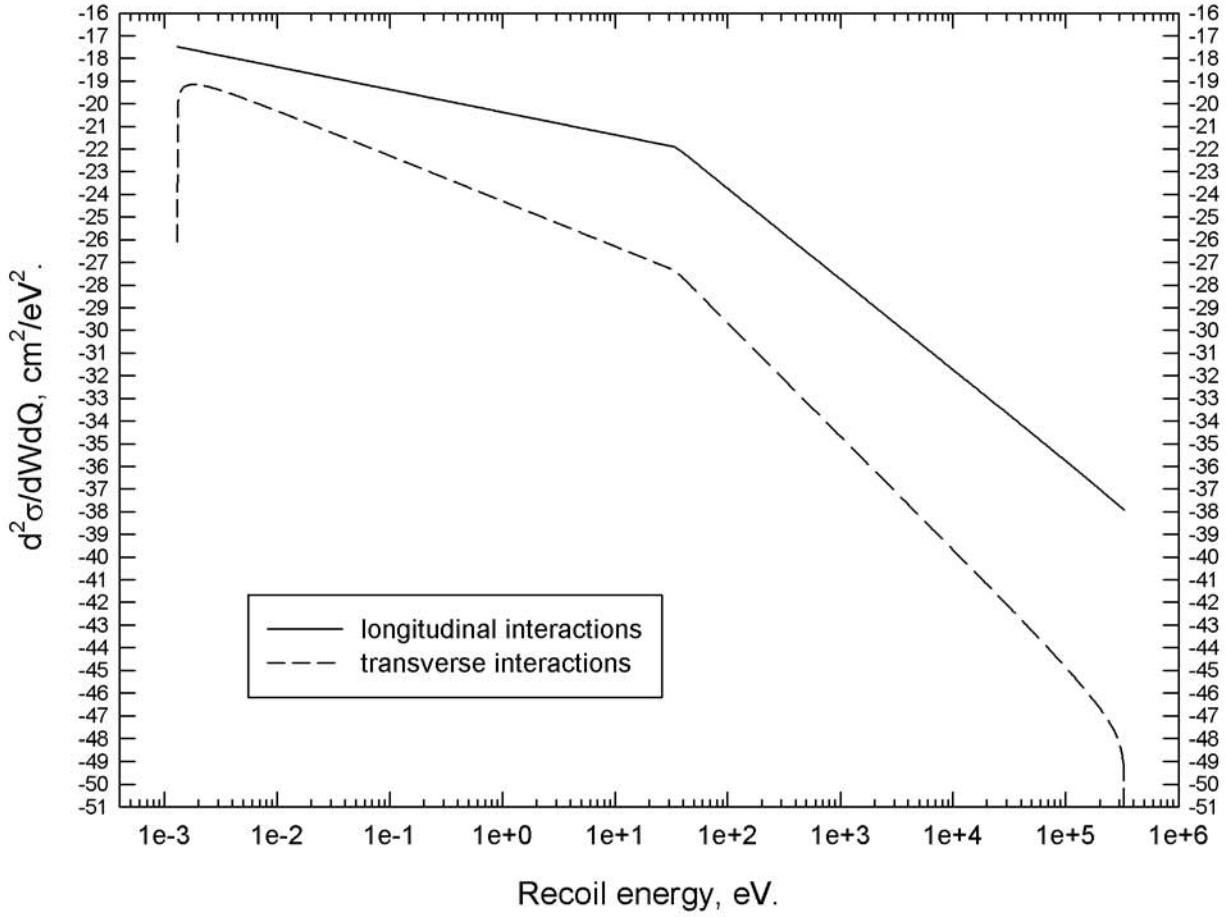

Figure 38. The energy loss and recoil energy differential interaction cross sections of 100 keV electrons with electrons from group three of calcium when the incident electrons experience 20 eV energy loss.

The energy loss and recoil energy differential interaction cross sections were calculated from the maximal energy loss that incident particles could experience in collisions with atomic electrons to zero energy loss, and from the minimal to the maximal recoil energy that incident particles could have at a given energy loss. The density with which the cross sections were calculated over the energy loss and recoil energy plane varied to ensure accurate integration of the cross sections by the recoil energy and by the energy loss.

The maximal energy loss, which incident electrons could experience in collisions with electrons of calcium, was calculated according to equation (45). Even though equation (45) does not account for the indistinguishability of incident and target electrons, and also for the binding of target electrons, the equation was still used for a calculation of the maximal energy loss. It was hypothesized during the course of calculations that the generalized oscillator strength function of calcium would account for binding and also for the orbital motion of target electrons, and collisions of incident particles with electrons of calcium could be considered as collisions with free electrons having zero initial linear momentums.

The maximal recoil energy, which incident electrons could have at different energy losses in collisions with electrons of calcium, was calculated according to equation (42). (The plus sign was applied in equation (42) during a calculation of the maximal recoil energy.) The minimal recoil energy, which incident electrons could have at different energy losses in collisions with electrons of calcium, was calculated according to equation (42) or equation (43). (If equation (42) was used for a calculation of the minimal recoil energy, then the minus sign was applied in the equation.) The choice between equations (42) and (43) was made according to a simple scheme. Initially, at large energy losses, equation (42) was used for a calculation of the minimal recoil energy. As soon as the minimal recoil energy, calculated according to equation (42),

turned equal to zero, equation (43) was engaged for a calculation of the minimal recoil energy. Once engaged, equation (43) was used for a calculation of the minimal recoil energy until the end of calculations performed for a given electron group of calcium.

Figure 39 shows the minimal and the maximal recoil energies that 100 keV electrons can have at different energy losses in collisions with electrons of calcium up to the energy loss equal to the kinetic energy of incident electrons. The stare-like shape of the graph for the minimal recoil energy, seen at small energy losses, as due to numerical errors in calculations performed according to equation (42).

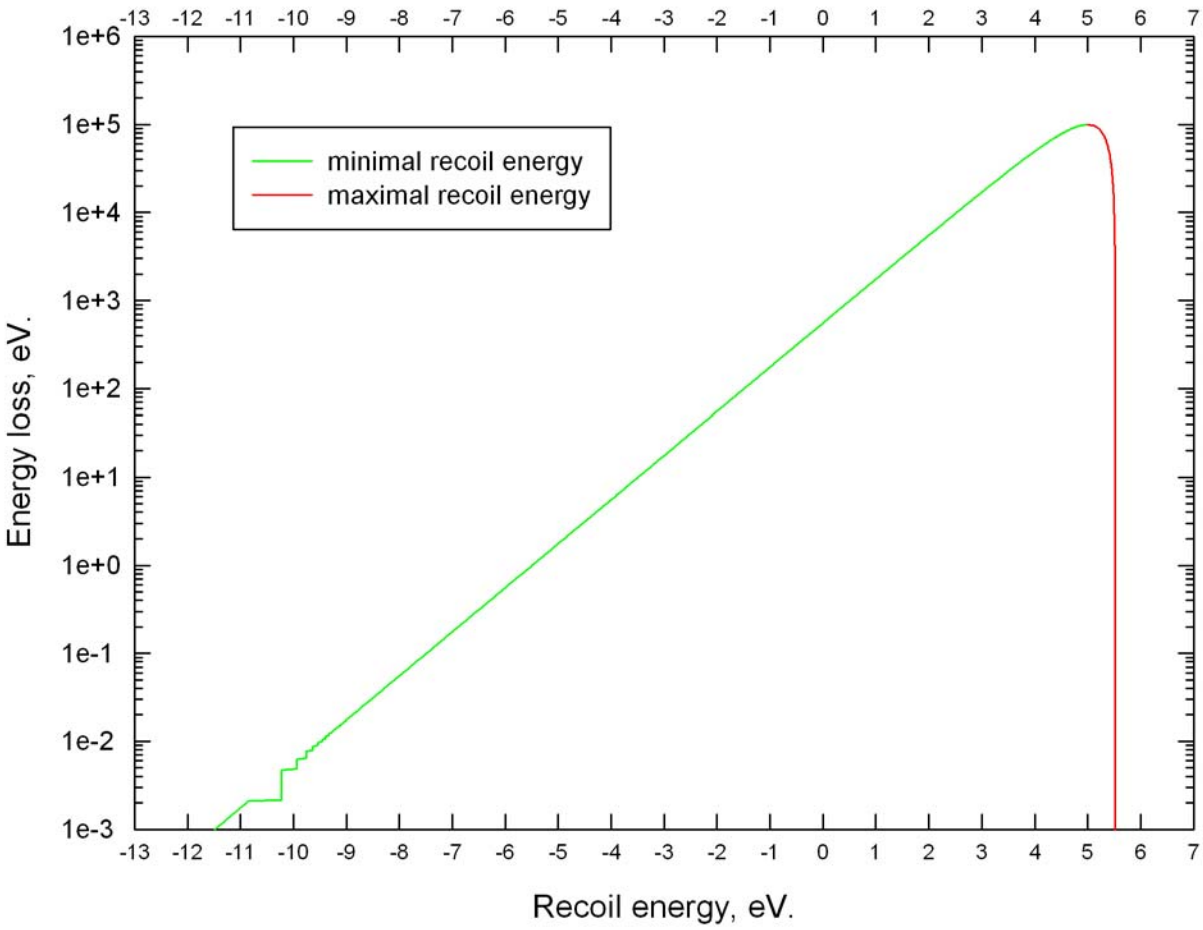

Figure 39. The minimal and the maximal recoil energies which 100 keV electrons can have at different energy losses in collisions with free electrons.

The energy loss differential interaction cross sections of 100 keV electrons with electrons of calcium were determined by an integration of the double differential interaction cross sections by the recoil energy. Calculations of the energy loss differential interaction cross sections were performed according to equation (40). Figure 40 shows the energy loss differential interaction cross sections of 100 keV electrons calculated for each electron group of calcium. The figure shows the cross sections which arise due to the longitudinal and the transverse interactions between incident electrons and electrons from the individual electron bands of metallic calcium, and the shells of atoms of calcium. The figure also shows the total longitudinal and the total transverse interaction cross sections obtained by a summation of the longitudinal and the transverse cross sections calculated for each electron group of calcium.

The energy loss differential interaction cross sections of 100 keV electrons with electrons of calcium were used for a calculation of the mean free path of and the stopping power to 100 keV electrons in calcium. The obtained values for the mean free path and the stopping power will be specified in the next section of the manuscript.

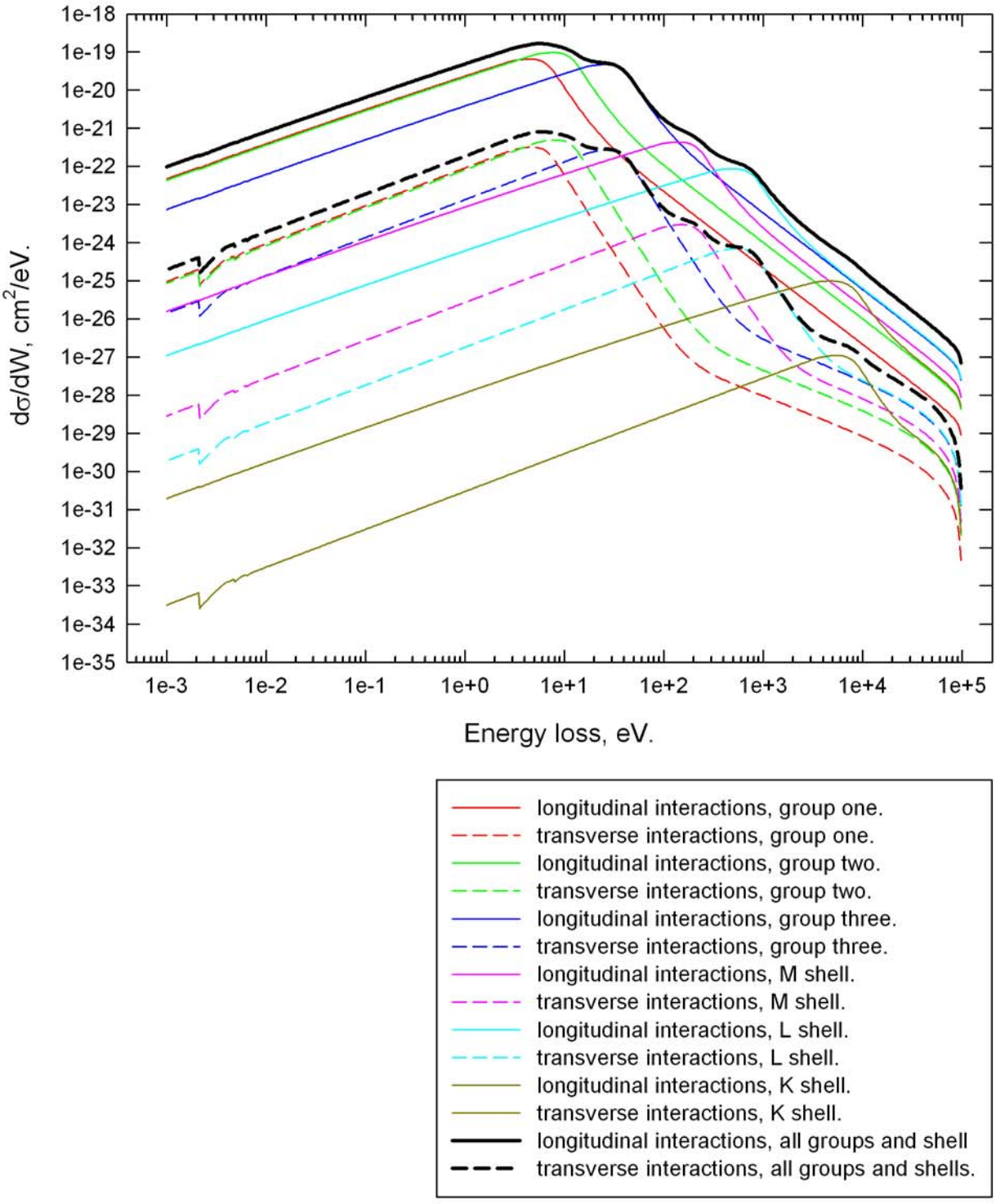

Figure 40. The energy loss differential interaction cross sections of 100 keV electrons with electrons of calcium.

The mean free path and the stopping power of electrons in calcium

The mean free path and the stopping power, calculated or measured for particles of a given kinetic energy, are just two scalar numbers. It is much more illustrative if one considers mean free paths and stopping powers of particles having different kinetic energy. Then one can plot the mean free paths and the stopping powers as a function of the kinetic energy of the particles.

The mean free paths and the stopping powers were calculated for electrons in calcium. Calculations were performed for electrons kinetic energy of which varied from 20 eV to 1 MeV. Calculations of the mean free path and of the stopping power were performed according to equations (46) and (47). The obtained mean free paths of electrons in calcium are plotted in figure 41. The stopping powers to electrons in calcium are plotted in figure 42.

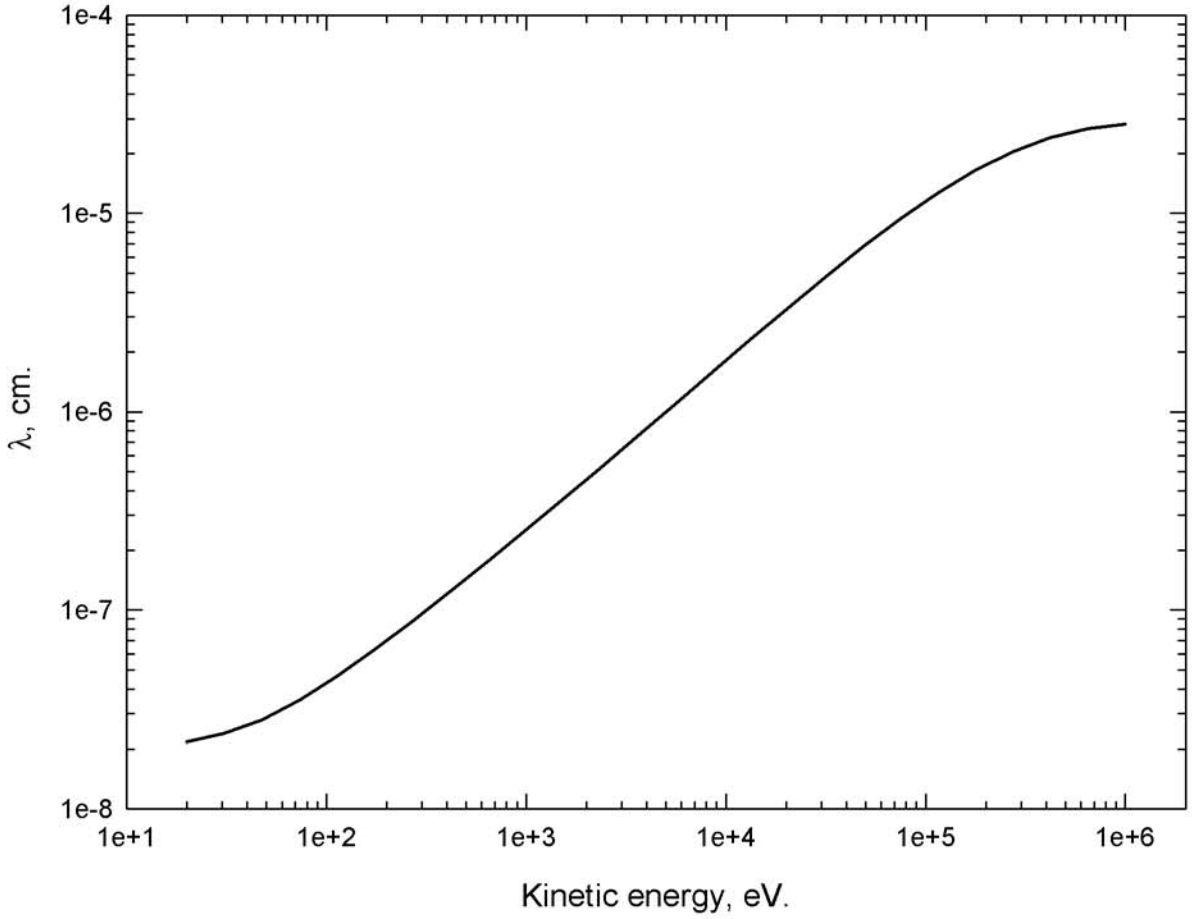

Figure 41. The mean free path of electrons having a given kinetic energy in calcium.

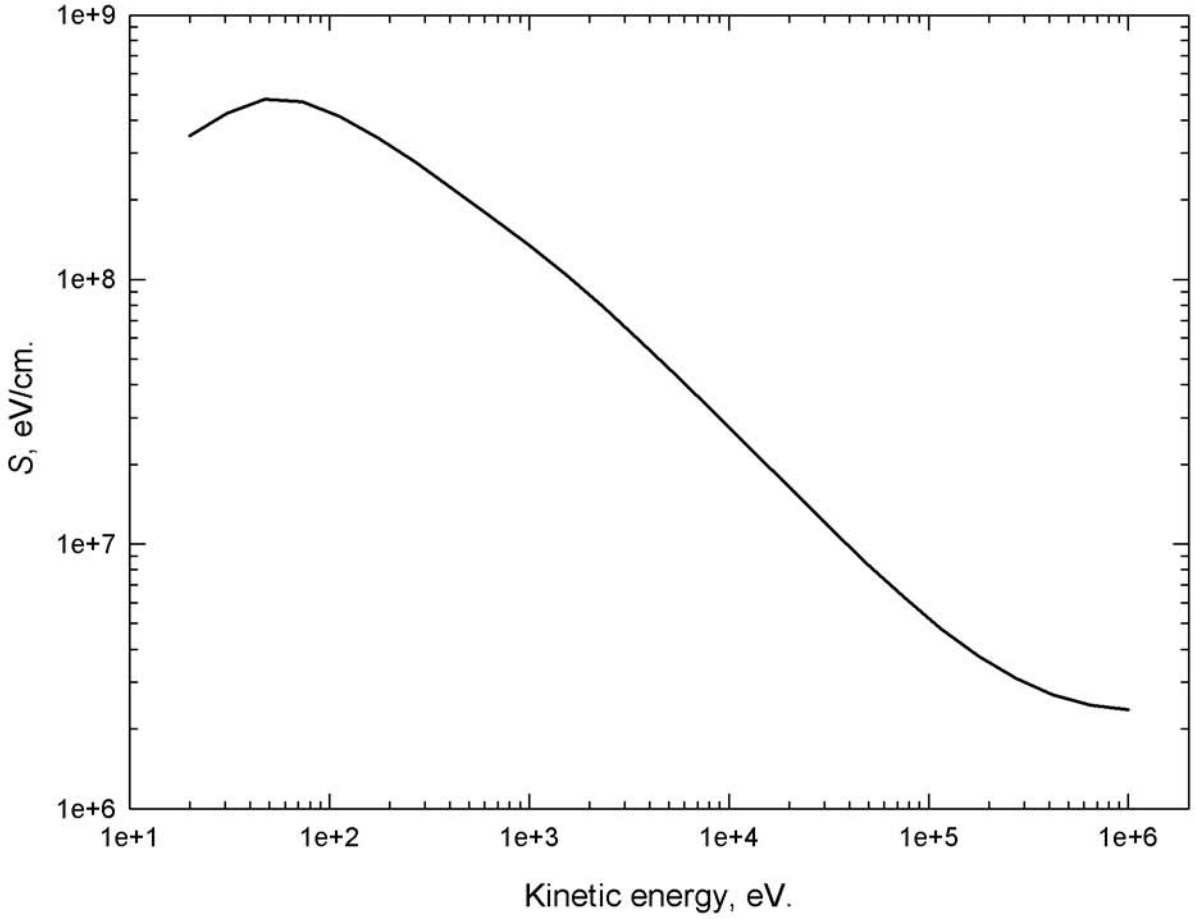

Figure 42. The stopping power to electrons having a given kinetic energy in calcium.

Unfortunately no data on interaction cross sections, the mean free path, or the stopping power of electrons in calcium were found in the literature. At this moment the cross sections, the mean free paths, and the stopping powers of electrons in calcium have to be taken as granted. There is, however, one reason to think that the cross sections, the mean free paths, and the stopping powers of electrons in calcium, calculated using the presented approach and the presented generalized oscillator strength function of calcium, are accurate. Similar calculations performed for protons in calcium yielded results which were in a reasonable agreement with the published material.

Interaction cross sections of 300 keV protons with electrons of calcium

Results of calculations of interaction cross sections of 300 keV protons with electrons of calcium are presented in the current section of the manuscript. One may argue that 300 keV protons have too small kinetic energy, and some of the conditions, at which the equations for interaction cross sections were derived, are not satisfied. At this moment the argument remains unanswered. In any case the goal of calculations, which happened to be performed for 300 keV protons, was to test the program which was written for a calculation of interaction cross sections, mean free paths, and stopping powers. Later calculations of interaction cross sections, mean free paths, and stopping powers included protons of much larger kinetic energy. The mean free paths and the stopping powers of different kinetic energy protons, including 300 keV protons, will be shown in the next section of the manuscript.

The energy loss and recoil energy differential interaction cross sections of protons with electrons of calcium were calculated according to equations (37) and (38). Equation (37) was used for a calculation of interaction cross sections which arise due to the longitudinal interactions between

incident charged particles and atomic electrons, while equation (38) was used for a calculation of interaction cross sections which arise due to the transverse interactions.

The total longitudinal energy loss and recoil energy differential interaction cross sections of 300 keV protons with electrons of calcium are shown in figure 43. The total longitudinal interaction cross sections were obtained by a summation of the longitudinal energy loss and recoil energy differential interactions cross sections calculated for each of the six electron groups of calcium. The total transverse energy loss and recoil energy differential interaction cross sections of 300 keV protons with electrons of calcium are shown in figure 44. The total transverse interaction cross sections were obtained by a summation of the transverse energy loss and recoil energy differential interactions cross sections calculated for the six electron groups of calcium.

Figure 45 shows the energy loss and recoil energy differential interaction cross sections of 300 keV protons with electrons of calcium calculated at 1 eV energy loss. The curves shown in the figure represent a cut through the surfaces shown in figures 43 and 44. Figure 45 shows the cross sections which arose due to the longitudinal and the transverse interactions between incident protons and calcium electrons. The figure shows the total longitudinal and the total transverse differential interaction cross sections obtained by a summation of the corresponding cross sections calculated for each of the six electron groups of calcium.

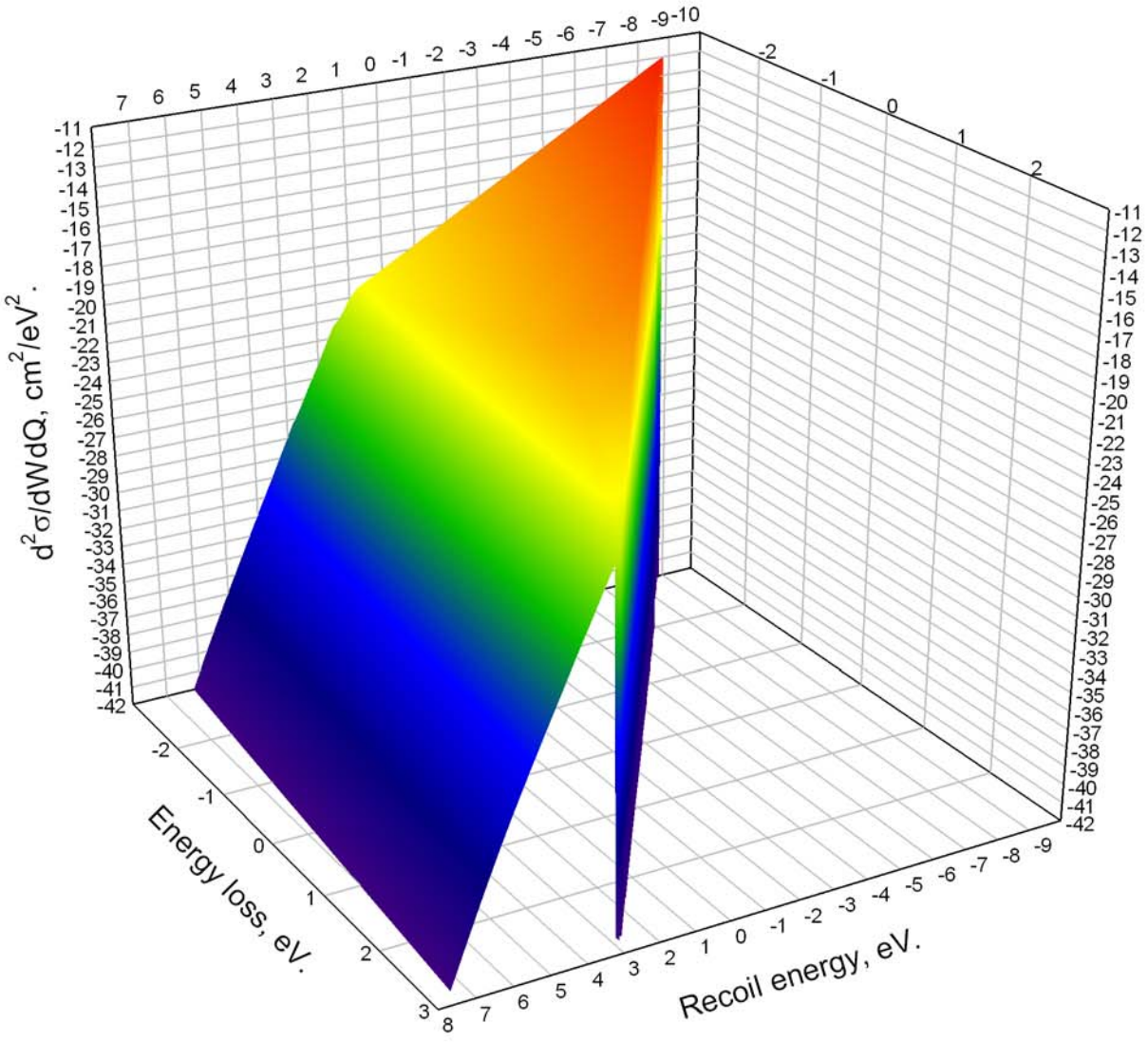

Figure 43. The energy loss and recoil energy differential interaction cross sections of 300 keV protons with electrons of calcium arising due to the longitudinal interactions between incident protons and target electrons.

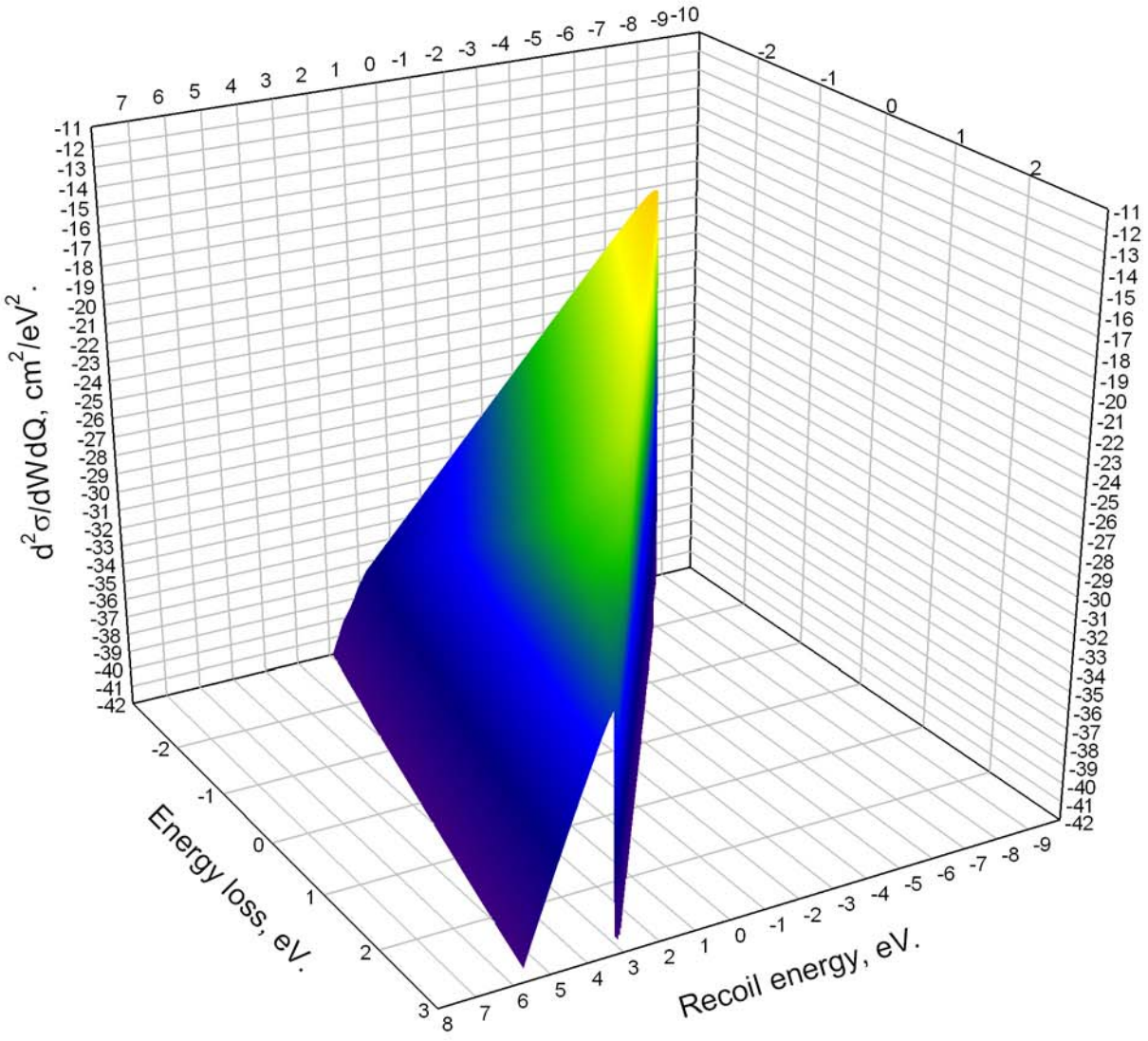

Figure 44. The energy loss and recoil energy differential interaction cross sections of 300 keV protons with electrons of calcium arising due to the transverse interactions between incident protons and target electrons.

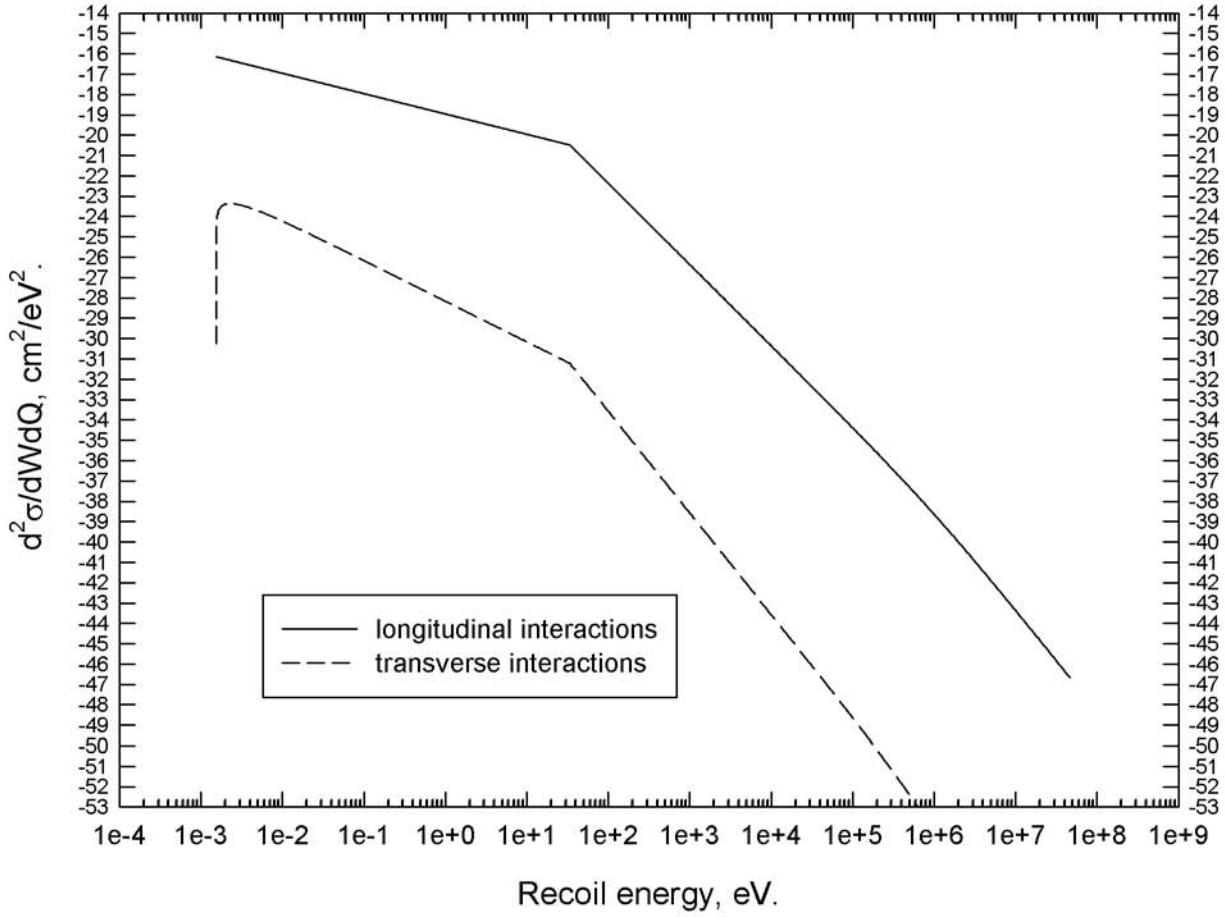

Figure 45. The energy loss and recoil energy differential interaction cross sections of 300 keV protons with electrons of calcium calculated at 1 eV energy loss.

The energy loss and recoil energy differential interaction cross sections of protons with electrons of calcium were calculated from the maximal energy loss that protons of a given kinetic energy could experience in collisions with electrons at rest to zero energy loss. The binding energies of electrons in bands of metallic calcium and in shells of calcium atoms were not considered during calculations of the maximal energy loss that protons could experience in collisions with electrons of calcium. In calculations of interaction cross sections it was assumed that the generalized oscillator strength function of the target material, calcium in the current case, accounts for the orbital motion and binding of target electrons. The maximal energy loss that protons of a given kinetic energy could experience in collisions with electrons of calcium was calculated according to equation (45).

The energy loss and recoil energy differential interaction cross sections of protons with electrons of calcium were calculated from the maximal to the minimal recoil energy that protons could have at a given energy loss. The minimal and the maximal recoil energies were calculated according to equation (42). The plus sign was used in equation (42) during a calculation of the maximal recoil energy. The minus sign was used in the equation during a calculation of the minimal recoil energy. If the minimal recoil energy turned equal to zero, then the energy loss and recoil energy differential interaction cross sections of protons with electrons from a given electron group of calcium were assumed equal to zero at the given energy loss and at any smaller energy losses. Figure 46 shows the minimal and the maximal recoil energies which 300 keV protons could have at different energy losses in collisions with calcium electrons which were basically assumed free and at rest.

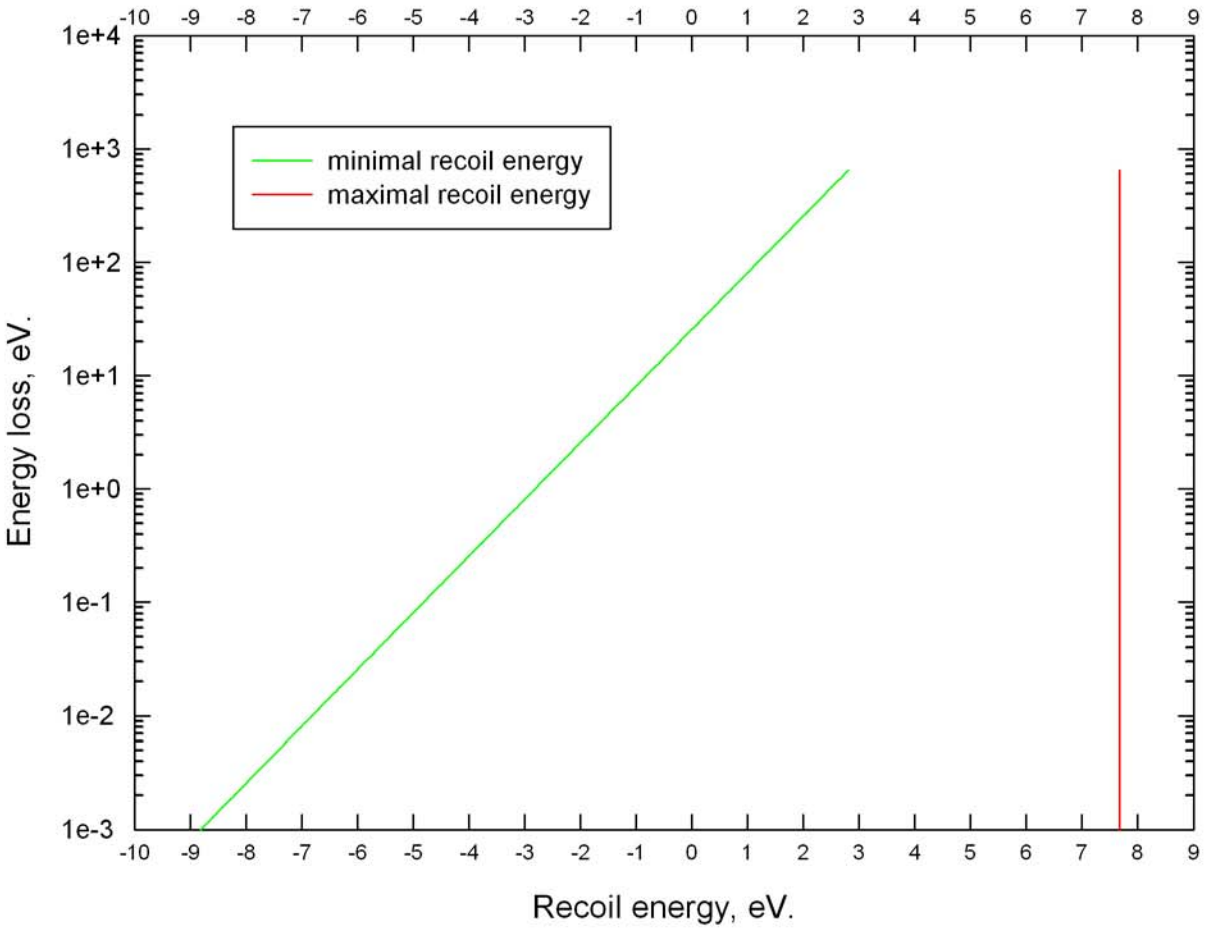

Figure 46. The minimal and the maximal recoil energies that 300 keV protons can have at different energy losses in collisions with electrons of calcium.

The energy loss differential interaction cross sections of protons with electrons of calcium were obtained by an integration of the double differential interaction cross sections by the recoil energy at each energy loss that protons could have in collisions with atomic electrons. Calculations of the energy loss differential interactions cross sections were performed according to equation (40).

The energy loss differential interaction cross sections of 300 keV protons with electrons of calcium are shown in figure 47. The figure shows the cross sections calculated for each electron group of calcium, and for the longitudinal and the transverse interactions between incident protons and calcium electrons. The total longitudinal and the total transverse energy loss differential interaction cross sections of protons with calcium electrons are also shown in the figure. The total longitudinal and the total transverse energy loss differential interaction cross sections were obtained by a summation of corresponding cross sections calculated for electrons from each of the six electron groups of calcium.

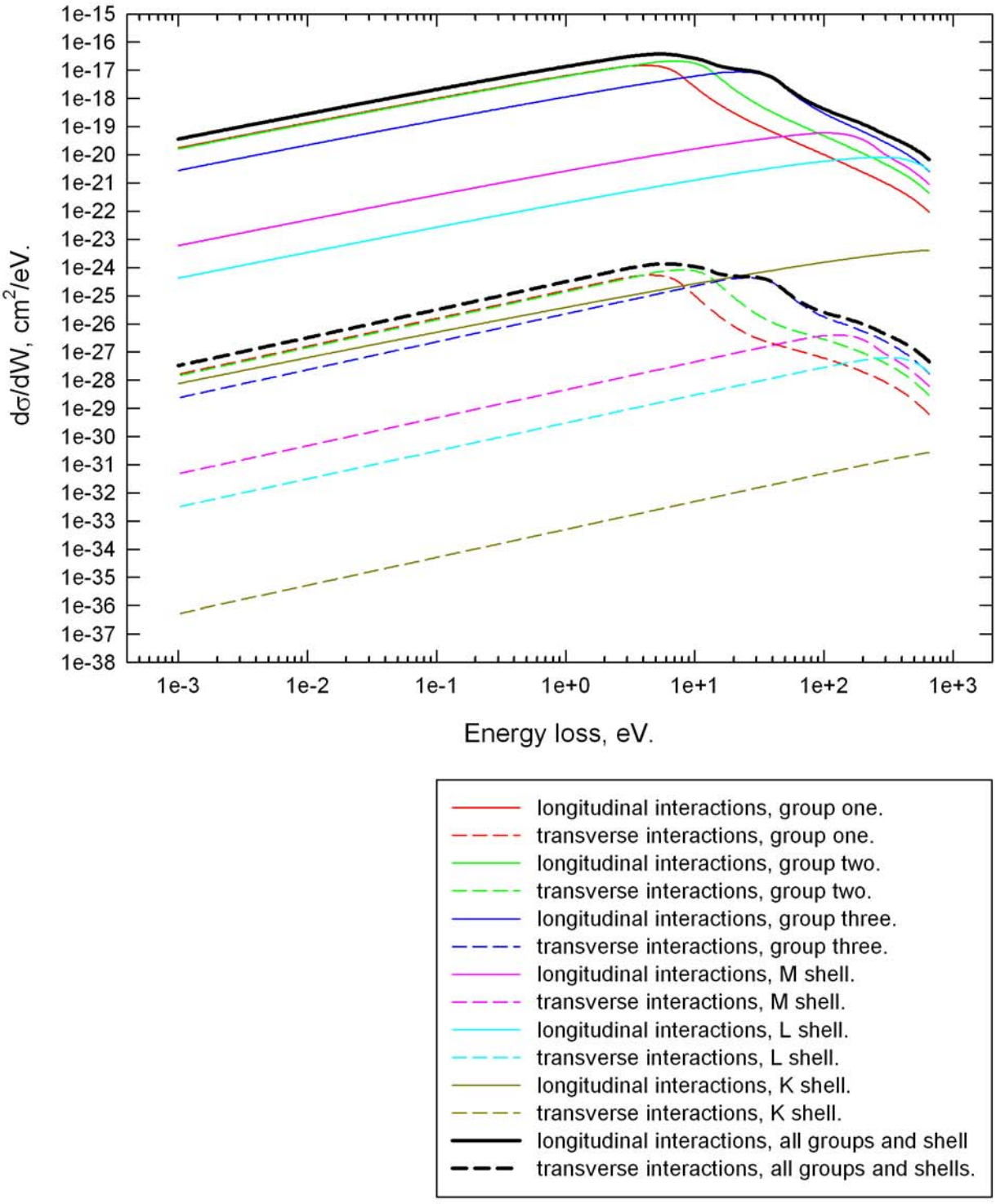

Figure 47. The energy loss differential interaction cross sections of 300 keV protons with electrons from the different electron groups of calcium.

The energy loss differential interaction cross sections of 300 keV protons with electrons of calcium were used for a calculation of the mean free path of and the stopping power to the protons in calcium. Calculations of the mean free path and the stopping power were performed according to equations (44), (46), and (47). Mean free paths and stopping powers of protons of different kinetic energy, including 300 keV protons, in calcium will be shown in the next section of the manuscript.

The mean free path and the stopping power of 1 keV to 10 GeV protons in calcium

The mean free paths of and the stopping powers to protons in calcium were calculated using the program developed over the course of the work. The mean free paths and the stopping powers were calculated for protons the kinetic energy of which varied from 1 keV to 10 GeV. Calculations of the mean free path and the stopping power of protons of any kinetic energy from the range were performed in a way completely similar to the one used for a calculation of interaction cross sections, the mean free path, and the stopping power of 300 keV protons in calcium. First the energy loss and recoil energy differential interaction cross sections of protons of a given kinetic energy with electrons of calcium were calculated. Then the cross sections were integrated by the recoil energy. The resulting energy loss differential interaction cross sections were used for a calculation of the mean free path and the stopping power of protons of the given kinetic energy in calcium.

Figure 48 shows the mean free paths of 1 keV to 10 GeV protons in calcium. Figure 49 shows the stopping powers to protons of the specified kinetic energy in calcium. Figure 49 also shows the data on the stopping power to protons in calcium found in the literature. Please see

the References section of the manuscript for the sources of the data on the stopping power of protons in calcium.

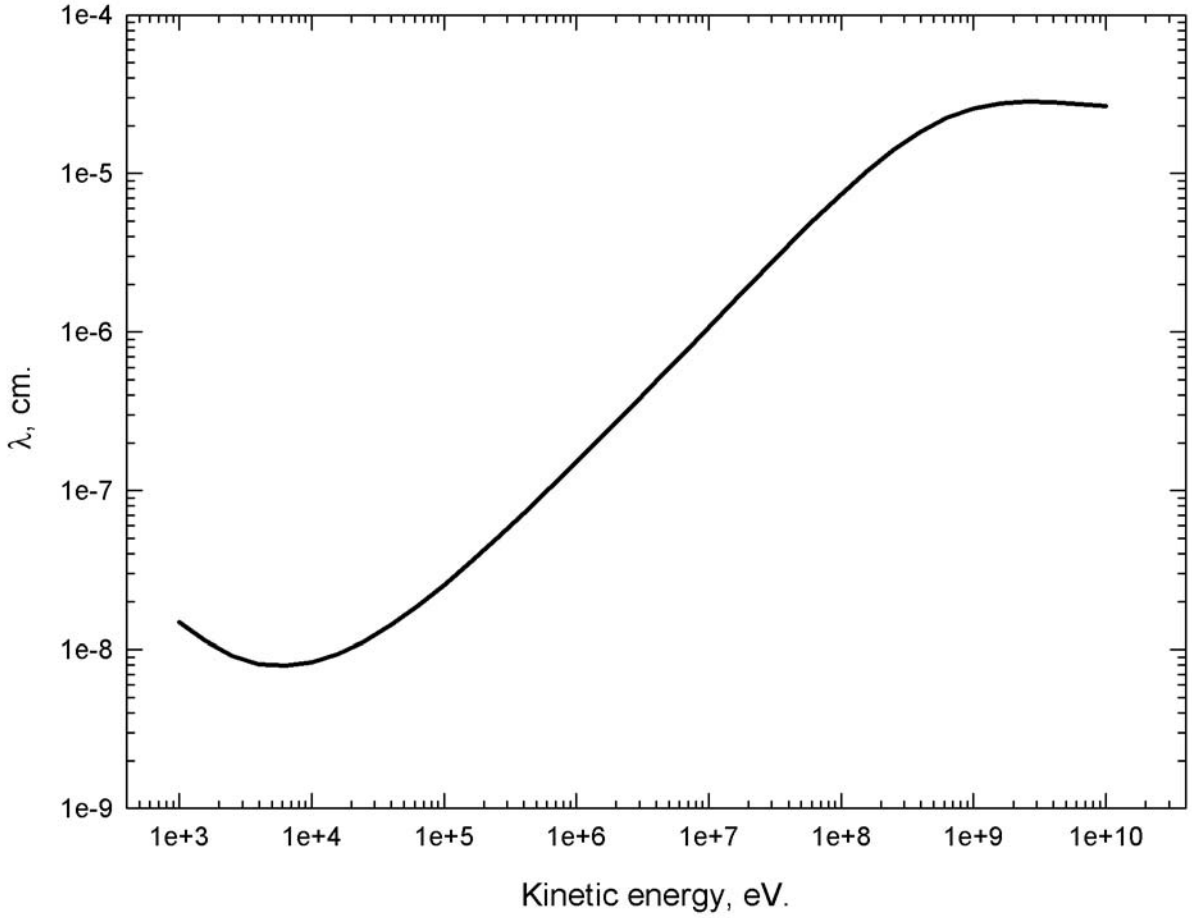

Figure 48. The mean free paths of protons of different kinetic energy in calcium.

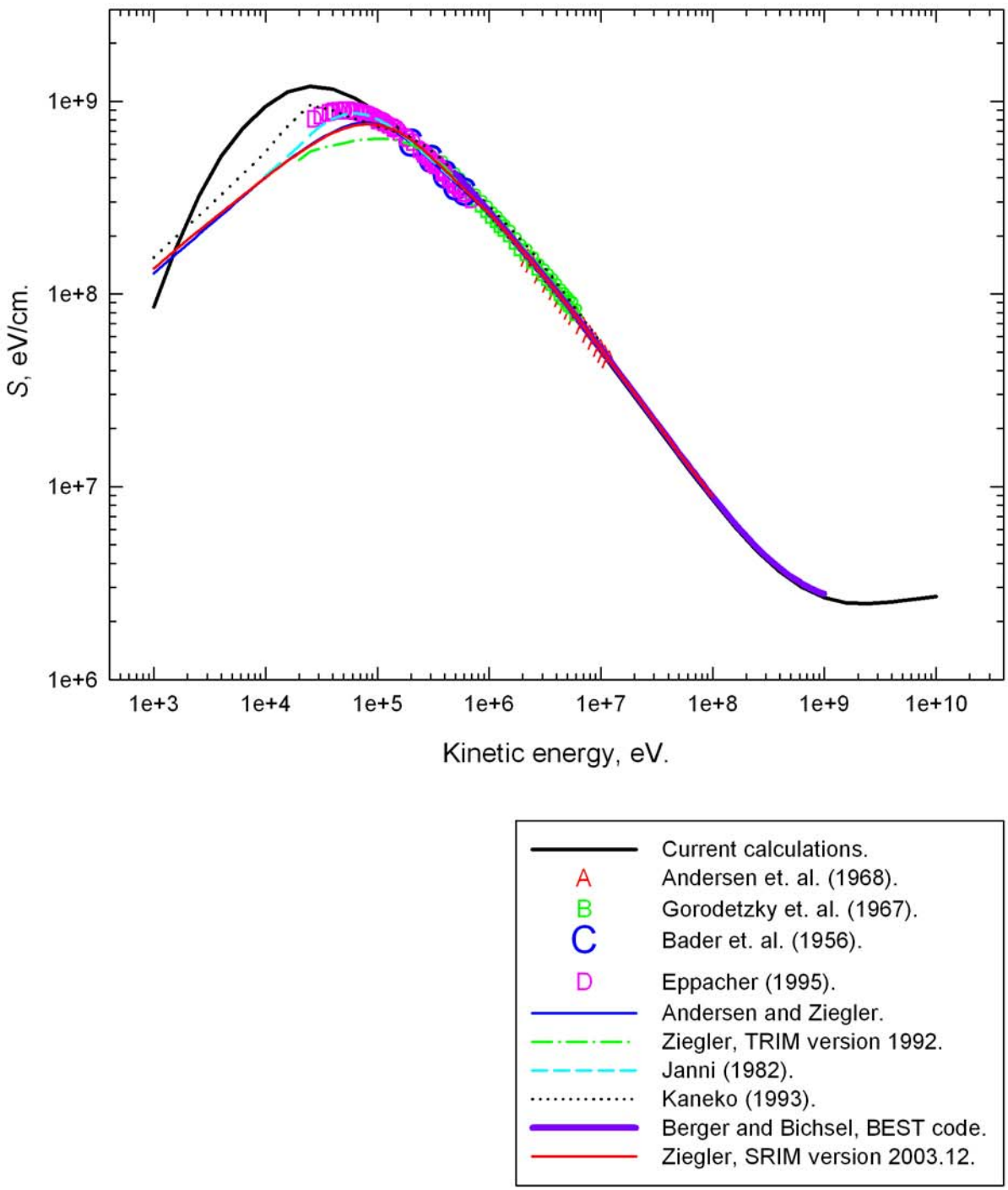

Figure 49. The stopping powers to protons of different kinetic energy in calcium.

Interaction cross sections of 2 MeV alpha particles with electrons of calcium

Calculations of interaction cross sections of alpha particles with electrons of calcium were performed in a way completely similar to the one used for a calculation of interaction cross sections of protons with electrons of calcium. Equations (37) and (38) were used for a calculation of the energy loss and recoil energy differential interaction cross sections of alpha particles of a given kinetic energy with electrons of calcium. The cross sections were calculated from zero to the maximal energy loss that alpha particles could experience in collisions with calcium electrons. Electrons of calcium were again assumed free and at rest. It was hypothesized in the course of calculations that the generalized oscillator strength function of calcium would account for binding and also for the orbital motion of target calcium electrons during calculations of interaction cross sections. The maximal energy loss, which alpha particles could experience in collisions with calcium electrons, was calculated according to equation (45). The maximal and the minimal recoil energies, which alpha particles could have at any given energy loss, were calculated according to equation (42). If the minimal recoil energy, calculated according to equation (42), turned equal to zero, then the double differential interaction cross sections, calculated for a particular electron group of calcium, were assumed equal to zero at the given and at any smaller energy losses. The energy loss differential interaction cross sections of alpha particles with electrons of calcium were obtained by an integration of the double differential interaction cross sections by the recoil energy. The energy loss differential interaction cross sections were used for a calculation of the mean free path and the stopping power of alpha particles of a given kinetic energy in calcium.

The energy loss and recoil energy differential interaction cross sections of 2 MeV alpha particles with electrons of calcium are shown in figures 50 and 51. Figure 50 shows the cross sections

which arise due to the longitudinal interactions between incident particles and target electrons, while figure 51 shows the cross sections which arise due to the transverse interactions. Please note that both figures show the total cross sections obtained by a summation of the cross sections, longitudinal or transverse, calculated for each electron group of calcium.

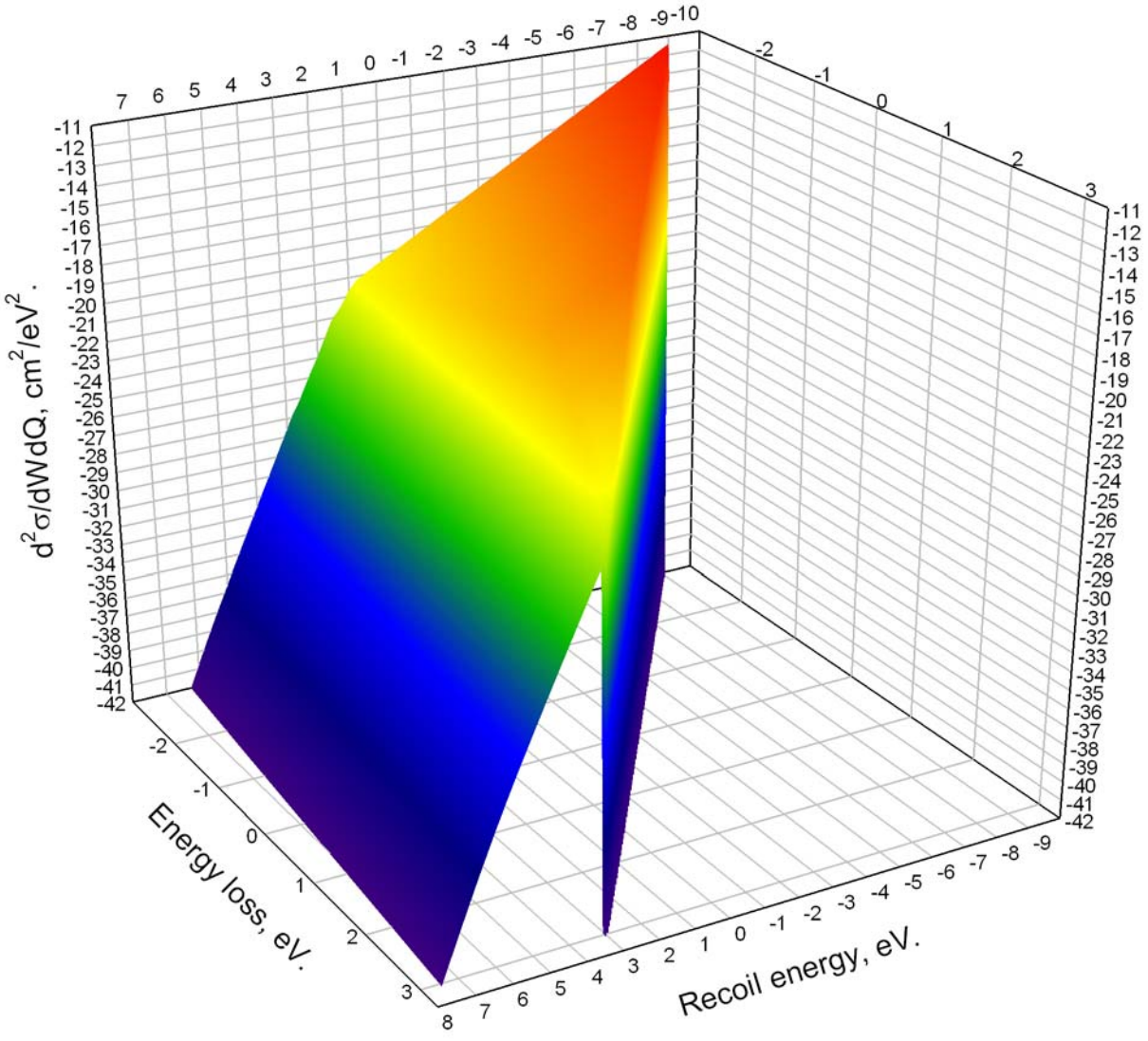

Figure 50. The energy loss and recoil energy differential interaction cross sections of 2 MeV alpha particles with electrons of calcium arising due to the longitudinal interactions between incident particles and target electrons.

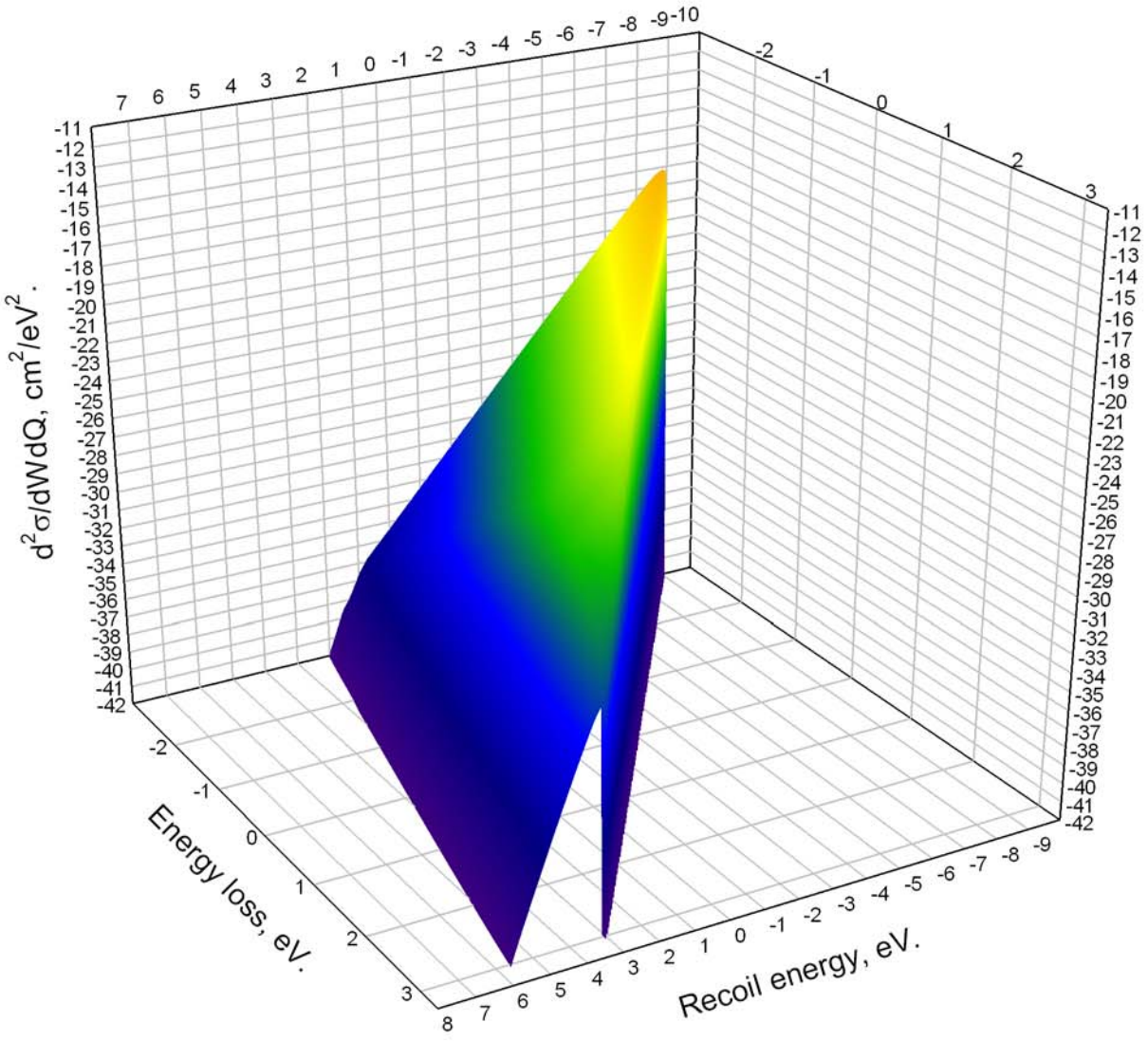

Figure 51. The energy loss and recoil energy differential interaction cross sections of 2 MeV alpha particles with electrons of calcium arising due to the transverse interactions between incident particles and target electrons.

The minimal and the maximal recoil energies, which 2 MeV alpha particles could have at different energy losses, are shown in figure 52. The figure shows the minimal and the maximal recoil energies for energy losses ranging from practically zero to the maximal energy loss which 2 MeV alpha particles could experience in collisions with calcium electrons. The curves for the minimal and the maximal recoil energy terminate in the limit of large energy losses at the maximal energy loss that 2 MeV alpha particles could experience in collisions with calcium electrons.

The energy loss differential interaction cross sections of 2 MeV alpha particles with electrons of calcium are shown in figure 53. The cross sections were obtained by an integration of the double differential interaction cross sections by the recoil energy. Figure 53 shows the cross sections for each electron group of calcium, and for the longitudinal and the transverse interactions between incident alpha particles and calcium electrons. The figure also shows the total longitudinal and the total transverse energy loss differential interaction cross sections obtained by a summation of corresponding energy loss differential interaction cross sections calculated for each electron group of calcium.

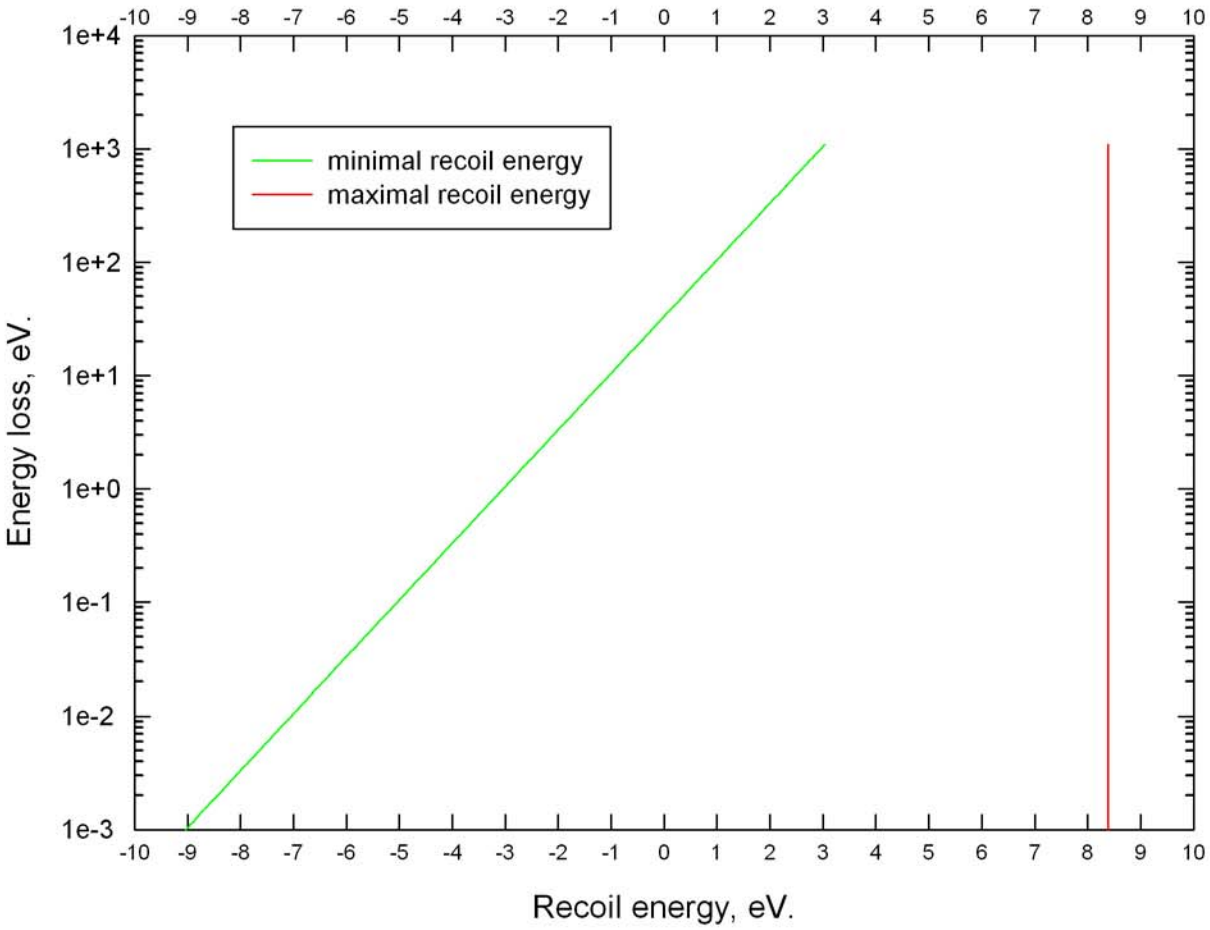

Figure 52. The minimal and the maximal recoil energies which 2 MeV alpha particles could have at different energy losses in collisions with calcium electrons.

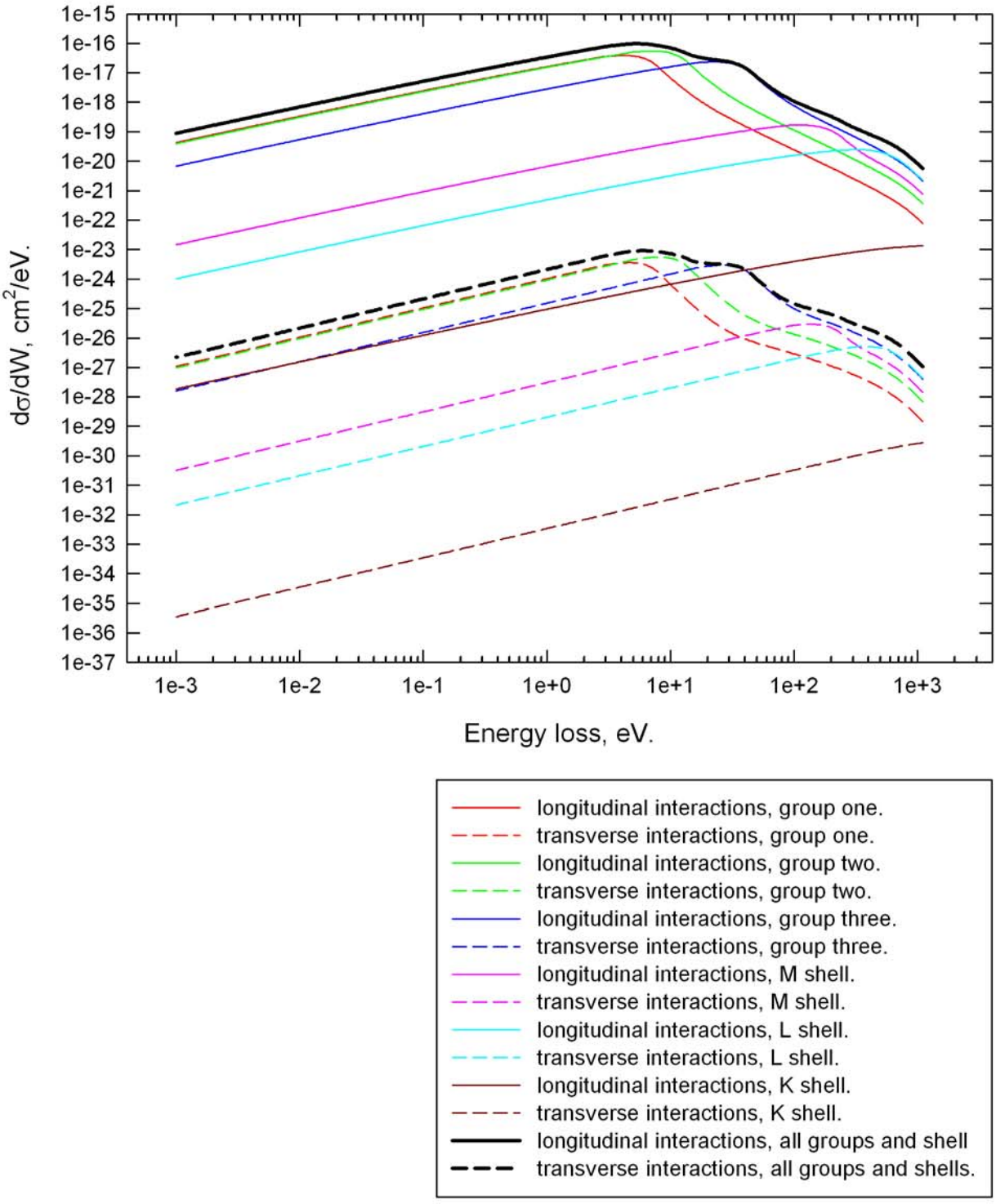

Figure 53. The energy loss differential interaction cross sections of 2 MeV alpha particles with electrons of calcium.

The energy loss differential interaction cross sections of 2 MeV alpha particles with calcium electrons were used for a calculation of the mean free path and the stopping power of the particles in calcium. The mean free paths of and the stopping powers to alpha particles of different kinetic energy in calcium are shown in the next section of the manuscript. The results, presented in the next section, include the mean free path and the stopping power calculated for 2 MeV alpha particles in calcium.

The mean free path and the stopping power of alpha particles in calcium

The mean free paths and the stopping powers were calculated for 6 keV to 60 MeV alpha particles in calcium. The mean free paths and the stopping powers were calculated in a way completely similar to the one described for 2 MeV alpha particles, or for 300 keV protons. Figure 54 shows the mean free path of 6 keV to 60 MeV alpha particles in calcium. Figure 55 shows the stopping power to alpha particles in calcium. Figure 55 also shows the stopping power to alpha particles in calcium found in the literature.

Considering figure 55 one may see that the curve, showing calculated stopping power to alpha particles in calcium, exhibit the same behavior as the curve and the data points showing the data found in the literature. The calculated stopping powers are, however, much larger then the stopping powers found in the literature for 2 MeV or smaller kinetic energy alpha particles. At this moment it is unclear why calculated stopping powers differ from the reported ones. One of the many reasons why calculated stopping powers differ from the reported stopping powers could be methodological one.

The mean free paths and the stopping powers of alpha particles in calcium were calculated using the energy loss differential interaction cross sections which, in their turn, were calculated by an

integration of the energy loss and recoil energy differential interaction cross sections. The energy loss and recoil energy differential interaction cross sections of alpha particles with electrons of calcium were calculated using the equations which were derived for spin ½ charged particles. The net spin of alpha particles, as is commonly known, is zero. The stopping powers, calculated for alpha particles, could deviate from the stopping powers reported in the literature due to the fact that the cross sections, used in calculations of the stopping powers, were calculated using the equations which might not be suitable for alpha particles.

Even though it was known from the very beginning that the equations for the energy loss and recoil energy differential interaction cross sections, equations (37) and (38), were derived for spin ½ charged particles, the equations were used for a calculation of interaction cross sections, the mean free paths, and the stopping powers of particles the spin of which differed from ½ in order to test a hypothesis about scaling of cross sections. The hypothesis about scaling of interaction cross sections is discussed in the next section of the manuscript.

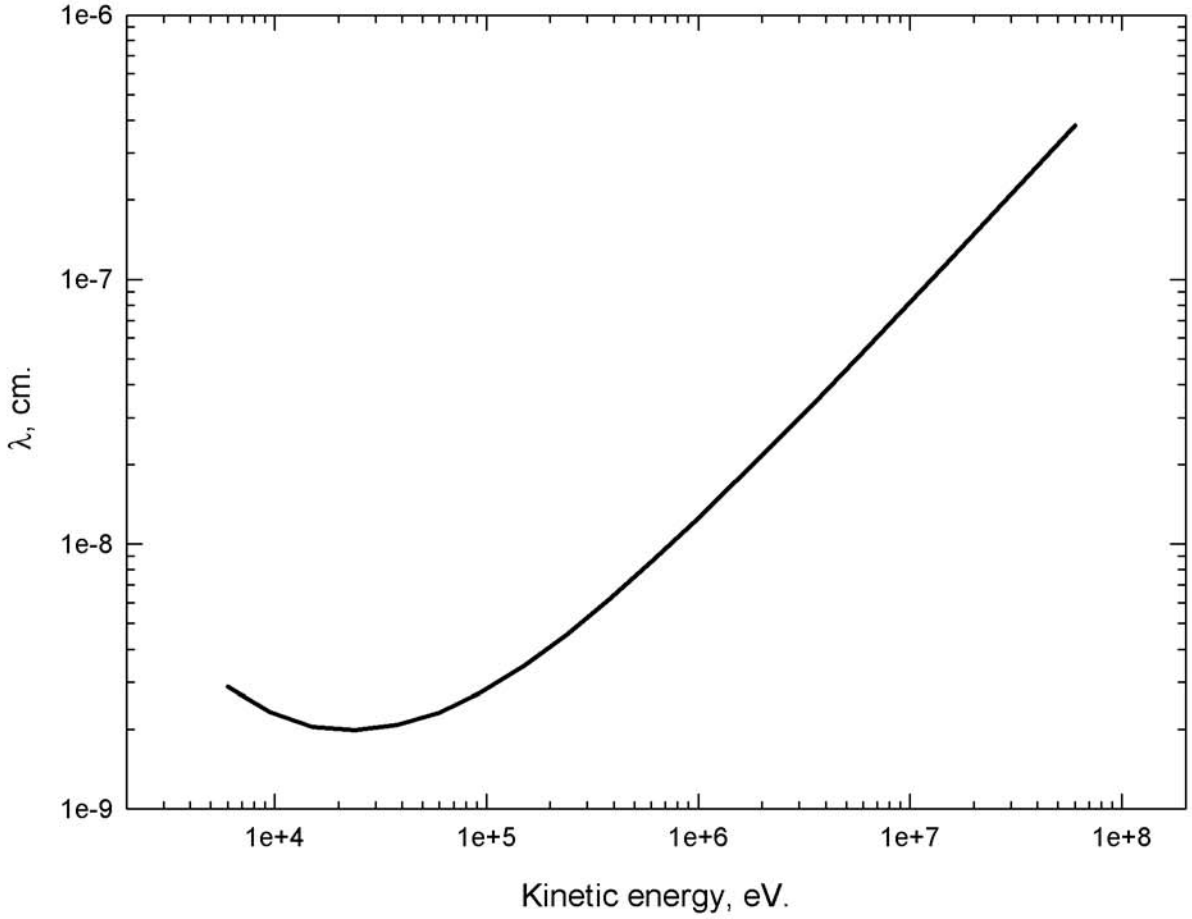

Figure 54. The mean free path of alpha particles in calcium.

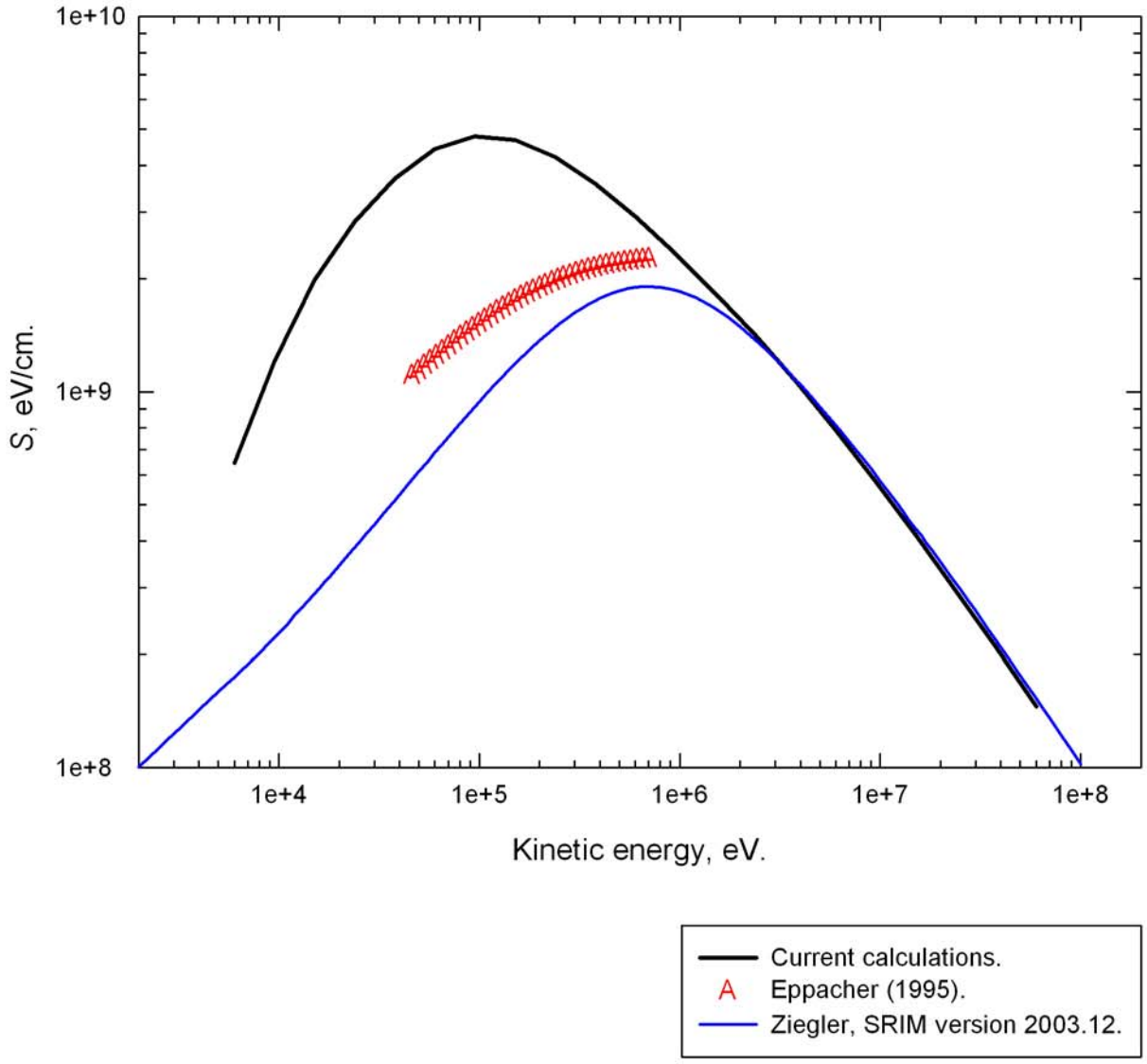

Figure 55. The stopping power to alpha particles in calcium.

Charge, speed, and mass scaling of interaction cross sections

It was hypothesized, private communications with Prof. Dingfelder, Dingfelder et al (2006), that the energy loss and recoil energy differential interaction cross sections of one particles with electrons of a given target material can be determined from interaction cross sections of other particles by scaling. The idea about scaling of interaction cross sections seemed very attractive. In computer programs, used for modeling passage of charged particles through media, the possibility for scaling interaction cross sections would eliminate the need for a repetitive calculation of the cross sections, would drastically increase the speed of computer calculations, would significantly reduce the demands for computer memory, etc. In the current section of the manuscript the hypothesis about scaling of interaction cross sections is presented and examined.

If one considers the equation for the energy loss and recoil energy differential interaction cross sections which arise due to the longitudinal interactions between incident particles and target electrons, equation (37), one will see that the cross sections depend only on the charge and the speed of incident particles. A ratio of interaction cross sections, calculated for particles carrying different charges and moving at different speeds, reduces to a ratio of charges of the particles squared, and a ratio of speeds of the particles squared.

Let $Z_{(R)}$ and $\upsilon_{(R)} = \beta_{(R)} \cdot c$ be the charge and the speed of particles for which the energy loss and recoil energy differential interaction cross sections, arising due to the longitudinal interactions between incident particles and target electrons, are known. Let $Z_{(U)}$ and $\upsilon_{(U)} = \beta_{(U)} \cdot c$ be the charge and the speed of particles for which the energy loss and recoil energy differential

interaction cross sections are being determined. A ratio of unknown interaction cross sections $\frac{d^2\sigma_{L,(U)}}{dWdQ}$ to known cross sections $\frac{d^2\sigma_{L,(R)}}{dWdQ}$ will be:

$$\frac{d^2\sigma_{L,(U)}}{dWdQ} \Big/ \frac{d^2\sigma_{L,(R)}}{dWdQ} = \left(\frac{Z_{(U)}}{Z_{(R)}}\right)^2 \cdot \left(\frac{\upsilon_{(R)}}{\upsilon_{(U)}}\right)^2 . \tag{49}$$

Now if one considers the equations for the energy loss and recoil energy differential interaction cross sections which arise due to the transverse interactions between incident particles and target electrons, equations (38) and (39), one will see that the cross sections depend on the charge, the speed, and, additionally, the mass of incident particles through parameter β_t. (Parameter β_t is the component of $\vec{\beta} = \vec{\upsilon}/c$ which is perpendicular to $\vec{q}$, the momentum transfer. For a definition of $\vec{\beta}$, $\vec{q}$, $\vec{p}$, and the other parameters please see the sections of the manuscript in which an introduction to the kinematics of inelastic collisions is provided, and the parameters, used for a description of incident particles before and after a collision, are introduced.)

In the case of interaction cross sections which arise due to the transverse interactions between incident particles and target electrons, a ratio of interaction cross sections, calculated for particles carrying different charges and moving at different speeds, reduces to a ratio of the charges of the particles squared, the speeds of the particles squared, and parameters β_t of the particles squared.

Let $\beta_{t,(R)}$ pertain to particles of mass $M_{(R)}$ for which the energy loss and recoil energy differential interaction cross sections, arising due to the transverse interactions between incident particles and target electrons, are known. Let $\beta_{t,(U)}$ pertain to particles of mass $M_{(U)}$ for which

the interaction cross sections are being determined. A ratio of unknown interaction cross sections $\frac{d^2\sigma_{T,(U)}}{dWdQ}$ to known cross sections $\frac{d^2\sigma_{T,(R)}}{dWdQ}$ will be:

$$\frac{d^2\sigma_{T,(U)}}{dWdQ} \Big/ \frac{d^2\sigma_{T,(R)}}{dWdQ} = \left(\frac{Z_{(U)}}{Z_{(R)}}\right)^2 \cdot \left(\frac{\upsilon_{(R)}}{\upsilon_{(U)}}\right)^2 \cdot \left(\frac{\beta_{t,(U)}}{\beta_{t,(R)}}\right)^2 . \tag{50}$$

Equations (49) and (50) clearly show that the energy loss and recoil energy differential interaction cross sections of particles having a given mass, carrying a given charge, and traveling at a given speed can be determined from interaction cross sections of particles having a completely different mass, charge, and speed. Such flexibility in scaling of interaction cross sections is very honorably, but it is also suspicious. Maybe because of such incredible flexibility of the approach it was proposed in the article by Dingfelder et al (2006) to apply scaling of interaction cross sections only to particles traveling at the same speed.

Scaling of energy loss and recoil energy differential interaction cross sections needs to be performed with caution. Particles having different masses and different kinetic energies will experience different maximal energy losses, and will have different minimal and maximal recoil energies in collisions with electrons of a given target material. One needs to assure that reference cross sections exist at requested energy loss and recoil energy during scaling of interaction cross sections of one particles from interaction cross sections of other particles. Extrapolation of reference interaction cross sections beyond kinematically allowed energy losses and recoil energies may not work in some cases. For example, considering cuts through the graphs showing the energy loss and recoil energy differential interaction cross sections of 100 keV electrons with electrons of calcium, figure 38, or 300 keV protons with electrons of calcium, figure 45, one may already have noticed that the cross sections, arising due to the transverse

interactions between incident particles and target electrons, drop to zero at the minimal and the maximal recoil energies. An extrapolation of the transverse differential interaction cross sections beyond the kinematically allowed minimal and maximal recoil energies will yield zero.

The hypothesis about scaling of interaction cross sections was tested by a calculation of interaction cross sections of alpha particles and protons with electrons of calcium, and a comparison of the cross sections. It is necessary to point out that calculations of the cross sections were performed for alpha particles and protons moving at the same speed. It is, of course, a special case. According to equations (49) and (50) the speeds of incident particles, for which the cross sections are being scaled, need not to be the same. Also it is necessary to point out that the energy loss differential interaction cross sections of alpha particles and protons were compared, not the energy loss and recoil energy differential interaction cross sections. At the time when the analysis was performed the interest was to see how kinematically allowed recoil energies affect the results of an integration of the double differential interaction cross sections by the recoil energy.

Calculations of interaction cross sections were performed for 2 MeV alpha particles and 503.4 keV protons. Please note that 503.4 keV protons travel at the same speed as 2 MeV alpha particles. The energy loss and recoil energy differential interaction cross sections of 2 MeV alpha particles with electrons of calcium, arising due to the longitudinal and the transverse interactions between incident particles and target electrons, were shown in figures 50 and 51. The energy loss differential interaction cross sections of 2 MeV alpha particles with electrons of calcium were shown in figure 53. The energy loss differential interaction cross sections of 503.4 keV protons with electrons of calcium are shown in figure 56. The figure shows the cross sections which arise due to the longitudinal and the transverse interactions between 503.4 keV

protons and electrons from each electron group of calcium. The figure also shows the total longitudinal and the total transverse energy loss differential interaction cross sections of protons obtained by a summation of corresponding energy loss differential interaction cross sections calculated for each electron group of calcium. The energy loss differential interaction cross sections of 2 MeV alpha particles and 503.4 keV protons were compared.

Figure 57 shows the total longitudinal and the total transverse energy loss differential interaction cross sections of 2 MeV alpha particles and of 503.4 keV protons. The figure also shows the proton cross sections multiplied by four. Four here comes from the charge of alpha particles squared. In figure 57 the graphs for the energy loss differential interaction cross sections of 503.4 keV protons multiplied by four clearly overlap with the graphs for the energy loss differential interaction cross sections of 2 MeV alpha particles. The fact that the graphs for the cross sections of protons multiplied by four overlap with the graphs for the cross sections of alpha particles confirms the hypothesis about scaling of interaction cross sections. A comprehensive analysis of the hypothesis about scaling of interaction cross sections should consider particles traveling at different speeds, and should focus on a comparison of the energy loss and recoil energy differential interaction cross sections.

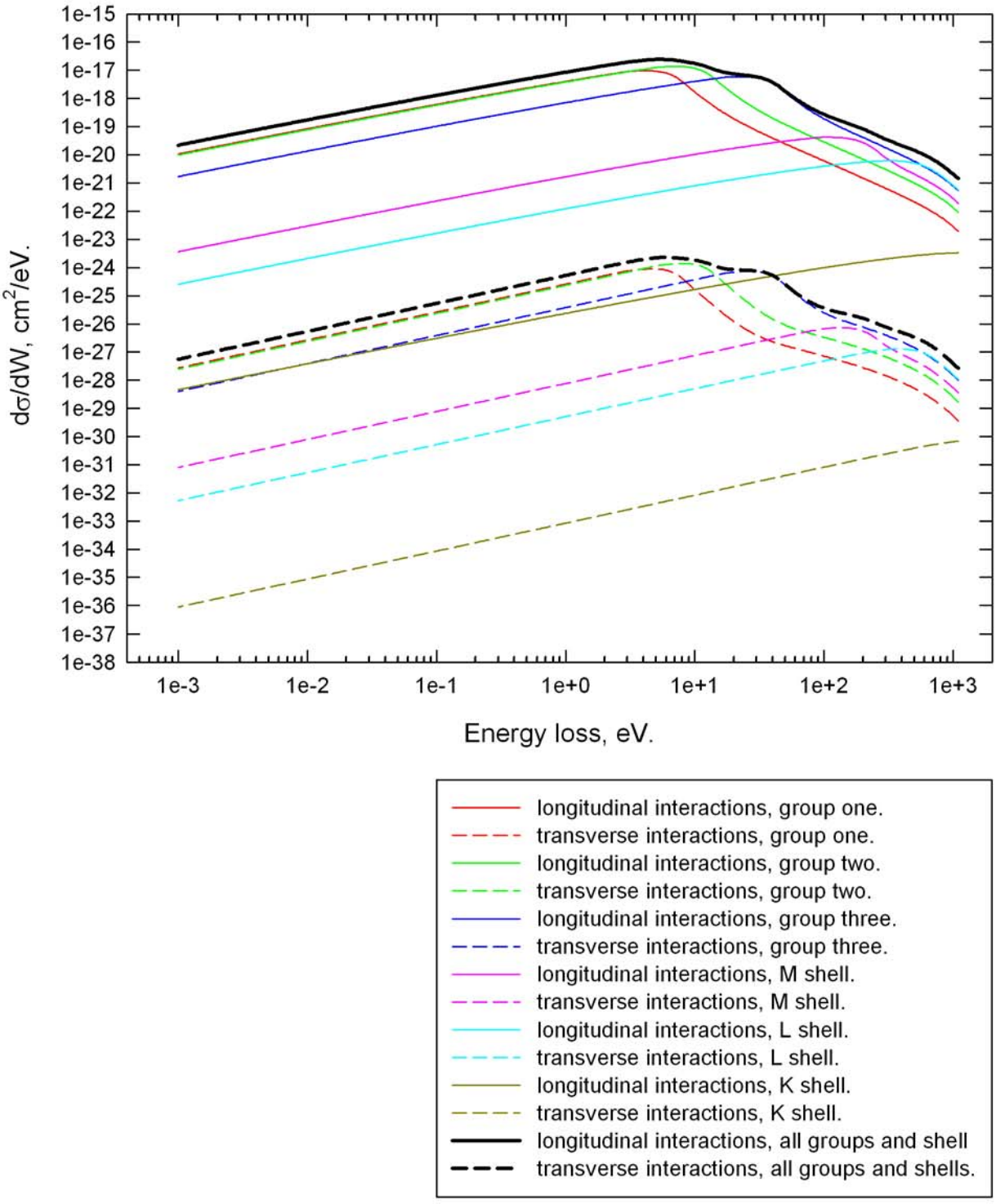

Figure 56. The energy loss differential interaction cross sections of 503.4 keV protons with electrons of calcium.

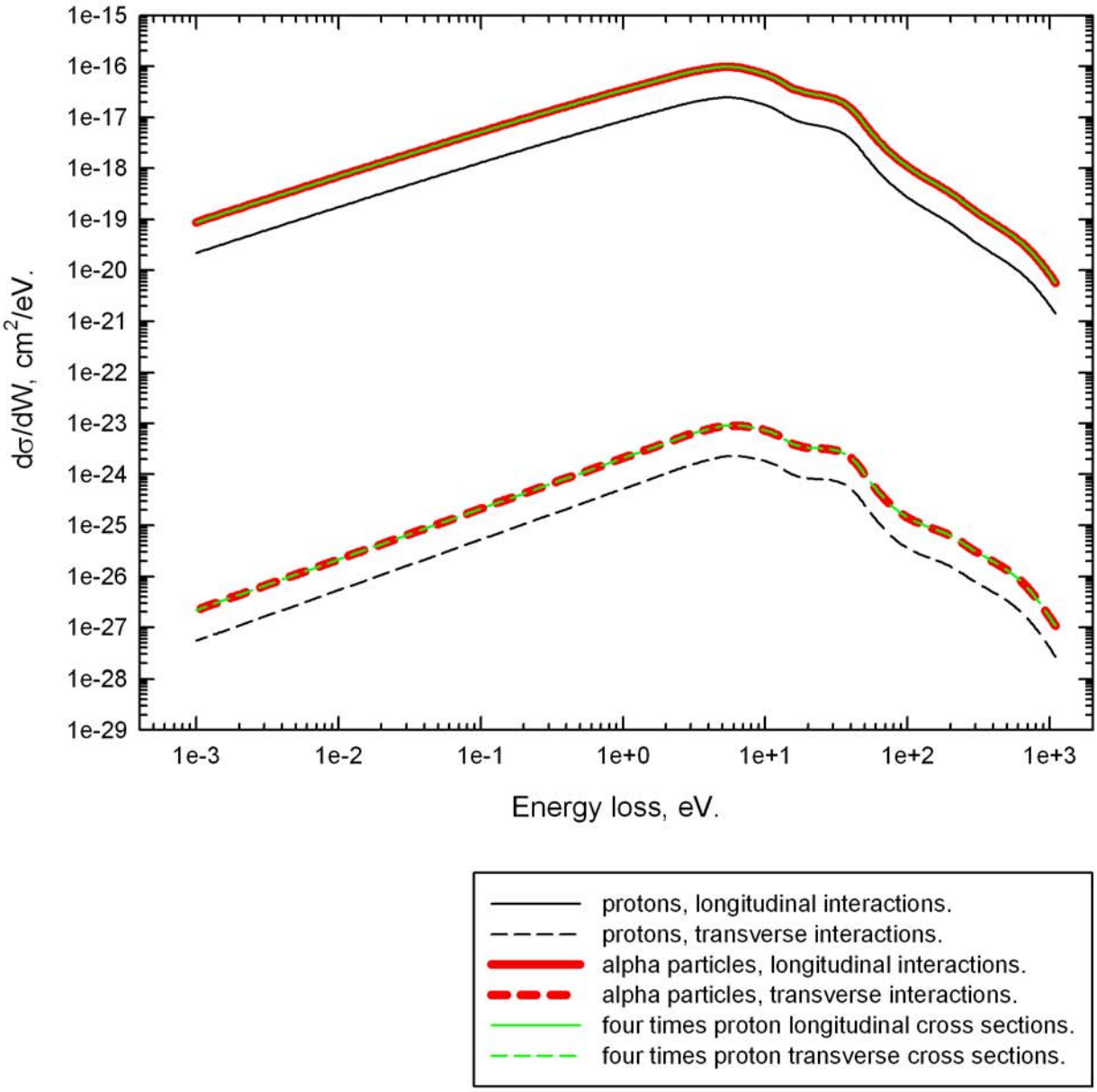

Figure 57. A comparison of the energy loss differential interaction cross sections of 503.4 keV protons and 2 MeV alpha particles.

Conclusions

The optical, the dielectric, and the energy loss functions of metallic calcium were derived from zero to infinite energy losses. The functions were based on the published material, derived using the Drude theory for small energy losses, and calculated using the photoelectric cross sections of calcium for large energy losses. The functions were used for a calculation of the oscillator strengths and the mean excitation energies of electrons from the bands of metallic calcium and the shells of atoms of calcium. The oscillator strengths and the mean excitation energies were used for modeling of the generalized oscillator strength (GOS) function of calcium. The GOS function of calcium was modeled with Gaussian functions extrapolated at small and at large energy losses with known slopes in order to accurately repeat the functions adopted for calcium.

A computer program was written which tabulated the generalized oscillator strength function of calcium, and which calculated interaction cross sections, mean free paths and stopping powers of electrons, protons and alpha particles in calcium. Stopping powers calculated for protons in calcium were in a very good agreement with the published results. Stopping powers calculated for alpha particles in calcium matched stopping powers published in the literature in the case of high kinetic energy alpha particles, but deviated from the published stopping powers in the case of small kinetic energy alpha particles. At this moment it is unknown which data, published in the literature or recently calculated, on the stopping power of alpha particles in calcium are more accurate. Unfortunately no data on interaction cross sections, mean free paths, or stopping powers of electrons in calcium were found in the literature. At this moment the results obtained for electrons in calcium have to be taken as granted. The computer program, which tabulated the GOS function of calcium, and which calculated interaction cross sections, mean free paths and stopping powers, was also used for testing the hypothesis about scaling of interaction cross

sections of one particles from interaction cross sections of other particles. Calculations of interaction cross sections of alpha particles and protons moving at the same speed confirmed the hypothesis about scaling of cross sections.

The computer program, written for modeling of the generalized oscillator strength function of calcium and for a calculation of interaction cross sections, mean free paths and stopping powers of charged particles in calcium, is organized in form of subroutines. The source code of the program is written in FORTRAN 77 computer language. Because the program is written in form of subroutines, the program can easily be integrated into any other computer program written in FORTRAN 77 language.

Accurate data on the optical and the dielectric properties of metallic calcium are highly desirable. The data would permit a creation of a more accurate model of the generalized oscillator strength function of metallic calcium. Measurements of interaction cross sections of charged particles with electrons of calcium and also measurements of mean free paths and stopping powers of charged particles in calcium are also highly desirable. Results of measurements of interaction cross sections, mean free paths and stopping powers would permit to test and improve the approach used for a calculation of interaction cross sections of charged particles not only with metallic calcium but with any metallic material.

References

Andersen H.H., Hanke C.C., Simonsen H., Sörensen H., and Vajda P., *"Stopping power of the elements Z=20 through Z=30 for 5-12-MeV protons and deuterons,"* Phys. Rev., Vol. 175, No. 2, (1968), 389–395.

Andersen H.H. and Ziegler J.F., *"Hydrogen stopping powers and ranges in all elements,"* Pergamon Press, Elmsford, New York, (1977).

Bader M., Pixley R.E., Mozer F.S., and Whaling W., *"Stopping cross section of solids for protons, 50-600 kev,"* Phys. Rev., Vol. 103, No. 1, (1956), 32–38.

Berger M.J. and Bichsel H., BEST code. The result of calculations performed for calcium using *BEST* program. *BEST*, *"BEthe STopping,"* is a computer program for a calculation of stopping powers of bare projectiles. The program was developed by Berger M.J. and Bichsel H., (1990/1994).

Dingfelder M., Jorjishvili I.G., Gersh J.A. and Toburen L.H., *"Heavy ion track structure simulations in liquid water at relativistic energies,"* Radiat. Prot. Dosim., Vol. 122, No. 1-4, (2006), 26-27.

Dressel M. and Grüner G., *"Electrodynamics of Solids: Optical Properties of Electrons in Matter,"* Cambridge University Press, 2002.

Eppacher Ch., Ph.D. Thesis, Univ. of Linz, Austria, Schriften der Johannes-Kepler-Universität Linz, Universitätsverlag Rudolf Trauner (1995).

Fernández-Varea J.M., Salvat F., Dingfelder M. and Liljequist D., *"A relativistic optical-data model for inelastic scattering of electrons and positrons in condensed matter,"* Nucl. Instr. and Meth. B, Vol. 229, (2005), 187-218.

Fox M., *"Optical Properties of Solids,"* Oxford University Press, 2001.

Gorodetzky S., Chevallier A., Pape A., Sens J.Cl., Bergdolt A.M., Bres M., and Armbruster R., *"Mesure des pouvoirs d'arrêt de C, Ca, Au Et CaF2 pour des protons d'énergie comprise entre 0.4 et 6 MeV,"* Nucl. Phys. A, Vol. 91, No. 1, (1967), 133–144.

Hunderi O., *"Optical properties of metallic calcium,"* J. Phys. F: Metal Phys., Vol. 6, No. 6, (1976), 1223-1229.

ICRU report 37, *"Stopping Powers for Electrons and Positrons,"* International Commission on Radiation Units and Measurements, Bethesda, MD (1984).

Janni J.F., *"Energy loss, range, path length, time-of-flight, straggling, multiple scattering, and nuclear interaction probability: In Two Parts. Part 1. For 63 Compounds. Part 2. For Elements $1 \leq Z \leq 92$,"* At. Data Nucl. Data Tabl., Vol. 27, No. 4-5, (1982), 341–529.

Kaneko T., *"Partial and Total Electronic Stopping Cross Sections of Atoms and Solids for Protons,"* At. Data Nucl. Data Tabl., Vol. 53, No. 2, (1993), 271–340.

Langkowski J., *"Electron-energy-loss experiments on calcium, strontium and barium,"* J. Phys. D: Appl. Phys., Vol. 8, (1975), 2058.

Liljequist D., *"A simple calculation of inelastic mean free path and stopping power for 50 eV–50 keV electrons in solids,"* J. Phys. D: Appl. Phys., Vol. 16, No. 8, (1983), 1567-1582.

Liljequist D., *"Simple generalized oscillator strength density model applied to the simulation of keV electron-energy-loss distributions,"* J. Appl. Phys., Vol. 57, No. 3, (1985), 657-665.

Marfaing J. and Vidal B., *"Sur la determination des constantes optiques du calcium a partir de couches epaisses,"* Opt. Commun., Vol. 25, No. 1, (1978), 9-13.

Mathewson A.G. and Myers H.P., *"Absolute values of the optical constants of some pure metals,"* Phys. Scripta, Vol. 4, (1971), 291-292.

Mendlowitz H., *"Optical constants of aluminium,"* Proc. Phys. Soc., Vol. 75, No. 5, (1960), 664-670.

Nilsson P.O. and Forssell G., *"Optical properties of calcium,"* Phys. Rev. B, Vol. 16, No. 8, (1977), 3352-3358.

Podgoršak E.B., *"Radiation Physics for Medical Physicists,"* Springer, 2006.

Potter M.R. and Green G.W., *"Optical properties of calcium in the vacuum ultraviolet,"* J. Phys. F: Metal Phys., Vol. 5, (1975), 1426-1432.

Segui S., Dingfelder M., Fernández-Varea J.M. and Salvat F., *"The structure of the Bethe ridge. Relativistic Born and impulse approximations,"* J. Phys. B: At. Mol. Opt. Phys., Vol. 35, (2002), 33-53.

Shiles E., Sasaki T., Inokuti M. and Smith D.Y., *"Self-consistency and sum-rule tests in the Kramers-Kronig analysis of optical data: Application to aluminum,"* Phys. Rev. B, Vol. 22, No. 4, (1980), 1612-1628.

Ziegler J.F., *TRIM ver. 1992*. The result of calculations performed for calcium using *TRIM* program. *TRIM*, *"Transport of Ions in Matter,"* is a computer program which calculates 3D distribution of projectile ions and kinetic phenomena associated with the ions' energy loss such as target damage, sputtering, ionization, and phonon production. Currently *TRIM* program in included in the *SRIM* program package. Ziegler J.F. is the leading scientist developing and supporting the *SRIM* program package. The *SRIM* program package is available online at www.srim.org as of Jan. 2013.

Ziegler J.F., *SRIM ver. 2003.12*. The result of calculations performed for calcium using the *SRIM* program package. *SRIM*, *"Stopping and Range of Ions in Solids,"* is a group of programs which calculate the stopping and range of ions in matter using a quantum mechanical treatment of ion-atom collisions. Ziegler J.F. is the leading scientist developing and supporting the *SRIM* program package. The *SRIM* program package is available online at www.srim.org as of Jan. 2013.

Photoelectric cross section databases

FFAST Chantler C.T., Olsen K., Dragoset R.A., Chang J., Kishore A.R., Kotochigova S.A. and Zucker D.S., *"X-Ray Form Factor, Attenuation and Scattering Tables"* (ver. 2.1). Available online at: http://physics.nist.gov/ffast (Jan. 24, 2006). National Institute of Standards and Technology, Gaithersburg, MD.

Originally published as

Chantler C.T., *"Detailed Tabulation of Atomic Form Factors, Photoelectric Absorption and Scattering Cross Sections, and Mass Attenuation Coefficients in the Vicinity of Absorption Edges in the Soft X-Ray (Z=30-36, Z=60-89, E=0.1 keV-10 keV), Addressing Convergence Issues of Earlier Work,"* J. Phys. Chem. Ref. Data, Vol. 29, No. 4, (2000), 597-1048, and

Chantler C.T., *"Theoretical Form Factor, Attenuation, and Scattering Tabulation for Z=1-92 from E=1-10 eV to E=0.4-1.0 MeV,"* J. Phys. Chem. Ref. Data, Vol. 24, No. 1, (1995), 71-643.

XCOM Berger M.J., Hubbell J.H., Seltzer S.M., Chang J., Coursey J.S., Sukumar R. and Zucker D.S., *"XCOM: Photon Cross Section Database"* (ver. 1.3). Available online at: http://physics.nist.gov/xcom (Jan. 24, 2006). National Institute of Standards and Technology, Gaithersburg, MD.

Originally published as

Berger M.J. and Hubbell J.H., *"XCOM: Photon Cross Sections on a Personal Computer,"* NBSIR 87-3597, National Bureau of Standards (former name of the NIST), Gaithersburg, MD (1987), and

Berger M.J. and Hubbell J.H., *"NIST X-ray and Gamma-ray Attenuation*

Coefficients and Cross Sections Database," NIST Standard Reference Database 8, Ver. 2.0, National Institute of Standards and Technology, Gaithersburg, MD (1990).